

การจัดการน้ำที่ตำแหน่งใต้ดินของแหล่งกักเก็บก๊าซธรรมชาติหลายชั้นซ้อนกัน



นาย พลพัฒน์ สุทธิโชติ

วิทยานิพนธ์นี้เป็นส่วนหนึ่งของการศึกษาตามหลักสูตรปริญญาวิศวกรรมศาสตรมหาบัณฑิต
สาขาวิชาวิศวกรรมปิโตรเลียม ภาควิชาวิศวกรรมเหมืองแร่และปิโตรเลียม

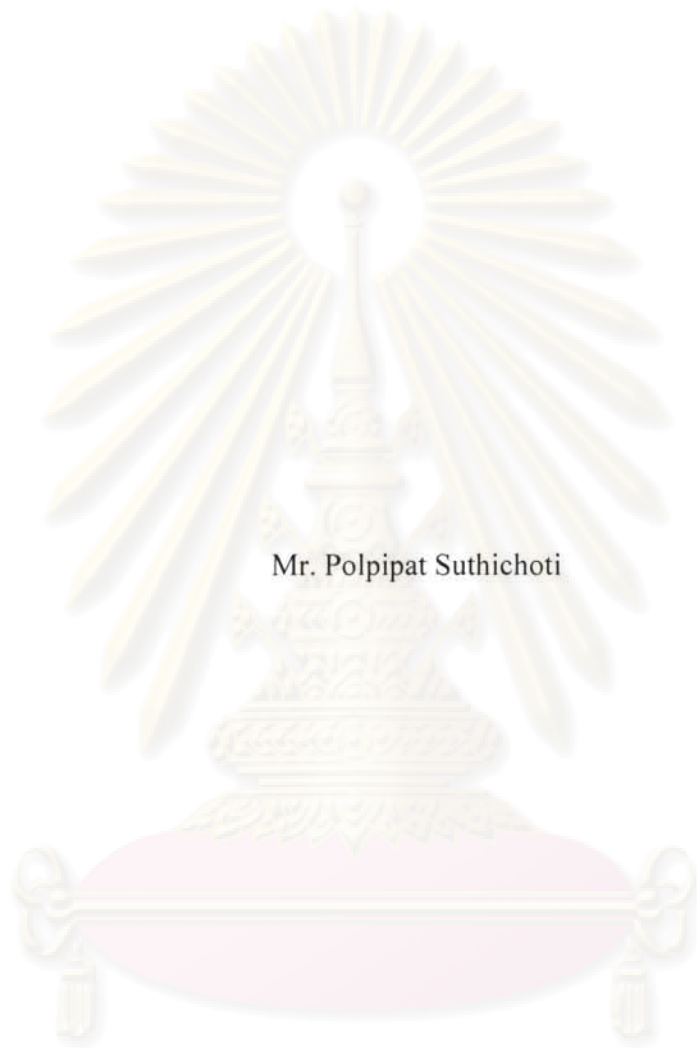
คณะวิศวกรรมศาสตร์ จุฬาลงกรณ์มหาวิทยาลัย

ปีการศึกษา 2550

ลิขสิทธิ์ของจุฬาลงกรณ์มหาวิทยาลัย

500565

SUBSURFACE WATER MANAGEMENT OF MULTI-STACKED
GAS RESERVOIRS



Mr. Polpipat Suthichoti

A Thesis Submitted in Partial Fulfillment of the Requirements
for the Degree of Master of Engineering Program in Petroleum Engineering

Department of Mining and Petroleum Engineering
Faculty of Engineering

Chulalongkorn University

Academic Year 2007

Copyright of Chulalongkorn University

พลพิพัฒน์ สุทธิโชติ : การจัดการน้ำที่ตำแหน่งใต้ดินของแหล่งกักเก็บก๊าซธรรมชาติหลาย
ชั้นซ้อนกัน (SUBSURFACE WATER MANAGEMENT OF MULTI-STACKED GAS
RESERVOIRS) อ.ที่ปรึกษา : ผศ.ดร. สุวัฒน์ อธิชนากร, อ.ที่ปรึกษาร่วม : ดร. ทศพล
ไชยอนันต์สุจริต, 141 หน้า

การผลิตน้ำในหลุมผลิตร่วมจากแหล่งกักเก็บก๊าซธรรมชาติเป็นปัญหาสำคัญต่อการเพิ่ม
ประสิทธิภาพในการผลิตก๊าซธรรมชาติออกจากแหล่งกักเก็บที่ชั้นขนาดเล็กให้ได้มากที่สุด
ในพื้นที่แอ่งปัดตานี อ่าวไทย หลังจากที่แหล่งกักเก็บหนึ่งแหล่งหรือมากกว่านั้นเริ่มผลิตน้ำ แหล่งกัก
เก็บก๊าซธรรมชาติอื่นๆจะได้รับผลกระทบจากความดันของน้ำหนักน้ำที่ผลิตเข้ามาในหลุมซึ่งจะ
ให้แหล่งกักเก็บอื่นผลิตด้วยประสิทธิภาพที่น้อยลงหรือไม่ผลิตเลย การปิดแยก (Shut off) แหล่งกัก
เก็บที่ผลิตน้ำเป็นวิธีที่สำคัญในการแก้ปัญหา

เป้าหมายของการศึกษาในวิทยานิพนธ์นี้ ได้มุ่งเป้าลงบนการคาดเดาอัตราการไหลวิกฤต
ของก๊าซธรรมชาติก่อนที่หลุมจะหยุดไหล และการคำนวณปริมาณสำรองก๊าซธรรมชาติของแต่ละ
แหล่งกักเก็บในหลุมผลิตร่วมโดยการสร้างแบบจำลองของแหล่งกักเก็บที่ผลิตจากหลุมเดียวกันและ
การปรับแบบจำลองโดยการเทียบกับข้อมูลการผลิตย้อนหลังจากการทดสอบหลุมและเครื่องมือ
สำรวจการผลิต (Production logging tool) เราสามารถใช้อัตราการไหลวิกฤตของก๊าซธรรมชาติ
ก่อนที่หลุมจะหยุดไหลเพื่อวางแผนสำหรับเวลาที่ดีที่สุดในการใช้เครื่องมือสำรวจการผลิต เพื่อหา
แหล่งกักเก็บที่ผลิตน้ำและปริมาณสำรองก๊าซธรรมชาติของแต่ละแหล่งกักเก็บเพื่อที่จะใช้ในการ
ตัดสินใจที่จะปิดแยกแหล่งกักเก็บที่ผลิตน้ำซึ่งจะช่วยเพิ่มอัตราส่วนความสำเร็จในการปิดแยกแหล่ง
กักเก็บที่ผลิตน้ำและเพิ่มประสิทธิภาพในการผลิตก๊าซธรรมชาติออกจากแหล่งกักเก็บในที่สุด

เราคาดหวังว่า ผลจากการศึกษานี้ จะเป็นเครื่องมือในการบริหารแหล่งกักเก็บเพื่อให้ได้การ
ผลิตก๊าซธรรมชาติขึ้นมามากที่สุด จากแหล่งกักเก็บขนาดเล็กที่ผลิตจากหลุมร่วมกันในพื้นที่อ่าว
ไทย

ภาควิชาวิศวกรรมเหมืองแร่และปิโตรเลียม
สาขาวิชาวิศวกรรมปิโตรเลียม
ปีการศึกษา 2550

ลายมือชื่อนิสิต.....

ลายมือชื่ออาจารย์ที่ปรึกษา.....

ลายมือชื่ออาจารย์ที่ปรึกษาร่วม.....

4771616021 : MAJOR PETROLEUM ENGINEERING

KEY WORD : /WATER/COMMINGLE/MULTI-TANK/OPTIMIZATION/ NEURAL NETWORK/CRITICAL GAS RATE/LOADING

POLPIPAT SUTHICHOTI. SUBSURFACE WATER MANAGEMENT OF MULTI-STACKED GAS RESERVOIRS. THESIS ADVISOR: SUWAT ATHICHANAGORN, Ph.D. THESIS CO-ADVISOR: THOTSAPHON CHAINANSUTCHARIT, Ph.D. 141 pp.

Water production in commingled monobore gas wells has been the crucial problem for maximizing recovery of multi-stack compartmentalized gas reservoirs in Pattani basin, Gulf of Thailand. After one or more sands produce a significant amount of water, the other sands suffer from the effect of hydrostatic backpressure from the produced water because they share the same wellbore. Shutting off water-out sand(s) is the major method to resolve this problem.

This study aims to improve sub-surface water management process. The main focus is on the prediction of critical velocity of gas well before it stops flowing and determination of individual zone gas reserve by building multi-tank commingled model and history match surface production and production logging data. By knowing critical gas velocity, best timing for production logging survey before well stop flowing can be planned to identify the water producing sand(s) as well as knowing OGIP of individual sand, better decision on water shut off intervention could be done with higher success ratio.

It is hoped that the outcome of the study will be used as the tool to improve reserve management to maximize recovery of these marginal gas reservoirs in the Gulf of Thailand.

Department of Mining and Petroleum Engineering

Field of study: Petroleum Engineering

Academic year: 2007

Student's signature.....

Advisor's signature *Suwat Athichanagorn*

Co-advisor's signature..... *Thotsaphon Chainansutcharit*

ACKNOWLEDGEMENTS

I would like to express my sincerest gratitude and appreciation to:

Dr. Suwat Athichanagorn, thesis advisor

Dr. Thotsaphon Chaianansutcharit, thesis co-advisor

Assoc. Prof. Sarithdej Pathanasetpong, thesis committee chairman

Dr. Jirawat Chewaroungroj, thesis committee

Nick Last, Chevron consulting PE

The management and colleagues of Chevron Thailand Exploration and Production,
Ltd

Classmates and Faculty Staff from the Department of Mining and Petroleum
Engineering — Chulalongkorn University

Pimra Suthichoti and Jirapun Paowarut;

Without their support and guidance, this work will never be accomplished.



ศูนย์วิทยทรัพยากร
จุฬาลงกรณ์มหาวิทยาลัย

TABLE OF CONTENTS

CHAPTER	Page
ABSTRACT (THAI).....	iv
ABSTRACT (ENGLISH).....	v
ACKNOWLEDGEMENTS.....	vi
TABLE OF CONTENTS.....	vii
LIST OF TABLES.....	x
LIST OF FIGURES.....	xii
NOMENCLATURE.....	xv
CHAPTER	
I. INTRODUCTION.....	1
II. LITERATURE REVIEW.....	3
2.1 Commingled reservoir model and method to determine individual properties.....	3
2.2 Critical Gas Well Loading Velocity	6
III. THEORETICAL CONSIDERATIONS.....	10
3.1 Non-linear regression analysis in Automatic History Matching	10
3.1.1 Gauss-Newton optimization method.....	10
3.1.2 Gauss-Newton-Levenberg-Marquardt Method.....	16
3.2 Theory behind MBAL to build Multi-Tank Model	18
3.2.1 Gas PVT	18
3.2.2 Gas Material Balance	22
3.2.3 Water influx model	26
3.2.4 Inflow Performance Relationship (IPR) of Each Individual Layer...27	
3.2.5 Relative Permeability.....	29
3.2.6 Vertical Lift Performance.....	31

จุฬาลงกรณ์มหาวิทยาลัย

CHAPTER	Page
3.3 Multi-Layer (feed-forward) Neural Net.....	32
3.3.1 Back- Propagation learning algorithm.....	34
3.3.2 Cost or Objective Functio.....	35
3.3.3 Activation Function.....	35
3.3.4 Gradient Descent Method.....	36
3.3.5 Input and output Encoding.....	36
3.3.6 Back-Propagation Rules.....	36
3.3.7 Termination Criteria.....	37
3.3.8 Learning Rate η	37
3.3.9 Momentum.....	38
3.3.10 Number of Hidden Layers and Node in the Network.....	38
3.3.11 Measure result of Testing Data Set.....	39
IV. WORK FLOW METHODOLOGY	40
4.1 Determination of OGIP and Aquifer size in multi –tank commingle model.....	40
4.1.1 Software for building and investigation of multi-tank commingle model with and without water production	40
4.1.2 Program coding for automatic history matching routine and its application	44
4.2 Determination of gas critical (terminal) velocity by Neural Network	47
V RESULT AND DISCUSSION.....	50
5.1 Determination of OGIP and Aquifer size	50
5.2 Construction and Testing of Neural Network for Gas Well Critical Loading Velocity Determination	102
5.2.1 Turner Critical Rate.....	102
5.2.2 Neural Network for Critical Gas Rate and its prediction result	107
VI CONCLUSIONS AND RECOMMENDATIONS.....	124
6.1 Zonal OGIP and aquifer determination	124
6.1.1 Conclusions.....	124

CHAPTER	Page
6.1.2 Recommendations for future work.....	127
6.2 Critical Gas Rate Prediction by Neural Network.....	127
6.2.1 Conclusions.....	127
6.2.2 Recommendations for future work	128
6.3 The comprehensive sub surface water management.....	128
REFERENCES.....	129
APPENDICES.....	131
APPENDIX A: EFFECT OF SHUTTING IN THE WELL ON GAP AND MBAL SOFTWARE.....	132
APPENDIX B: PROCEDURE TO SET UP COMMINGLE MODEL WITH MBAL AND PROCEDURE TO USE AUTOMATIC HISTORY MATCHING SPREADSHEET.....	134
APPENDIX C: AUTOMATIC HISTORY MATCHING MACRO CODE.....	140
VITAE.....	141



 ศูนย์วิทยทรัพยากร
 จุฬาลงกรณ์มหาวิทยาลัย

LIST OF TABLES

TABLE	Page
5.1 Two-Tank commingle system reservoir property data.....	50
5.2 Summary of commingle multi-tank model study	58
5.3 Reservoir properties used in this case 2.1.....	59
5.4 Depth data of two different reservoirs in case 2.1.....	59
5.5 Reservoir properties used in case 3.....	65
5.6 Result of automatic history match with depletion drive model	67
5.7 Result of automatic history matching of case 1.1.1.....	67
5.8 Summary of automatic history match on simulation data of Multi-tank Model with Aquifer Model on tank 77-5	70
5.9 Summary of automatic history matching result of case 4.1.....	71
5.10 Result of history match of case 4.1#3.....	72
5.11 Summary of automatic history matching of case 4.2.....	75
5.12 Reservoir data of three-tank commingled system	76
5.13 Result of automatic history matching of case 5.....	77
5.14 Comparison of various normalized ΣR^2 from converged solution	77
5.15 Result of history matching from case 5#4, normalized weighing factor 10 times on PLT data	78
5.16 Reservoir properties for well A	81
5.17 Result of trial of automatic history matching parameters on well A	83
5.18 Comparison of various normalized ΣR^2 from converged solution	83
5.19 Result of automatic history match case 6#4.....	84
5.20 OGIP of individual layer of well A compared with various method.....	85
5.21 Reservoir properties for all sands in well B	87
5.22 Result of various trials of automatic history matching parameters	89
5.23 Comparison of various normalized ΣR^2 from converged solution	90
5.24 Comparison of OGIP of individual sands with different methods(software).....	90
5.25 Result of automatic history matching case 7#4.....	91
5.26 Reservoir properties for all layers modeled in well C	94
5.27 Relative permeability for well C from Boatman correlation	95

TABLE	Page
5.28 Result of various trial of automatic history matching parameters	97
5.29 Result of automatic history matching case 8#5.....	99
5.30 Result of new trials performed with normalized error in the algorithm.....	102
5.31 Comparison of various normalized ΣR^2 from converged solution	103
5.32 Result of automatic history matching case 8#4 normalized error	104
5.33 Turner's critical gas loading velocity and rate	108
5.34 Training and validated data set records	110
5.35 Testing data set records	112
5.36 Training result	117
5.37 Training result sorted by ascending training error	118
5.38 Training result sorted by ascending validation error	119
5.39 Training result sorted by ascending testing R^2	120
7.1 Tank 77-5 production profile during shut in simulated with GAP.....	131
7.2 Tank 70-2 production profile during shut in simulated with GAP.....	132
7.3 Tank 70-2 production profile simulated by MBAL.....	133
7.4 Tank 77-5 production profile simulated by MBAL.....	133


 ศูนย์วิทยทรัพยากร
 จุฬาลงกรณ์มหาวิทยาลัย

LIST OF FIGURES

FIGURE	Page
3.1 Flowchart of Gauss-Newton Algorithm	15
3.2 Flow chart of Levenberg-Marquardt algorithm.....	17
3.3 Cole plot to detect addition drive energy in gas reservoir.....	25
3.4 Multi-layer back-propagation Neural Network diagram.....	33
4.1 Flow chart of data communication and calculation between IPM and automatic history matching spreadsheet.....	45
5.1 IPR of each tank and composite IPR Case 1.....	51
5.2 Comparison of total gas rate (Case1.1).....	52
5.3 Comparison of pressure of tank 70-2 (Case1.1).....	53
5.4 Comparison of gas rate of tank 70-2 (Case1.1).....	53
5.5 Comparison of pressure of tank 77-5 (Case1.1).....	53
5.6 Comparison of gas rate of tank 77-5 (Case1.1).. ..	54
5.7 Comparison of total gas rate (Case1.2).....	55
5.8 Comparison of pressure of tank 70-2 (Case1.2).....	55
5.9 Comparison of gas rate of tank 70-2 (Case1.2).....	56
5.10 Comparison of pressure of tank 77-5 (Case1.2).....	56
5.11 Comparison of gas rate of tank 77-5 (Case1.2).....	57
5.12 IPR of all reservoirs in the system for case 2.1.....	60
5.13 Plot of difference in total gas production between GAP and MBAL, all tanks having depletion drive.....	60
5.14 Difference in tank 59-1 pressure profile between GAP and MBAL, all tanks having depletion drive.....	61
5.15 Difference in tank 59-1 gas rate profile between GAP and MBAL, all tanks having depletion drive.....	61
5.16 Difference in tank 78-6 pressure profile between GAP and MBAL, all tanks having depletion drive.....	62
5.17 Difference in tank 78-6 gas production rate between GAP and MBAL, all tanks having depletion drive.....	62

FIGURE	Page
5.18 Difference in total water production profile between MBAL and GAP (scenario 1 and 2).....	63
5.19 Difference in total WGR profile between MBAL and GAP (scenario 1 and 2).....	63
5.20 Difference in total gas production profile MBAL and GAP (scenario 1 and 2).....	64
5.21 Result of automatic history matching of well gas rate case 3.1#1.....	67
5.22 Result of automatic history matching of tank gas rate case 3.1#1.....	67
5.23 Result of automatic history matching of tank pressure case 3.1#1.....	68
5.24 Plot of gas WT history match result of case 4.1#3.....	72
5.25 Chart of tank pressure history match result of case 4.1#3.....	73
5.26 Chart of tank gas rate history match result of case 4.1#3.....	73
5.27 System and individual IPR for case 5.....	79
5.28 Gas WT matching result of case 5#4.....	79
5.29 Chart of tank pressure history matching result of case 5#4.....	79
5.30 Chart of tank gas rate history matching result of case 5#4.....	79
5.31 IPR of commingle system – well A.....	82
5.32 Well test automatic history matching result of case 6#4.....	84
5.33 Tank pressure matching result of case 6#4.....	85
5.34 Tank gas rate matching result of case 6#4.....	85
5.35 IPR of commingle system – well B.....	88
5.36 WT gas rate matching result of case 7#4.....	92
5.37 Tank pressure matching result of case 7#4.....	92
5.38 Tank gas rate matching result of case 7#4.....	92
5.39 Relative permeability curve calculated from Boatman correlation.....	95
5.40 IPR of commingle system – well C.....	96
5.41 WT water rate match result of case 8#5.....	100

FIGURE	Page
5.42 WT gas rate match result of case 8#5.....	100
5.43 Tank pressure matching result of case 8#5.....	100
5.44 Tank gas rate matching result or case 8#5.....	101
5.45 Tank water rate matching result of case 8#5.....	101
5.46 WT water rate matching result of case 8#4 normalized error	106
5.47 Result of WT water matching result case 8#4 normalized error	106
5.48 Result of tank pressure matching result case 8#4 normalized error.....	106
5.49 Result of tank gas rate matching result of case 8#4 normalized error	107
5.50 Result of tank water rate matching result of case 8#4 normalized error	107
5.51 Data distribution histogram.....	113
5.52 Summary of the result from all network.....	121
5.53 Training and validating result of Network #20.....	122
5.54 Training and validating progress chart of Network #20.....	122
5.55 Testing result of network #20, comparison with Turner's.....	123
7.1 System production profile simulated by GAP during shut in.....	131
7.2 System production profile during shut in simulated with MBAL.....	132

NOMENCLATURE

CHAPTER 2

G	=	Original gas in place, MMScf
G_p	=	Cumulative gas produced, MMScf
J_g	=	real gas flow coefficient, MScf Cp/D/psi ²
n _{layer}	=	number of layer in a commingled system
OGIP	=	Original Gas in Place, MMScf
P	=	Pressure, psia
<i>prod</i>	=	production
<i>pl</i>	=	production log
T	=	Temperature, Rankin
V	=	Velocity, ft / sec
Z	=	Gas deviation factor
\mathcal{E}	=	error term, dimension less subscript
A	=	Flow area of conduit, ft ²
A_p	=	Projected area, ft ²
C_d	=	Drag coefficient
d_p	=	Diameter of liquid drop, ft
d_m	=	Maximum diameter of liquid drop, ft
g	=	Local acceleration of gravity, ft / sec ²
g_c	=	Gravitational constant = 32.17 lb mass / lb ft sec ²
$m(\bar{p})$	=	real gas pseudo-pressure at average reservoir pressure, psi ² /Cp
$m(p_{wf})$	=	Pseudo-pressure at bottom hole flowing pressure, psi ² /Cp

m_p	=	Mass of falling particle, lb mass
N_{re}	=	Reynolds number
N_{we}	=	Weber number
p_i	=	initial reservoir pressure, psia
q_g	=	gas production rate, MScf/D
q_t	=	total flow rate in commingled system, MScf/D
V_t	=	terminal velocity of free falling particle, ft / sec
μ_g	=	Gas phase viscosity, lb mass / ft sec
μ_L	=	Liquid phase viscosity, lb mass / ft sec
ρ_g	=	Gas phase density, lb mass / ft ³
ρ_L	=	Liquid phase density, lb mass / ft ³
ρ_p	=	Density of particle, lb mass / ft ³
σ	=	interfacial tension, dynes / cm

CHAPTER 3

$H_m^c(\bar{p})$ = the calculated value corresponding to measurement H_m^{obs}

W_m = the weighting coefficient of measurement m

f_m = m^{th} residual is a measure of the closeness of the match on that particular pair of calculating/measured value

N_r = number of residual

P = Matching (model) parameters, total n parameters (G_i, A_i)

N_r = Total number of residual ($Q_g^k, Q_w^k, Q_g^{id}, Q_w^{id}, p^{id}$)

k = Total number of well test point

i	=	Tank ID
d	=	sequence order number of PLT survey
M_w	=	Molecular weight
V	=	Volume in Scf
n	=	mole in lb-mole
R	=	gas constant which is 10.73
T	=	Temperature in degrees Rankin (deg F+460)
Z	=	Gas compressibility factor, dimensionless
ρ	=	gas density, 1/cc
P	=	pressure (psia)
T	=	Temperature Rankin
M_w	=	molecular weight of gas
G	=	initial reservoir gas, or OGIP, Scf
B_g	=	Gas formation volume facto, bbl/Scf
B_{gi}	=	Initial gas formation volume factor, bbl/Scf
C_w	=	Water isothermal compressibility, psi^{-1}
S_{wi}	=	Initial or connate water saturation
C_f	=	Formation isothermal compressibility, psi^{-1}
$\Delta\bar{P}$	=	Change in average reservoir pressure, psia
W_e	=	Water influx into reservoir, bbl
G_p	=	Cumulative gas production, Scf
B_w	=	Water formation volume factor, bbl/STB

W_p	=	Cumulative produced water, STB
W	=	Aquifer original water in Place (OWIP), res bbl
P_i	=	Initial aquifer or reservoir pressure
$m(\bar{p})$	=	Pseudo average reservoir pressure, psi^2/Cp
$m(p_{wf})$	=	Pseudo wellbore pressure, psi^2/Cp
q	=	Gas flow rate, Scf per day
k	=	Permeability, mD
h	=	Formation thickness
r_e	=	Reservoir radius, ft
r_w	=	Wellbore radius, ft
S	=	Skin factor, dimensionless
F	=	Non Darcy coefficient,
\bar{P}_r	=	Average reservoir pressure, psi
P_{wf}	=	Wellbore pressure at sand face, psi
C	=	performance coefficient, $\text{Mscf}/\text{day}/\text{psi}^2$
n	=	an exponent
A	=	Laminar pressure drop coefficient, $\text{psi}^2/(\text{Mscf}/\text{day})$
B	=	turbulent pressure drop coefficient, $\text{psi}^2/(\text{Mscf}/\text{day})^2$
E_x	=	end point of phase x
S_x	=	Phase saturation
S_{rx}	=	Phase residual saturation
S_{mx}	=	Phase maximum saturation
nx	=	Covey exponent

F_x	=	Fractional flow of phase x
Q_x	=	Flow rate phase x at surface
B_x	=	Formation volume factor of phase x
Q_y	=	Formation volume factor of phase y
B_y	=	Formation volume factor of phase y
K_{rx}	=	Relative permeability of phase x
K_{ry}	=	Relative permeability of phase y
μ_x	=	Viscosity of phase x
μ_y	=	Viscosity of phase y
y	=	l output vector
μ	=	m input vector
n	=	Number of neurons in the hidden layer
$\Delta W_{previous}$	=	Previous weight adjustment
α	=	momentum, $0 \leq \alpha < 1$

ศูนย์วิทยทรัพยากร
จุฬาลงกรณ์มหาวิทยาลัย

CHAPTER I

INTRODUCTION

Nick Last^[1] stated that the prevalent completion strategy of all operators to economically develop gas field in the Gulf of Thailand of which reservoirs have the nature of multiple stacked-sand horizons over long pay window (up to 5000 TVD) is to utilize tubingless monobore slimhole well design. These monobore wells penetrate multiple sands in particular fault blocks and produce gas comingled from these several different reservoirs into one wellbore. One of most significant factors impairing recovery efficiency from these wells is water production, the source of which cannot usually be predicted in advance. Gas productivity from non-watered out reservoirs is impaired or even stops when gas velocity falls below the limit of which water can be lifted out of the wellbore. The phenomenon called liquid loading occurs when accumulated liquid column formed in the wellbore and increases hydrostatic head that creates additional back pressure to other gas reservoirs penetrated by wellbore. Shutting off water producing sands is the prevalent intervention to resolve this liquid problem.

To identify water producing sands, memory production logging tool (MPLT) is run to investigate flow profile of multiple sands and identify the phase of fluid. The problem is what should be the best time to run PLT. The timing to run PLT is needed before the gas flow rate falls below the critical rate. In this work, critical velocity prediction is investigated empirically by Neural Network. After water sands are identified, decision to shut off water sand depends on the benefit of the potential of the rest of sands in term of reserve left and the cost of water shut off intervention. Ability to determine individual Original Gas In Place (OGIP) of each sand with petroleum expert software (MBAL, GAP, Prosper) by using multi tank model and calibration of the model by prediction and MPLT data will certainly improve decision process whether watered out sand(s) should be shut off as well as improve success rate of water shut off (WSO) intervention. The study investigates incorporation of automatic history matching algorithm to construct multi tank model to reduce the task of model calibration with all available data since this feature is not available in existing software features.

Apart from improving the success rate of WSO intervention, multi-tank model is also beneficial for flow profile prediction of individual tank, investigating the likelihood of cross flow when perforating later batches. Another goal of this thesis is to bring simplicity to build and history match multi-tank model which should improve its popularity and promote it to become standard reserve determination methodology as well as demonstrate its benefit on production optimization related decision making improvement in commingled production.



ศูนย์วิทยทรัพยากร
จุฬาลงกรณ์มหาวิทยาลัย

CHAPTER II

LITERATURE REVIEW

2.1 Commingled Reservoir Model and Method to Determine Individual Layer Properties

El-Banbi and Wattenbarger ^[2] presented a method to match the production data of commingled tight gas reservoirs with a simple computer program that used to history match the production data, estimate the individual OGIP and productivity of each layer and forecast the total performance of the well. Their method is based on a layered model that couples the material balance equation for gas reservoirs with the stabilized gas flow equation for each later in the commingled system.

The volumetric material balance equation for gas reservoirs (Equation 2.1) and the flow equation (Equation 2.2) are coupled by gas flow rate (q_g) and cumulative gas production (Equation 2.3). The material balance and gas flow equation for individual layer are described below:

$$\frac{P}{Z} = \left(\frac{P}{Z} \right)_i \left(1 - \frac{G_p}{G} \right) \quad (2.1)$$

$$q_g = J_g \left[m(\bar{p}) - m(p_{wf}) \right] \quad (2.2)$$

$$G_p = \int_0^t q_g(t) dt \quad (2.3)$$

The performance from single layer stabilized flow model can be added for all layers in the commingled system with Equation 2.4

$$q_r(t) = \sum_{j=1}^{nlayer} q_{gj}(t) \quad (2.4)$$

where

G = Original gas in place, MMScf

G_p = Cumulative gas produced, MMScf

J_g	=	real gas flow coefficient, MScf cp/D/psi ²
$m(\bar{p})$	=	real gas pseudo-pressure at average reservoir pressure, psi ² /cp
$m(p_{wf})$	=	Pseudo-pressure at bottom hole flowing pressure, psi ² /cp
n _{layer}	=	number of layer in a commingled system
OGIP	=	Original Gas in Place, MMScf
P	=	pressure, psia
p_i	=	initial reservoir pressure, psia
q_g	=	gas production rate, MScf/D
q_t	=	total flow rate in commingled system, MScf/D
Z	=	real gas correction factor

The parameters to be determined are OGIP and J_g for each layer. The analysis of commingled system is carried out by assuming values for OGIP and J_g for each layer and calculating the total performance (rate vs. time) for the entire commingled system. The error in the model is compared with observed values (total gas rate from well test vs. time). The sum of the squares of the errors is treated as the objective function for a multi variable optimization routine. The optimization routine is used to minimize the errors between the data and the model forecast by adjusting OGIP and J_g for each layer until the sum of the squares of the errors is minimal. El-Banbi and Wattenbarger model assumed p_{wf} is known for each layer, no turbulence skin and pseudo steady state (pss) is reached. Therefore, this model is only good after the data are acquired when all the layers are in pseudo-steady state; otherwise, conservative estimates of OGIP and prediction are obtained. The model is also only good for moderate permeability formation of which turbulent skin does not play important role in pressure drop across formation. In addition, the optimization routine may converge to a wrong minimum when field data for history match is not good enough.

Spivey ^[3] presented a fully-coupled reservoir/wellbore single well analytical simulator for multilayer unconventional gas reservoirs that automatically history matches production and production log data simultaneously. His simulator accounts for transient and boundary-dominated flow in each layer and pressure drop in the wellbore, including pressure drop between adjacent layers and pressure drop from the reservoir to the surface. By history matching data from multiple production logs as well as surface production data, this simulator provides estimate of individual layer properties such as permeability, fracture length, and drainage area. There are different wells, reservoirs, and outer boundary models available. Well models include fully penetrating vertical well, finite-conductivity hydraulically fractured well, and horizontal well models. Reservoir models include homogenous, pseudo steady state dual porosity, and transient dual porosity models. Outer boundary models include infinite reservoir, closed circular reservoir, closed rectangular reservoir, and infinite or finite radial composite reservoirs. The simulator calculates layer and total well flow rates for a specified pressure history which could be either wellhead pressures or sandface pressures. Levenberg-Marquardt non-linear regression algorithm is used. This algorithm combines the rapid convergence of the Gauss-Newton Method, when the near solution, with the guaranteed decrease in the objective function of the steepest descent algorithm when far from the solution. The objective function for minimization is shown in Equation 2.5

$$= \sum_{j=1}^{N_{prod}} \mathcal{E}_{prodj}^2 + \sum_{j=1}^{N_{pl}} \left[\sum_{k=1}^{N_{layer}} \mathcal{E}_{plj,k} \right] \quad (2.5)$$

where

\mathcal{E}_{prod} = error term
 production

pl = production log

\mathcal{E}_{prod} can be either cumulative production (G_p) or incremental production data (ΔG_p), and \mathcal{E}_{pl} is the gas rate of individual layer at particular PLT survey. At most 3 different matching parameters would be allowed to vary for each layer. It is

recommended that as many parameters as possible be eliminated independently. For vertical wells, recommended matching parameters are permeability, skin factor, and drainage area. For hydraulically fractured wells, permeability fracture half length, fracture conductivity, and drainage area are available as matching parameters.

Nick Last^[1] developed CWM (commingle wellbore model), a spreadsheet-based commingled well simulator with the intention of estimating individual reservoir volumes, by adjusting input zone areas until simulated well performance matched PLT survey results and production history.

2.2 Critical Gas Well Loading Velocity

Turner *et al.*^[12] describe the nature of liquid in Gas well as follow:

“Gas phase hydrocarbon produced from reservoir will have liquid phase material associated with them. Liquid could come from two obvious sources : liquid condensed from gas owing to wellbore heat loss and free liquids produced into wellbore with gas such as water from aquifer bearing formation or water influx encroachment to gas reservoir. In either case, higher density liquid phase, being essentially discontinuous, must be transported to the surface by the gas. In late event that gas does not provide sufficient transport energy to lift liquid out of wellbore, the accumulation of liquid will impose back pressure on the formation that significantly affect the production capacity of the well. In low pressure wells, the liquid may completely kill the well and in high pressure wells, there can occur a variable degree of slugging or churning of liquids, which can affect calculation in routine well test and bottom hole pressure calculation.” He proposed a droplet model to calculate minimum velocity of gas that breaks liquid into droplets and transports these droplets out of the wellbore. The liquid is treated as freely falling particles in a fluid medium. The particles will reach a terminal velocity, which is the maximum velocity that can attain under the influence of gravity alone when the drag forces equal gravitational force. If the gas were moving at a velocity sufficient to hold a drop in suspension, then gas velocity would be equal to the free fall terminal velocity of the drop which can be defined as follows:

$$V_t = \sqrt{\frac{2gm_p(\rho_p - \rho)}{\rho_p \rho A_p C_d}} \quad (2.6)$$

where

ρ_p	=	Density of particle, lb mass / ft ³
A_p	=	Projected area, ft ²
C_d	=	Drag coefficient
g	=	Local acceleration of gravity, ft / sec ²
m_p	=	Mass of falling particle, lb mass
ρ	=	Fluid medium density, lb mass / ft ³

Equation 2.6 can also be presented in terms of drop diameter

$$V_t = 6.55 \sqrt{\frac{d(\rho_L - \rho_g)}{\rho_d C_d}} \quad (2.7)$$

where

d	=	Diameter of a drop, ft
ρ_g	=	Gas phase density, lb mass / ft ³
ρ_L	=	Liquid phase density, lb mass / ft ³
ρ_d	=	Droplet density, lb mass / ft ³

The bigger the droplet, the higher terminal velocity is required. Hinze showed that liquid drops moving relative to a gas are subjected to force that tries to shatter the drops, while surface tension of the liquid acts to hold the drops together. He determined that it is antagonism of two pressures, the velocity pressure, $V^2 \rho_g / g_c$ and the surface tension, σ / d that determines the maximum Weber number, $N_{we} = V^2 \rho_g d / \sigma \cdot g_c$. Hinze showed that if the ratio exceeds a critical value, a liquid drop would shatter. This ratio was found to be 20 to 30. From Weber number definition above, if we substitute N_{we} by 30 and solve for droplet diameter with the following equation below.

$$d_m = \frac{30\sigma \cdot g_c}{\rho_g V_i^2} \quad (2.8)$$

Substituting Equation 2.8 into Equation 2.7, we obtain a new equation

$$V_i = \frac{1.3\sigma^{1/4}(\rho_L - \rho_g)^{1/4}}{\rho_d^{1/4} C_d^{1/4}} \quad (2.9)$$

Interfacial tension can be obtained from Chemical Engineering handbook. Drag coefficient depends on the Drop Reynolds number (N_{re}). A correlation of C_d vs. N_{re} range from 1,000 to 200,000 indicates that the drag coefficient is approximately constant in this range of Reynold number. For typical field condition, N_{re} ranges from 10^4 to 10^5 in which C_d is constant at 0.44. Substituting the value of C_d into Equation 2.9, we have

$$V_i = \frac{1.593\sigma^{1/4}(\rho_L - \rho_g)^{1/4}}{\rho_g^{1/2}} \quad (2.10)$$

Equation 5 in reference 12 was wrong. This equation was taken from reference 13. Analysis of this equation with field data shows the need for adjustment of Equation 2.10 to Equation 2.11

$$V_i = \frac{1.912\sigma^{1/4}(\rho_L - \rho_g)^{1/4}}{\rho_g^{1/2}} \quad (2.11)$$

The field testing result showed that the wellhead conditions were the controlling condition. Surface tension of low molecular weight Hydrocarbon varies only slightly with change in molecular weight and temperature. For water, 60 dynes/cm can be used. Density of water is relatively constant at 67 lb mass/cu.ft. Terminal velocity for water droplet becomes

$$V_g(\text{water}) = \frac{5.3(67 - \rho_g)^{1/4}}{\rho_g^{1/2}} \quad (2.12)$$

Converting to gas rate at standard conditions, we obtain

$$q_g (\text{MMscf} / D) = \frac{3.06 P V_g A}{T_z} \quad (2.13)$$

Turner^[12] stated that the liquid gas ratio does not affect V_g in the observed range of liquid gas ratio up to 130 bbl / MMscf.

A	=	Flow area of conduit, ft ²
d_p	=	Diameter of liquid drop, ft
g_c	=	Gravitational constant = 32.17 lb mass / lb ft sec ²
N_{re}	=	Reynolds number
N_{we}	=	Weber number
P	=	Pressure, psi
q_g	=	Gas flow rate, MMscf / D
T	=	Temperature, Rankin
V	=	Velocity, ft / sec
V_t	=	terminal velocity of free falling particle, ft / sec
Z	=	Gas deviation factor
μ_g	=	Gas phase viscosity, lb mass / ft sec
μ_L	=	Liquid phase viscosity, lb mass / ft sec
σ	=	interfacial tension, dynes / cm

Coleman^[13] concluded that critical gas velocity calculated with initial proposal (Equation 2.10) by Turners should be used (without 20% uplift). A well that exhibits slugging behavior may not follow the liquid droplet model because of different transport mechanism. He also confirmed that in most cases, wellhead conditions can be used to predict the onset of liquid load up.

CHAPTER III

THEORETICAL CONSIDERATION

3.1 Non-linear Regression Analysis in Automatic History Matching

A process to improve reservoir description is in a sense, the “inverse” of simulation to predict reservoir performance. The approach generally adopted is to search for the set of properties that defines a reservoir model so that a simulation based on this model will produce calculated reservoir behavior that represents the closest match to the observed behavior. This search is referred to as “history matching”. By far, the largest fraction of this modeling is performed manually – i.e. by running a number of simulations and altering the model between successive simulations as needed to improve the match between model output and historical data. Due to the lengthy and unstructured nature of this trial and error of the process, there is an incentive to provide an automated version of the process. Some algorithms adjust the model (matching) parameters according to certain predetermined guideline. The quality of the match is quantified in term of objective function, a relationship that reflects the difference between observed and calculated reservoir behavior. The goal is to find the model that will optimize the objective function, i.e., minimizing the error. The process is generally referred to as “automatic history matching”. The most common objective function is the sum of squares of the difference between observed and calculated data

3.1.1 Gauss-Newton optimization method

Consider \bar{p} as the parameter vector and the components $\{P_1, P_2, \dots, P_n\}^T$ to be estimated. For this work, the OGIP (G_i) each layer and aquifer size of particular layer(s) are the parameters of interest. The objective function can be written as

$$E(\bar{p}) = \sum_{m=1}^{N_r} W_m^2 [H_m^c(\bar{p}) - H_m^{obs}]^2 \quad (3.1)$$

or

$$E(\bar{p}) = \sum_{m=1}^{N_r} f_m^2(\bar{p}) \quad (3.2)$$

$$f_m(\bar{p}) = W_m [H_m^c(\bar{p}) - H_m^{obs}] \quad (3.3)$$

where

$H_m^c(\bar{p})$ = the calculated value corresponding to measurement H_m^{obs}

W_m = the weighting coefficient of measurement m

f_m = m^{th} residual is a measure of the closeness of the match on that particular pair of calculating/measured value

N_r = number of residual

In a regression method, the derivatives of the objective function with respect to each variable are analyzed concurrently to determine the optimum direction for the parameter ΔP_i . The effects of all variables on each residual are included simultaneously.

From objective of function, Equation 3.2 for $E(\bar{p})$ to be minimum at $P' + \Delta P$, the following equation must be satisfied;

$$\frac{\partial E}{\partial P_i} = 2 \sum_{k=1}^{N_r} f_k(P' + \Delta P) \frac{\partial f_k(P' + \Delta P)}{\partial P_i} = 0 \quad (3.4)$$

for $i = 1, 2, \dots, n$

A Taylor-series expansion about P_i including only the first derivative gives

$$f_k(P' + \Delta P) = f_k(P') + \sum_{j=1}^n \Delta P_j \frac{\partial f_k(P')}{\partial P_j} \quad (3.5)$$

Upon substituting, Equation 3.4 becomes

$$\sum_{k=1}^{N_r} \left[f_k(P') + \sum_{j=1}^n \Delta P_j \frac{\partial f_k(P')}{\partial P_j} \right] \frac{\partial f_k(P' + \Delta P)}{\partial P_i} = 0 \quad (3.6)$$

For $i = 1, 2, \dots, n$

$$\frac{\partial f_k(P' + \Delta P)}{\partial P_i} \approx \frac{\partial f_k(P')}{\partial P_i}$$

Rearranging gives

$$\sum_{j=1}^n \sum_{k=1}^{Nr} \frac{\partial f_k}{\partial P_i} \frac{\partial f_k}{\partial P_j} \Delta P_j = - \sum_{k=1}^{Nr} f_k(P') \frac{\partial f_k}{\partial P_i} \quad (3.7)$$

for $i = 1, 2 \dots n$ and where all derivatives are evaluated at P' . Equation 3.7 has the form

$$A \Delta P = b$$

where

$$A_{i,j} = \sum_{k=1}^{Nr} \frac{\partial f_k}{\partial P_i} \frac{\partial f_k}{\partial P_j}, \quad 1 \leq i \leq n, \quad 1 \leq j \leq n$$

And

$$b_i = - \sum_{k=1}^{Nr} f_k(P') \frac{\partial f_k}{\partial P_i}, \quad 1 \leq i \leq n$$

For this study, the measurements to be historically matched are;

- 1) Well test gas rate at particular dates (Q_g^k).
- 2) Well test water rate on the same dates as particular date (Q_w^k). This is optional if water needed to be matched.
- 3) Tank gas flow rate of particular tank from particular PLT survey (q_g^{id}). This is optional if PLT match is to be selected.
- 4) Tank flow water rate of particular tank from particular PLT survey (q_w^{id}). This is optional if PLT and water match are to be selected.
- 5) Pressure (average reservoir pressure) of particular tank on particular PLT survey (p^{id}). This is optional if PLT match is selected.

Matching or model parameter are

- 1) OGIP of particular tank, G_i ,
- 2) Aquifer size of watered-out tank, A_i ,

For example, the matrix A and b can be written as:

$$A_{i,j} = \begin{matrix} & j & = & 1, & 2, & \dots & n \\ \begin{matrix} i \\ = \\ 1 \\ 2 \\ \dots \\ n \end{matrix} & \left(\begin{array}{cccc} \sum_{k=1}^{Nr} \frac{\partial f_k}{\partial P_1} \frac{\partial f_k}{\partial P_1} & \sum_{k=1}^{Nr} \frac{\partial f_k}{\partial P_1} \frac{\partial f_k}{\partial P_2} & \dots & \sum_{k=1}^{Nr} \frac{\partial f_k}{\partial P_1} \frac{\partial f_k}{\partial P_n} \\ \sum_{k=1}^{Nr} \frac{\partial f_k}{\partial P_2} \frac{\partial f_k}{\partial P_1} & \sum_{k=1}^{Nr} \frac{\partial f_k}{\partial P_2} \frac{\partial f_k}{\partial P_2} & \dots & \sum_{k=1}^{Nr} \frac{\partial f_k}{\partial P_2} \frac{\partial f_k}{\partial P_n} \\ \dots & \dots & \dots & \dots \\ \sum_{k=1}^{Nr} \frac{\partial f_k}{\partial P_n} \frac{\partial f_k}{\partial P_1} & \sum_{k=1}^{Nr} \frac{\partial f_k}{\partial P_n} \frac{\partial f_k}{\partial P_2} & \dots & \sum_{k=1}^{Nr} \frac{\partial f_k}{\partial P_n} \frac{\partial f_k}{\partial P_n} \end{array} \right) \end{matrix} \quad (3.9)$$

ศูนย์วิทยทรัพยากร
จุฬาลงกรณ์มหาวิทยาลัย

$$b_i = \begin{bmatrix} -\sum_{k=1}^{N_r} f_k(P^1) \frac{\partial f_k}{\partial P_j} \\ -\sum_{k=1}^{N_r} f_k(P^2) \frac{\partial f_k}{\partial P_j} \\ \cdot \\ \cdot \\ -\sum_{k=1}^{N_r} f_k(P^n) \frac{\partial f_k}{\partial P_j} \end{bmatrix} \quad (3.10)$$

where

P = Matching (model) parameters, total n parameters (G_i, A_i)

N_r = Total number of residual ($Q_g^k, Q_w^k, Q_g^{id}, Q_w^{id}, p^{id}$)

k = Total number of well test point

i = Tank ID

d = sequence order number of PLT survey

The first derivatives are obtained by numerical method, i.e. perturbing the variable P_i once at a time while holding the other variables constant and computing the effect on each residual f_k

$$\frac{\partial f_k}{\partial P_i} = \frac{f(P_{i+1}) - f(P_{i-1})}{2h} \quad (3.11)$$

where

h = 0.00000001

(P_{i+1}) = $P_i \times 1.00000001$

$$(P_{i-1}) = P_i \times (1 - 0.00000001)$$

Steps for Gauss-Newton algorithm are shown in Figure 3.1

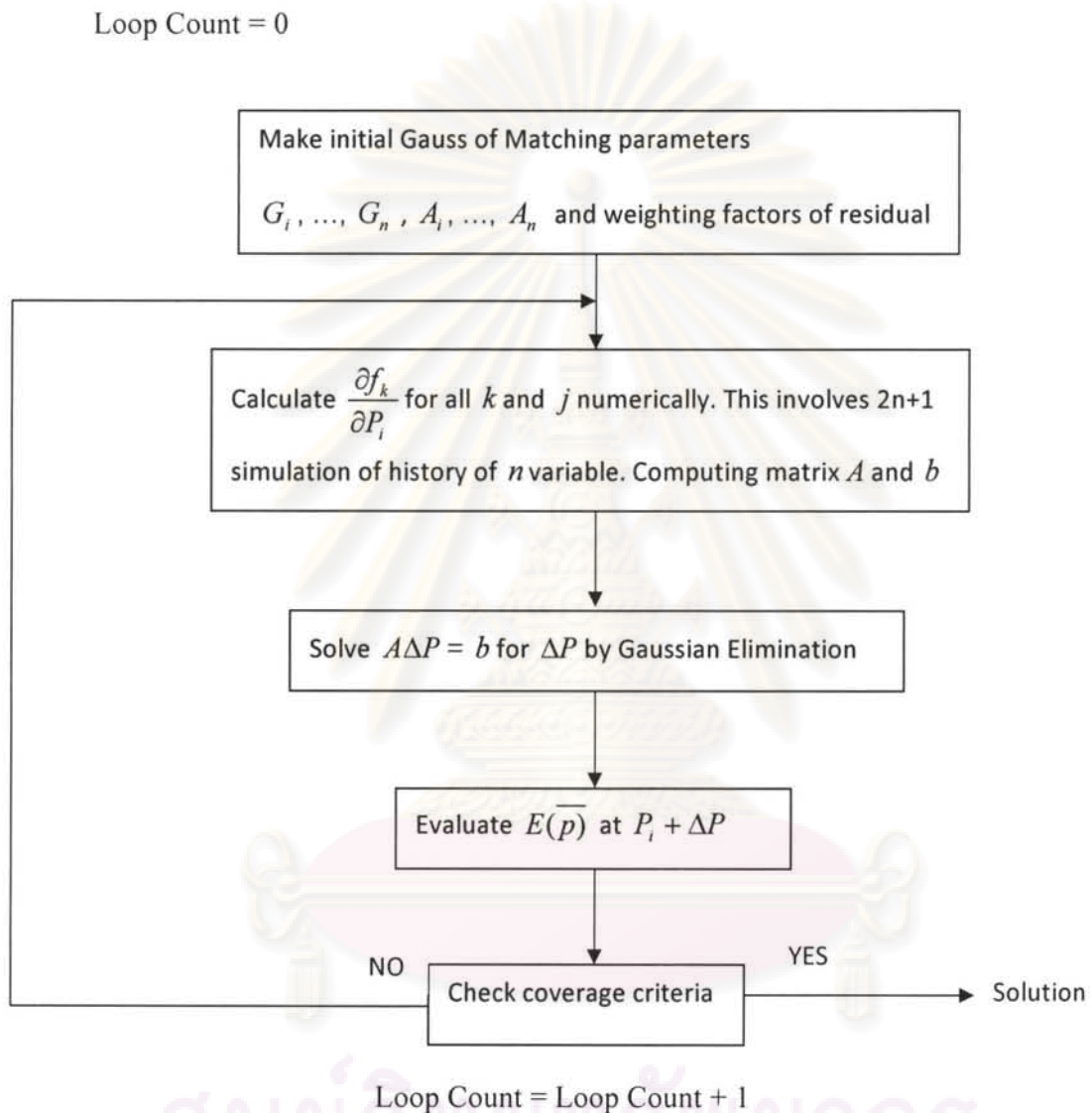


Figure 3.1 Flowchart of Gauss-Newton Algorithm

ศูนย์วิจัยทรัพยากร
จุฬาลงกรณ์มหาวิทยาลัย

Convergence criteria

Three converged criteria are used in automatic history matching algorithm:

- 1) $|E(\bar{p}_k) - E(\bar{p}_{k-1})| \leq 0.005$
- 2) $E(\bar{p}) \leq 0.005$
- 3) $|E(\bar{p}_k) - E(\bar{p}_{k-1})| / E(\bar{p}_{k-1}) \leq 0.001$

3.1.2 Gauss-Newton-Levenberg-Marquardt Method

The Levenburg-Marquardt method is one way to guarantee that $E(p_{k+1}) \geq E(p_k)$, i.e., the objective function of the next iteration is lower than previous iteration. Levenburg- Marquardt (LM) method includes an additional term added to A to avoid singularity:

$$(A + \lambda_m I) \Delta P = b \quad (3.12)$$

where λ_m (lamda) is a coefficient and I is the identity matrix

When $\lambda_m = 0$, the method reduces to Gauss-Newton, and if λ_m tends to infinity, Δp_k turn to so-called steepest descent direction and the size Δp_k tends to zero. Therefore $E(p_{k+1}) \leq E(p_k)$ can always be expected by increasing the value of λ_m . Press *et al.* (1988) have given the procedure for selecting λ_m as follows:

- 1) Complete $E(p_k)$
- 2) Pick a modest value for λ_m , says $\lambda_m = 0.001$
- 3) Solve the linear system of Equation 3.12 to find ΔP_k and calculate $E(p_k + \Delta p_k)$
- 4) If $E(p_k + \Delta p_k) > E(p_k)$, increase λ_m by a factor of 10 and go back to 3)
- 5) If $E(p_k + \Delta p_k) < E(p_k)$, decrease λ_m by a factor of 10, update the trial solution, i.e., replace p_k by $p_k + \Delta p_k$ and go to next iteration

These steps are illustrated in Figure 3.2.

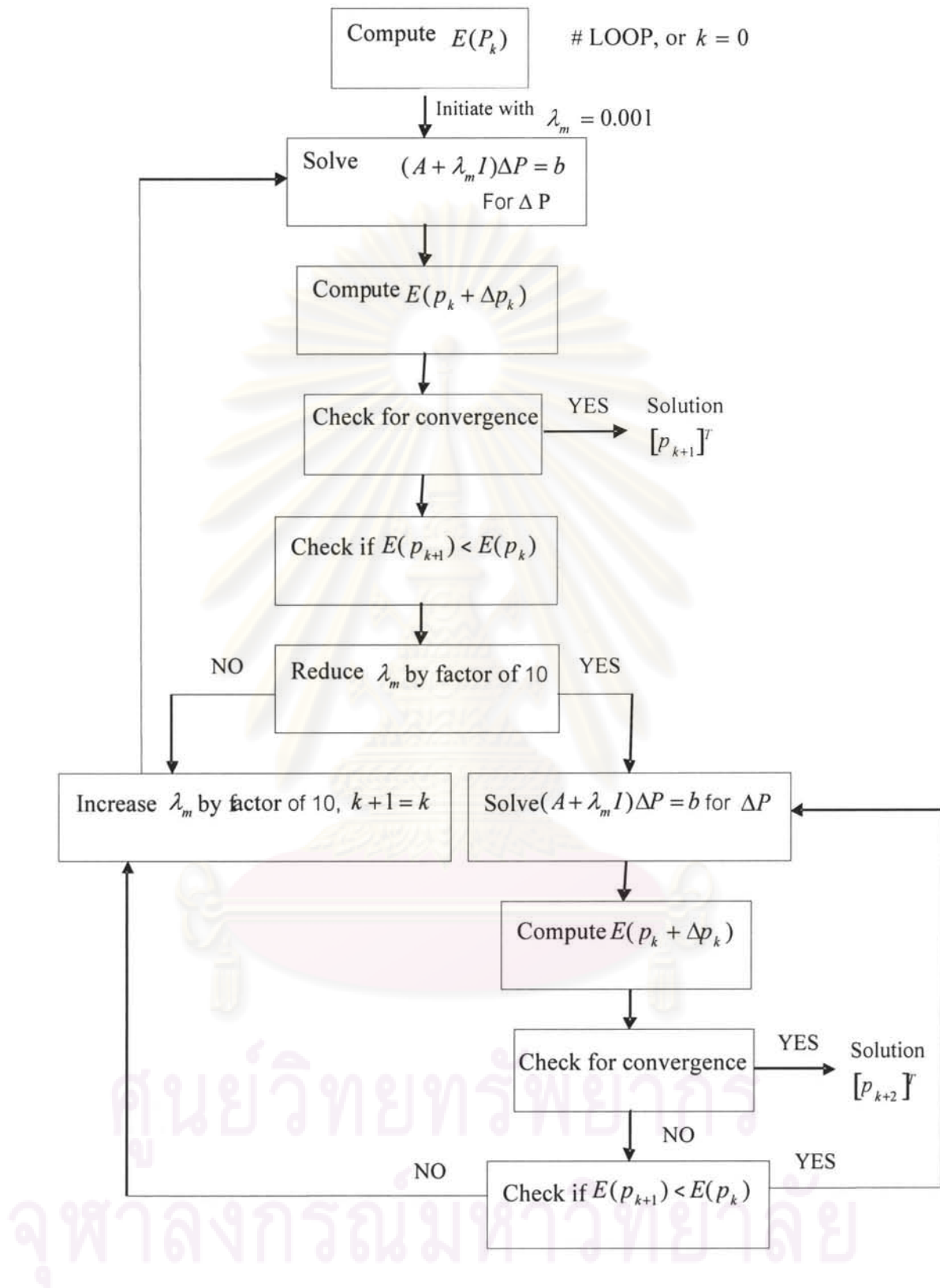


Figure 3.2 Flow chart of Levenberg-Marquardt algorithm

3.2 Theory behind MBAL to build Multi-Tank Model

Calculation of MBAL that models the production of multiple reservoirs through the same wellbore is simple dynamic nodal analysis. Constraints such as manifold pressure (tubing head pressure) or specified flow rate are given to MBAL. MBAL uses VLP curve to calculate the bottomhole pressure. Knowing the bottom pressure, fluid production rate can be calculated with a specified IPR. Depending on saturation of the tank at the current time step, associated fluid can be calculated from fractional flow equation derived from relative permeability curve (function of saturation) and viscosity (function of PVT). Calculated flow rate and specified time step dictate the withdrawal amount of fluid from the reservoir (tank). Material balance equation is used to relate fluid withdrawal, fluid influx, expansion of rock and connate water and calculate the average reservoir pressure at the end of each time step. This new average reservoir pressure is used for updating new IPR of each tank, and the process repeats again to calculate the flow rate from specified constraint of the subsequent time steps. The equation or theory behind MBAL is described in this section.

3.2.1 Gas PVT ^[5]

3.2.1.1 Specific Gas Gravity

$$\gamma_g = \frac{M_w}{28.97} \quad (3.13 \text{ a})$$

Density

$$\rho_g = Z \frac{PM_w}{RT} \quad (3.13 \text{ b})$$

Real gas equation

$$PV = ZnRT \quad (3.14)$$

where

$$M_w = \text{Molecular weight}$$

$$P = \text{Pressure in psi}$$

$$V = \text{Volume in Scf}$$

n	=	mole in lb-mole
R	=	gas constant which is 10.73
T	=	Temperature in degrees Rankin (deg F+460)
Z	=	Gas compressibility factor, dimensionless

3.2.1.2 Pseudo reduced pressure and temperature

Pseudo reduced pressure and temperature correlation by Sutton is good for a range of $-0.57 < \gamma_g < 1.68$

$$P_{pc} = 756.8 - 131.0 \gamma_g - 3.6 \gamma_g^2 \quad (3.15)$$

$$T_{pc} = 169.2 + 349.5 \gamma_g - 74.0 \gamma_g^2 \quad (3.16)$$

3.2.1.3 Z Factor

The Z factor correlation by Dranchuk and Abou-Kassem is good for the range

$$0.2 < P_{pr} < 30$$

$$1.0 < T_{pr} < 30$$

$$Z = 1 + C_1(T_{pr})\rho_r + C_2(T_{pr})\rho_r^2 - C_3(T_{pr})\rho_r^3 + C_4(\rho_r, T_{pr}) \quad (3.17)$$

where

$$\rho_r = 0.27 P_{pr} / Z T_{pr} \quad (3.17 a)$$

$$C_1(T_{pr}) = A_1 + A_2 / T_{pr} + A_3 / T_{pr}^3 + A_4 / T_{pr}^4 + A_5 / T_{pr}^5 \quad (3.17 b)$$

$$C_2(T_{pr}) = A_6 + A_7 / T_{pr} + A_8 / T_{pr}^2 \quad (3.17 c)$$

$$C_3(T_{pr}) = A_9 (A_7 / T_{pr} + A_8 / T_{pr}^2) \quad (3.17 d)$$

$$C_4(\rho_r, T_{pr}) = A_{10} (1 + A_{11} \rho_r^2) (\rho_r^2 / T_{pr}^3) \exp(-A_{11} \rho_r^2) \quad (3.17 e)$$

Constant $A_1 - A_{11}$ are as follows:

$$\begin{array}{lll}
 A_1 = 0.3265 & A_2 = -1.0700 & A_3 = -0.5339 \\
 A_4 = 0.01569 & A_5 = -0.05165 & A_6 = 0.5475 \\
 A_7 = -0.7361 & A_8 = 0.1844 & A_9 = 0.1056 \\
 A_{10} = 0.6134 & A_{11} = 0.7210 &
 \end{array}$$

3.2.1.4 Formation volume factor, B_g

$$B_g = \frac{P_{sc} ZT}{T_{sc} P} \quad (3.18)$$

P_{sc} is 14.7 psia, T_{sc} is 60 deg F

$$B_g = 0.00504 \frac{ZT}{P} \text{ bbl/Scf} \quad (3.18 \text{ a})$$

$$= 0.02829 \frac{ZT}{P} \text{ ft}^3/\text{Scf} \quad (3.18 \text{ b})$$

3.2.1.5 Isothermal compressibility, C_g

$$C = -\frac{1}{V} \frac{dV}{dP} \quad (3.19)$$

$$C_g = \frac{1}{P} - \frac{1}{Z} \frac{dZ}{dP} \quad (3.19 \text{ a})$$

$$C_r = C_g P_{pc} = \frac{1}{P_{pr}} - \frac{1}{Z} \frac{dZ}{dP_{pr}} \quad (3.19 \text{ b})$$

Matter, Bror and Aziz developed an analytical expression for calculating C_r

$$C_r = \frac{1}{P_{pr}} - \frac{0.27}{Z^2 T_{pr}} \left[\frac{(\partial Z / \partial \rho_r) T_{pr}}{1 + (\rho_r / Z)(\partial Z / \partial \rho_r) T_{pr}} \right] \quad (3.19 \text{ c})$$

Taking derivative of equation 3.17, equation of state developed by Dranchuk and Abou-Kassem correlation, we have

$$\left(\frac{\partial Z}{\partial \rho}\right)_{T_{pr}} = C_1(T_{pr}) + 2C_2(T_{pr})\rho_r - 5C_3(T_{pr})\rho_r^4 + \frac{\partial}{\partial \rho_r} [C_4(T_{pr}, \rho_r)] \quad (3.19 d)$$

and

$$\frac{\partial}{\partial \rho_r} (C_4(T_{pr}, \rho_r)) = \frac{2A_{10}\rho_r}{T_{pr}^3} [1 + A_{11}\rho_r^2 + (A_{11}\rho_r^2)^2] \exp(-A_{11}\rho_r^2) \quad (3.19 e)$$

3.2.1.6 Gas viscosity, μ_g

Lee, Gonzalez, and Eakin developed a semi empirical for the following range

$$100 < P(\text{psia}) < 8000$$

$$100 < TC \text{ deg F} < 340$$

$$0.9 < CO_2 \text{ (mole \%)} < 3.2$$

$$\mu_g = (10^{-4}) K \exp(X\rho^Y) \quad (3.20)$$

where

$$\rho = 1.4935(10^{-3}) \frac{PM_w}{ZT} \quad (3.20 a)$$

$$K = \frac{(9.4 + 0.02M_w)T^{1.5}}{(209 + 19M_w + T)} \quad (3.20 b)$$

$$X = 3.5 + \frac{986}{T} + 0.01M_w \quad (3.20 c)$$

$$Y = 2.4 - 0.2X \quad (3.21)$$

Where

$$\rho = \text{gas density, l/cc}$$

$$P = \text{pressure (psia)}$$

T = Temperature (Rankin)

M_w = molecular weight of gas

3.2.2 Gas Material Balance ^{[5][6][7]}

Material balance or tank model is zero dimensions, i.e. no difference in reservoir properties across the given reservoir because it considers properties of any point in reservoir as single average value. Whether material balance can be applied to a hydrocarbon accumulation as a whole depends upon how rapidly any pressure disturbance is equilibrated in the reservoir so that it may be treated as zero dimensional. This, in turn, is dependent on the magnitude of the hydraulic diffusivity constant $k/\phi\mu c$. The larger the value of this parametric group, the more rapidly is pressure equilibrium achieved.

$$G(B_g - B_{gi}) + GB_{gi} \left[\frac{C_w S_{wi} + C_f}{1 - S_{wi}} \right] \Delta \bar{P} + W_e = G_p B_g + B_w W_p \quad (3.22)$$

where

G = initial reservoir gas, or OGIP, Scf

B_g = Gas formation volume factor, bbl/Scf

B_{gi} = Initial gas formation volume factor, bbl/Scf

C_w = Water isothermal compressibility, psi^{-1}

S_{wi} = Initial or connate water saturation

C_f = Formation isothermal compressibility, psi^{-1}

$\Delta \bar{P}$ = Change in average reservoir pressure, psia

W_e = Water influx into reservoir, bbl

G_p = Cumulative gas production, Scf

B_w = Water formation volume factor, bbl/STB

W_p = Cumulative produced water, STB

Initial standard cubic feet of gas in place by the volumetric method expressed as:

$$G = \frac{43,560(\phi)(1 - S_{wi})}{B_{gi}} \quad \text{Scf/Acre-ft} \quad (3.23)$$

$$\text{Connate water volume} = 43,560(\phi)(S_w) \quad \text{ft}^3/\text{Acre-ft} \quad (3.23 \text{ a})$$

$$\text{Reservoir gas volume} = 43,560(\phi)(1 - S_w) \quad \text{ft}^3/\text{Acre-ft} \quad (3.23 \text{ b})$$

$$\text{Reservoir pore volume} = 43,560(\phi) \quad \text{ft}^3/\text{Acre-ft} \quad (3.23 \text{ c})$$

After the reservoir is flooded by influx water

$$\text{Water volume} = 43,560(\phi)(1 - S_{gr}) \quad \text{ft}^3/\text{Acre-ft} \quad (3.23 \text{ d})$$

$$\text{Reservoir gas volume} = 43,560(\phi)(S_{gr}) \quad \text{ft}^3/\text{Acre-ft} \quad (3.23 \text{ e})$$

S_{gr} is residual gas saturation which is immovable gas portion which is trapped after infused water invades the gas reservoir. Water will move into the pores of gas saturated rock by imbibitions (due to capillary forces) and displacement (due to viscous force). These mechanisms are sometimes referred to as spontaneous imbibition and forced imbibitions, or imbibitions displacement and dynamic displacement. As water moves into the reservoir, some of the gas becomes trapped behind the water due to capillary forces and residual gas saturation being developed.

S_{gr} can be measured in the laboratory on representative core samples.

Table 3.3 in Reference 5, page 80 gives residual gas saturations that were measured on core samples from a number of producing horizons and on the same synthetic laboratory samples. The values range from 16 to 50% and average near 30%. When there are well-defined continuous beds of higher and lower permeability, the water advances more rapidly through the more permeable beds so that when a gas is abandoned, owing to excessive water production, considerable unrecovered gas remains in the less permeable beds.

Correlation of S_{gr} was founded to decrease with increasing porosity. Agawal^[14] also recommended that S_{gr} is about 50% of the initial saturation (S_{gi})

Equation 3.23 can be rearranged as

$$F = G(E_g + E_{fw}) + W_e B_w \quad (3.24)$$

$$\begin{aligned} F &= G_p B_g + W_p B_w \\ &= \text{Total gas and water production (rcf)} \end{aligned} \quad (3.24 \text{ a})$$

$$\begin{aligned} E_g &= B_g + B_{gi} \\ &= \text{underground gas expansion (rcf/Scf)} \end{aligned} \quad (3.24 \text{ b})$$

$$\begin{aligned} E_{fw} &= \frac{B_{gi}(C_w S_{wc} + C_f)}{1 - S_{wc}} \Delta P \\ &= \text{expansion of connate water and reduction of pore space} \end{aligned} \quad (3.24 \text{ c})$$

For normal pressure reservoirs and practical case, $E_{fw} \leq E_g$. Therefore, Equation 3.24 reduces to

$$F = GE_g + W_e B_w \quad (3.24 \text{ d})$$

When dividing both sides by E_g , we have

$$\frac{F}{E_g} = G + \frac{W_e B_w}{E_g} \quad (3.24 \text{ e})$$

The equation is similar to Cole plot^[7], which is used to detect drive mechanism of gas reservoirs. Plotting $\frac{F}{E_g}$ or $\frac{G_p B_g}{E_g}$ (Cole plot) vs. G_p can give the idea of the strength of aquifer which reflects on the slope of the plot as shown in figure 3.3

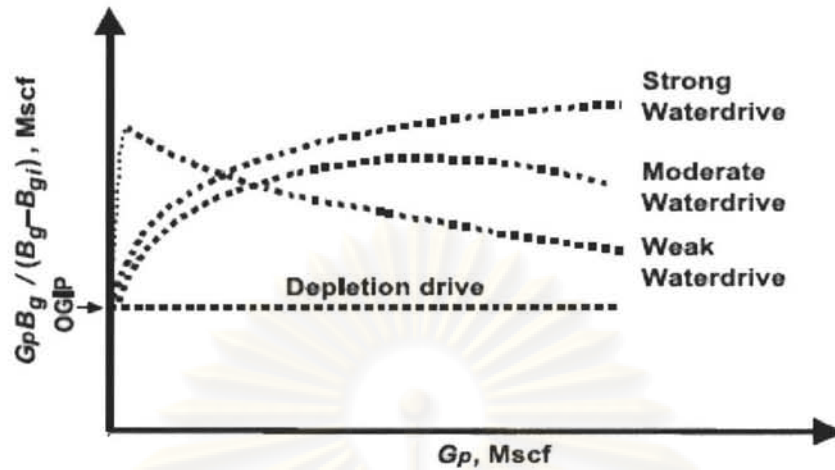


Figure 3.3 Cole plot to detect addition drive energy in gas reservoir

$$\text{Pore volume (PV)} = GB_{gi} \left(\frac{1}{1 - S_{wc}} \right) \quad (3.24 f)$$

$$\text{Hydrocarbon pore volume (HCPV)} = GB_{gi} \quad (3.24 g)$$

$$\text{Movable gas volume (MGV)} = GB_{gi} \left(\frac{1 - S_{gr} - S_{wc}}{1 - S_{wc}} \right) \quad (3.24 h)$$

When water influxes into the reservoir, $W_e B_w$ invades gas reservoir, the volumetric sweep is

$$\alpha = \frac{W_e B_w}{GB_{gi}} \left(\frac{1 - S_{gr} - S_{wc}}{1 - S_{wc}} \right) \quad (3.24 i)$$

The volume of gas that was trapped behind the water front can be expressed at standard condition as

$$\frac{\alpha(PV)S_{gr}}{B_g} = \alpha G \frac{S_{gr}}{1 - S_{wc}} \frac{B_{gi}}{B_g} = \alpha \frac{GS_{gr}}{1 - S_{wc}} \frac{P/Z}{P_i/Z_i} \quad (3.24 j)$$

The material balance at abandonment can be written as:

$$\text{Production at abandonment} = \text{OGIP} - \text{Trapped residual gas} - \text{By passed gas}$$

$$G_p = G - \left[\alpha G B_{gi} \frac{S_{gr}}{1 - S_{wc}} + (1 - \alpha) G B_{gi} \right] \frac{1}{B_{gabd}} \quad (3.24 \text{ k})$$

To express Equation 3.24 k in term of P/Z , we can write it as

$$\frac{P}{Z_{ab}} = \frac{P_i}{Z_i} \frac{(1 - \frac{G_p}{G})}{\alpha (\frac{S_{gr}}{1 - S_{wc}} + \frac{1 - \alpha}{\alpha})} \quad (3.24 \text{ l})$$

Recovery efficiency (RE) is described by dividing Equation 3.24 k by G as follows:

$$RE = \alpha \left(1 - \frac{(P/Z)_{abd} S_{gr}}{(P/Z)_i S_{gi}} \right) + (1 - \alpha) \left(1 - \frac{(P/Z)_{abd}}{(P/Z)_i} \right) \quad (3.24 \text{ m})$$

Or

$$RE = \alpha \left(1 - \frac{S_{gr} / B_{gabd}}{S_{gi} / B_{gi}} \right) + (1 - \alpha) \left(1 - \frac{B_{gi}}{B_{gabd}} \right) \quad (3.24 \text{ n})$$

3.2.3 Water influx model^[7]

If the aquifer is relatively small and in good communication with the hydrocarbon reservoir, and permeability is sufficiently high, the aquifer can be represented with the pot aquifer model which is described as

$$W_e = (C_w + C_f) W (P_i - P) \quad (3.25)$$

where

W = Aquifer original water in Place (OWIP), res bbl

P_i = Initial aquifer or reservoir pressure

P = Current aquifer pressure assumed to be same as reservoir pressure

^[8]The equation is simply a re-statement of basic definition of compressibility and only applicable to very small aquifers. For large aquifers, a mathematical model which includes time dependence to respond fully to pressure change in the reservoir is

required. For the pot aquifer model, any drop in reservoir pressure is instantaneously transmitted throughout the entire aquifer.

3.2.4 Inflow Performance Relationship (IPR) of Each Individual Layer

IPR of each layer is calculated from the data of multirate PLT. Multirate PLT is conducted by taking PLT survey during normally three stabilized flow rates by changing the choke size with additional shut in survey. Conventional PLT which takes one survey on normal flowing condition with shut-in survey can be used with lesser confidence in model accuracy because only two points were used for IPR fitting.

From PLT survey, P_{wf} vs. Q_g and perhaps Q_w (if any) will be acquired after choosing best fitted model to these points. Interception on the y-axis (P_{wf}) is the average reservoir pressure which is another data point for history matching.

Steady state inflow equation for gas can be written as

$$m(\bar{p}) - m(p_{wf}) = \frac{1422Tq}{kh} \left(\ln \frac{r_e}{r_w} - \frac{1}{2} + S \right) + Fq^2 \quad (3.26)$$

where

$m(\bar{p})$ = Pseudo average reservoir pressure, psi²/cp

$m(p_{wf})$ = Pseudo wellbore pressure, psi²/cp

T = Temperature, Rankin

q = Gas flow rate, Scf per day

k = Permeability, mD

h = Formation thickness

r_e = Reservoir radius, ft

r_w = Wellbore radius, ft

S = Skin factor, dimensionless

F = Non-Darcy coefficient,

The pseudo pressure is defined as

$$m(p) - m(p_w) = \int_{p_w}^p \frac{1}{\mu B_g} dP \quad (3.27)$$

In practical, these parameters are unknown; therefore, from data points of IPR for each layer from PLT, we can use deliverability equation to describe IPR of each layer.

1) Back pressure : C and n

where

$$q = C(\bar{P}_r^2 - P_{wf}^2)^n$$

q = Gas flow rate, MMscf/D

\bar{P}_r = Average reservoir pressure, psi

P_{wf} = Wellbore pressure at sand face, psi

C = performance coefficient, Mscf/day/psi²

n = an exponent which varies between 1 for laminar flow and 0.5 for completely turbulent flow.

Normally, C and n can be determined from a plot of Q vs. $(\bar{P}_r^2 - P_{wf}^2)$ on log-log scale.

We assume C and n are constant in the model, but actually C will change with the pressure and flow rate. The viscosity (μ) and gas deviation factor (Z) are pressure dependent. The rate dependent skin factor will vary with flow rate. The effect of variations in these terms on the value of C must be considered for accurate long range prediction of q .

2) Forchheimer equation

$$(\bar{P}_r^2 - P_{wf}^2) = Aq_g + Bq_g^2 \quad (3.29)$$

where

A = Laminar pressure drop coefficient, $\text{psi}^2/(\text{Mscf}/\text{day})$

B = turbulent pressure drop coefficient, $\text{psi}^2/(\text{Mscf}/\text{day})^2$

The pseudo pressure may be used instead of pressure square yielding an equation which is similar to Equation 3.29

$$m(\bar{P}_r) - m(P_{wf}) = Aq_g + Bq_g^2$$

A practical solution to obtain the parameters A and B from this equation is to plot

$(\bar{P}_r^2 - P_{wf}^2)/q_g$ or $m(\bar{P}_r) - m(P_{wf})/q_g$ vs. q_g on a linear scale. The result is a straight line with intercept A and slope B.

3.2.5 Relative Permeability

In order to determine relative permeability of water displacing gas^[9], steady state technologies must be used to generate full-curve data. Water and gas are injected simultaneously into the core sample at incremental water-gas ratio. As the system reaches pressure equilibrium (indicating steady-state flow) at each incremental ratio, relative permeability both water and gas are measured and the increase in S_w determined. Several such measurements are made to generate decreasing relative permeability to gas and increasing relative permeability to water curve versus increasing water saturation.

Many correlations are available in the literature:

Wyllie

$$K_{rw} = (S^*)^4 \quad (3.30 \text{ a})$$

$$K_{rg} = (1 - S^*)^2 (1 - S^*)^2 \quad (3.30 \text{ b})$$

Boatman

$$K_{rw} = (S^*)^{1.5} (S_w)^3 \quad (3.30 \text{ c})$$

$$K_{rg} = (1 - S^*)^2 (1 - S^{*0.25} (S_w^{0.5}))^{0.5} \quad (3.30 d)$$

For both cases,

$$S^* = \frac{S_w - S_{wi}}{1 - S_{wi} - S_{gr}} \quad (3.30 e)$$

Boatman correlation gives water end points equal to 1; Willie correlation gives water end point to a much lower value. Both correlations give gas end point equal to 1.

Corey function can be used to represent data from each correlation for easier data entry

Corey function

$$K_{rx} = E_x \left(\frac{S_x - S_{rx}}{S_{mx} - S_{rx}} \right)^{nx} \quad (3.30 f)$$

where

E_x = end point of phase x

S_x = Phase saturation

S_{rx} = Phase residual saturation

S_{mx} = Phase maximum saturation

nx = Corey exponent

MBAL calculates phase production from IPR and fraction flow which corresponds to average tank saturation at particular time step.

$$F_x = \frac{Q_x B_x}{Q_x B_x + Q_y B_y} \quad (3.30 g)$$

where

F_x = Fractional flow of phase x

Q_x = Flow rate phase x at surface

B_x = Formation volume factor of phase x

Q_y = Formation volume factor of phase y

B_y = Formation volume factor of phase y

$$F_x = \frac{\frac{K_{rx}}{\mu_x}}{\frac{K_{rx}}{\mu_x} + \frac{K_{ry}}{\mu_y}} \quad (3.30 \text{ h})$$

where

K_{rx} = Relative permeability of phase x

K_{ry} = Relative permeability of phase y

μ_x = Viscosity of phase x

μ_y = Viscosity of phase y

3.2.6 Vertical Lift Performance (VLP)

Vertical lift performance correlation describes various methods of calculating pressure losses in inclined pipes. While the basic form of the pressure loss equation is the same for all correlations, the treatment of multi phase friction and gas/liquid slip (hold up) varies considerably. VLP is generated from the combination of various pressure traverse curve of corresponding required flow rate.

The calculation of pressure traverse curve comes from calculation of multi phase pressure drop from bottom hole tubing intake to surface end node.

The general pressure gradient equation is

$$\frac{dP}{dL} = \frac{g}{g_c} \rho_s \sin \theta + \frac{f \rho_f V_m^2}{2 g_{cd}} + \frac{\rho V_m dV_m}{g_c dL} \quad (3.31)$$

(ΔP Elevation)
(ΔP Friction)
(ΔP Acceleration)

The pressure drop caused by elevation change depends on the density of two-phase mixture and usually calculated using a liquid hold-up value. Except for conditions of high velocity, most of the pressure drop in vertical flow is caused by this component. The pressure drop caused by friction losses required evaluation of a two-phase friction factor. The pressure drop caused by accelerating the fluid is sometime considered negligible and usually calculated only for cases of high flow velocities.

Many correlations have been developed for predicting two-phase flowing pressure gradient. These correlations give liquid hold-up, friction factor by dividing flow condition into patterns or regimes. Each flow regime has corresponding correlation for its specific condition.

Various VLP correlations were captured from specific data sets of lab and field data. They can therefore be expected to perform best for field conditions that fell in the range of the captured lab or field conditions. There is no universal rule for selecting best VLP correlation for a given well. By calculating pressure gradient traverses using different correlations, the range of estimate pressures can be assumed. We select a VLP correlation on the basis of flow regime and closeness of fit to the measured pressure.

3.3 Multi-Layer (feed-forward) Neural Net

^[10] Multi-layer neural network is the most well known and popular neural network. Figure 3.4 shows a general architecture of a multi-layer feed-forward neural network.

Basically, a neural network consists of an input layer, one or multiple hidden layers, and an output layer. The units in the hidden later plays key role in the internal representation of the input patterns.

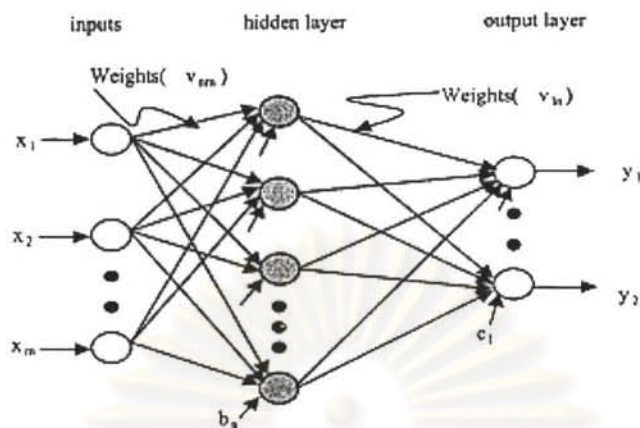


Figure 3.4 Multi-layer back-propagation Neural Network diagram

The input-output flow of the network model is determined by the strength of the connection and operation function of the neurons. The operation of a single neuron consists of a weighted sum of the incoming signals and a bias term feed through our activation function $f(\cdot)$ resulting in the output value of neuron. This is shown mathematically as

$$y_i = f\left(\sum_{r=1}^n W_{ir} \cdot f\left(\sum_{j=1}^m V_{rj} - \mu_j + b_r\right) + C_i\right) \quad i = 1, \dots, l \quad (3.32)$$

where

y = l output, vector

μ = m input, vector

n = Number of neurons in the hidden layer

v and w = Weight factor

b_r and c_i = Bias values of the neuron in the hidden and in the output layer

$f(\cdot)$ = Activation function, normally sigmoid function

The knowledge to map input patterns into appropriate classification is given by the strength of the weights. The process of finding a suitable set of weight is called training.

The rationale of most of the learning algorithms is based on search directions according to an objective function's derivative information and this is what the parameter learning of the neural networks is all about. The most common methods are the steepest descent method and Newton's method, as well as some modifications such as Gauss-Newton method (e.g. Levenburg-Marquardt). The steepest descent methods use the second derivatives of the cost function.

3.3.1 Back- Propagation learning algorithm

Back-propagation learning algorithm is the classical least mean squares algorithm, which modifies the network weights using gradient descent search in the weight space to minimize the mean squares error between the desired and actual output of the network. It is the simple steepest descent method. The back-propagation algorithm could also modify the weights in all of the intermediate layers (hidden layers) of any multilayer feed forward neural network.

Back-propagation uses supervised learning rules. By doing so, the network is trained using data for which the input and output are known. Once the training is completed, the network weights are frozen, and the network model can be used to compute output values for unseen data (fresh data set). The drawback of the back-propagation algorithm is its slowness by need of a considerable number of iterations to train a network. It can also be easily trapped in local minimum and thus learning procedure can fail to solve the problem, despite the network configuration (i.e. number of hidden layers and neurons). One way to overcome is to introduce a momentum term in the learning rule. This procedure is based mainly on heuristics and lacks a theoretical support. Therefore, result is not always guaranteed.

Two steps for application of back-propagation are

1) Input vector is presented to the network and propagated forwards through the hidden layer(s) to the output layer. Then, the desired output and the calculated output are compared to each other, and the error signal is calculated.

2) The error is propagated backwards through the network to each hidden layer(s)

The process is repeated for every layer until the input layer is reached.

3.3.2 Cost or Objective Function ^[11]

Most popular cost or objective function is the sum of square error (SSE)

$$SSE = \sum_{record} \sum_{outputnode} (actual - output)^2 \quad (3.33)$$

It is analogous to the residuals in regression. The weights are to be determined to minimize SSE. In EasyNN software which is the software used in this study, the error is normalized. Individual (not summed) and average error of the network is recorded (dividing by number of record).

3.3.3 Activation Function

The most common activation function is the sigmoid function

$$y = \frac{1}{1 + e^{-x}} \quad (3.34)$$

This function combines nearly linear behavior, curvilinear behavior and nearly constant behavior depending on the value of the input.

Much of center of the domain of input x (i.e. $-1 < x < 1$), $f(x)$ is nearly linear. As it moves away from the center, $f(x)$ becomes curvilinear. When the input reaches extreme values, $f(x)$ becomes nearly constant.

3.3.4 Gradient Descent Method

A prevalent optimization algorithm during the learning step to find vector of (weight) $W = W_0, W_1, \dots, W_m$ that minimizes SSE employs a gradient-descent method to find direction of the adjustment.

$$W_{new} = W_{current} + \Delta W_{current}$$

The gradient of SSE with respect to the vector of weights W is the vector derivative.

$$\nabla SSE(w) = \left[\frac{\partial SSE}{\partial W_0}, \frac{\partial SSE}{\partial W_1}, \dots, \frac{\partial SSE}{\partial W_m} \right] \quad (3.35)$$

The direction of adjusting $W_{current}$ is $\frac{\partial SSE}{\partial W_{current}}$

$$\eta = \text{learning rate, range 0 to 1}$$

η is adjustment to derivatives

$$\Delta W_{current} = -\eta(\partial SSE / \partial W_{current}) \quad (3.36)$$

3.3.5 Input and Output Encoding

All attribute values must be encoded in a standardized manner, taking value between 0 and 1. Min – Max normalization is applied as follows:

$$X^* = \frac{X - \text{Min}(X)}{\text{Range}(X)} = \frac{X - \text{Min}(X)}{\text{Max}(X) - \text{Min}(X)} \quad (3.37)$$

3.3.6 Back-Propagation Rules

$$W_{ijnew} = W_{ijcurrent} + \Delta W_{ij}$$

where

$$\Delta W_{ij} = \eta \partial_j X_{ij}$$

∂_j = “responsibility” for particular error or node j

∂_j = Output j (1- Output j)(actual j - Output j) for an output layer nodes

OR = Output j (1- Output j) $\sum_{downstream} W_{jk} \partial_j$ for hidden layer nodes

(3.38)

3.3.7 Termination Criteria

One can set termination based on threshold limit of SSE or number of iterations which is directly resulted from training time willing to spent on training operation. However, too low SSE causes the network to be over fitting, memorizing the pattern in the training set instead of retaining generalization ability to unseen data.

Therefore, most networks adopt the following cross validation termination procedure:

- 1) Retain part of data for validity
- 2) Proceed to train the remaining data
- 3) Apply weight learn to validating data
- 4) Monitor two sets of weights, one “current” set of weights produced by the training data, and one “best” set of weights as measured by the lowest SSE so far on the validating data.
- 5) When the current set of weights has significant greater SSE than best set of weights, then terminate the algorithm.

3.3.8 Learning Rate η

If the learning rate is small, weight adjustment will be small. It will take a long time (more iteration) to converge. If it is too large, it may overshoot when the solution is near optimal. One solution is to change the value of η as training move forward.

Therefore, it may start with relatively large value and when the network is near optimum SSE, it should be reduced to avoid overshooting.

3.3.9 Momentum

$$\Delta W_{current} = -\eta(\partial SSE / \partial W_{current}) + \alpha \Delta W_{previous} \quad (3.39)$$

where

$$\Delta W_{previous} = \text{Previous weight adjustment}$$

$$\alpha = \text{momentum, } 0 \leq \alpha < 1$$

$\alpha \Delta W_{previous}$ represents a fraction of previous weight adjustment for a given weight.

The momentum represents inertia which influences current weight adjustment to the same direction of previous adjustment.

The momentum, α , will help dampen the oscillations around the optimum point. It will, in the initial stage, increase the rate at which the weight approaches the neighborhood of optimum. The momentum is helpful when $\partial SSE / \partial W_i$ is flat. If α is too large, it will overshoot the optimum. It can help avoid being stuck at local minimum but it can also shoot global minimum to other local minimum. The parameters η and α need to be experimented for the best result.

Global minimum can also be determined by trial of W_i with fair value of different initial weights which are set randomly with certain network configuration.

3.3.10 Number of Hidden Layers and Nodes in the Network

The number of nodes needs to be less than a certain limit so that the total number of connection are less than training samples to provide sufficient degree of freedom.

If the number is too big, it will be overfitted. Baum & Haussler^[10] proposed the following relation to determine the number of training sample on the basis of the desired accuracy on the set.

$$P > \frac{|W|}{(1-a)} \quad (3.40)$$

where

P = Number of Samples

$|W|$ = Number of Weight to be trained

a = Accuracy on the test (if test accuracy =95%, $a=0.95$)

We can see that if we want high test accuracy, we need higher number of samples relative to number of weights.

3.3.11 Measured Result of Testing Data Set

After getting the best network, a dedicated set of testing data is used to test the parameters of the network. Input variables are fed into the network, and the output is compared with actual value. The correlation coefficient of the predicted output and the actual value can be computed using the following equation.

$$r = \frac{\sum(X - \bar{X})(Y - \bar{Y})}{\sqrt{\sum(X - \bar{X})^2 \sum(Y - \bar{Y})^2}} \quad (3.41)$$

If $r^2 = 1$, it means $X = Y$.

ศูนย์วิทยทรัพยากร
จุฬาลงกรณ์มหาวิทยาลัย

CHAPTER IV

WORK FLOW METHODOLOGY

4.1 Determination of Individual OGIP and Aquifer Size in Multi-tank Commingled Model

4.1.1 Software for Building and Study Multi-tank Commingled Model with and without Water Production

The model is built with software, namely Integrated Production Model (IPM) from Petroleum Experts Limited (PetEx). This software suite is composed of three major components, i.e., GAP, MBAL and PROSPER. GAP (General Allocation Package) is the software that can solve and optimize network of production and injection systems that are connected via common manifolds and pipelines to a fixed system pressure called separator in GAP. It can be used to build multi-tank commingled model by connecting the network of reservoir models from MBAL and well bore model above the top most tank by sets of vertical lift performance curve (VLP) generated from Prosper. The pressure drop between tanks is modeled with a multi-phase correlation available in GAP. It is also capable of modeling surface network of various equipments in the topside area. Prediction function can be used to simulate production profile and history match the production data to determine the unknown reservoir parameters.

The program has the optimizer function that can be used for maximizing production by optimizing choke size, allocating gas lift rate, determining ESP operating frequency while honoring constraints at the gathering system, well and reservoir level

MBAL is a package made up of various tools designed to help the engineer to gain a better understanding of reservoir behavior and perform prediction run. Various tools are available in MBAL but the only tool used in this work from MBAL is Material Balance. Material balance is a reservoir modeling tool using classical material balance calculation as discussed in section 3.2.2, Chapter 3. It can be used for history matching by graphical methods (like Havlena-Odeh, Cole, etc.) and predictions in association with relative permeabilities to predict the amount of the associated phase

productions with or without well models. In this study, MBAL was used to built multi-tank commingled production with well model from the wellhead down to the top most producing reservoir by VLP curve generated from Prosper. Prediction function was used to generate production profile to history match the production data in the same manner as GAP is used to determine unknown parameters.

Prosper is the Production and Systems Performance analysis software. Prosper can be used for predicting tubing and pipeline hydraulics and temperatures. The tool can be used for modeling reservoir inflow performance (IPR) for single, multilayer, multilateral wells with complex and highly deviated completions. The multiphase flow correlations implemented can be adjusted to match measured field data to generate vertical lift performance curve (VLP) to be used in GAP and MBAL which is the main utilization of Prosper in this study.

Openserver feature is designed to provide open architecture for PetEx products. This allows PetEx programs to be directly access and driven by other programs (such as Excel, or program written with Visual Basic) via PetEx public function. These can then be accessed by an external program in an automated procedure.

Both MBAL and GAP are capable of modelling commingled production from multiple reservoirs but each has its own flaws. Below are the discussion on Pros and Cons of both softwares.

MBAL

Pro

- Easier to use - The only requirement is VLP (Vertical Lift Performance) generated from Prosper. Other than that, the system can stand alone.
- Ability to incorporate aquifer effect to material balance calculation
- Well can be modeled using VLP generated from Prosper.
- Water production can be simulated from fractional flow which relates water production to average water saturation in the tank. The fractional flow curve is obtained from relative permeability which corresponds to saturation change due to water influx. Water production can be simulated throughout production history if relative permeability and IPR data are available.

- Can model effect of cross flow between layers whenever the BHP is higher than the average reservoir pressure. Nevertheless, this might not be an accurate model since cross flow needs transient solution.
- Fast run time.

Cons

- Does not include calculation function to calculate pressure drop between tanks. All tanks are assumed to be at the same datum level. Nonetheless, there is a function to apply dP shift to include a negative ΔP to account for the pressure drop for the deeper tanks. However, this pressure drop is not constant and can change if there is a different rate and fluid hold up in the wellbore.
- Does not have regression calculation to automatically history match the total production when using multi-tank model to determine OGIP and aquifer properties.

GAP

Pro

- There is a function to calculate pressure drop between sands having different datum. Sometimes cross flow can be modeled unless the BHP is higher than the average reservoir pressure of all tanks, such as during a shut-in period. In this case, GAP will show result as if there is injection from the surface to all reservoirs.
- There is an optimizer function to optimize an objective function chosen by the user.

Con

- Need VLP from Prosper and reservoir material balance model from MBAL. It requires more steps; therefore, it is more complicated and difficult to set up the model.
- Result in wrong answer when the simulating well is shut in and, in some scenarios, when cross flow between layers cannot be modeled correctly.
- Slow run time.

Even though MBAL does not have the feature to model pressure drop between the layers, it can model cross flow between layers. Despite this, cross flow might not be perfectly modeled because MBAL uses steady state solution while cross flow is actually a transient problem.

Since GAP has features to calculate pressure drop between sands but cannot handle cross flow between sands during shut in, we cannot use it to a build model and perform history matching of actual wells. Most of the wells operated in the GOT need to be shut in for several reasons, especially good producing wells which are used as swing wells. These wells are main candidate for building multi-tank model for individual tank OGIP. Material balance will never be correct since there will be cross flow from high pressure sands to low pressure sands in a commingled system as long as the pressure is not equalized. MBAL must be used for the reason that it can model cross flow among sands during shut in even though it does not model pressure drop between sands. Please read further in Appendix A for details of this particular problem.

Therefore, in this study, multi-tank model is built with MBAL and history matching is preferred by an automatic history matching spreadsheet. Procedures on how to built and run MBAL commingled multi-tank model and how to use automatic history matching spreadsheet are given in Appendix B as well as program code of macro of automatic history matching spreadsheet. A typical 2 7/8" monobore tubing completion was used in all cases. PROSPER was used to create VLP curves with PetEx 2 correlation. This VLP curves were imported to MBAL to represent well pressure drop model. The procedure to set multi-tank commingled model with MBAL can be found in Appendix B.

Regarding to the aquifer, a steady state pot aquifer model which is available in MBAL is selected since its assumption does not violate the geological setting of the reservoirs in the area of this study (small compartment and relatively high permeability for water producing sands). The model is easy to use and only requires aquifer volume as the input. If the other water influx models are to be used, there is no way to prove its validity due to lack of individual tank data for Havlena-Odeh plot which is used for identifying correctness of each aquifer model. There is also no geological and geometry data of the aquifer to prove its validation. Above all, we are not really

interested in obtaining the correct aquifer size but only need the aquifer model which can match pressure and water production rate of the water producing sand(s).

Relative permeability data are subject to uncertainty. There is no experimental core test to identify actual relative permeability from the area in this study. Due to this reason, correlation described in Section 3.2.5 is used in this study.

The first two cases examine the effect of water in commingled system and the effect of model with and without pressure drop between sands (difference between models built with MBAL and GAP).

Case 1: simulation of two-tank commingled model with different aquifer sizes compared with all-volumetric drive system to investigate the effect of water on production in a commingled system. This case is subdivided into 2 cases to compare the effect of different aquifer sizes to volumetric drive.

Case 1.1: Comparison of all volumetric drive system vs. 25 MMRB pot aquifer on water drive tank

Case 1.2: Comparison of all volumetric drive system vs. 50 MMRB pot aquifer on water drive tank

Case 2: simulation of two-tank systems with and without aquifer by the model that considers the pressure drop between tanks (GAP) compared with the model that does not consider the pressure drop between tanks (MBAL).

4.1.2 Program Coding for Automatic History Matching Routine and its Application

Nonlinear regression optimization algorithm as described in Section 3.1 is used to build an automatic history matching routine to be utilized with the commingled model built with the selected IPM software. Nonlinear regression optimization routine is written in VBA in Excel as it is easy to enter input and display the result. The objective of non-linear regression optimizing routine is to assist engineers by automating the history matching process which is the major time consuming portion of the multi-tank commingled model construction to get best possible match with the least residual. The calculation in the algorithm is done by Excel VBA which sends

the matching parameters to and receive residual values from Petex software via Openserver until the convergence criteria are met. The flow chart of this architecture is Figure 4.1.

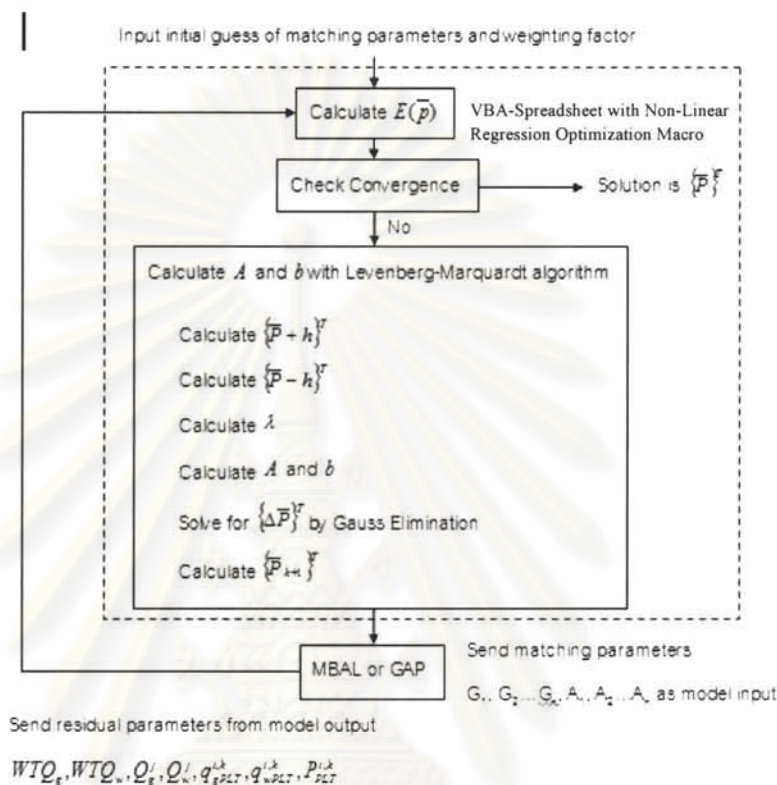


Figure 4.1 Flow chart of data communication and calculation between IPM and automatic history matching spreadsheet

Levenberg-Marquardt algorithm and other necessary Visual Basic procedures for data communication with Petex software as well as data interface/display for automatic/semi automatic (manual) history matching are written in VBA language for macro operation in Excel spreadsheet. The detail of this VBA code is in Appendix C.

Automatic history matching spreadsheet coupled with multi-tank model is tested with simulated and actual field data with the following cases:

Case 3: Investigation of automatic history matching spreadsheet on a two-tank commingled model with water drive on one tank. The simulated data of the two-tank commingled model with aquifer drive on one tank without pressure drop between the tanks is generated, then the following models are used to history match the data:

Case 3.1: Use a two-tank commingled model with volumetric drive on both tank to history match data in Case 1 before water breakthrough.

Case 3.2: Use a two-tank commingled model with one aquifer model on the tank which has water breakthrough to history match data in Case 1 after the breakthrough (at the time we know which tank has an aquifer).

Case 4: Investigate the effect of using a model which does not take into the account of pressure drop between tanks to history match data generated by the model which has the pressure drop between the tanks.

Case 4.1: Simulated data of a two-tank commingled model which considers the pressure drop between the tanks. Both tanks are volumetric drive. Then, we use a two-tank commingled model without the pressure drop between the tanks, both with depletion drive to history match respective data.

Case 4.2: Simulated data of a two-tank commingled model which considers the pressure drop between the tanks. The upper tank is volumetric drive, and the bottom one is water drive. Then, we use a two-tank commingled model without the pressure drop between the sands, one tank is depletion drive and the other is water drive to history match respective data.

Case 5: Investigation of the capability of automatic history matching spreadsheet for three-tank commingled model. Simulated data of a three-tank commingled model, all with volumetric drive, is generated. The same model is used with an automatic history match spreadsheet to find the correct solution.

Case 6 to 8 are the examination of multi-tank commingled model and automatic history match spreadsheet to actual field data.

Case 6: Actual field data, well A, with two-tank commingled system without water production.

Case 7: Actual field data, well B, with six-tank commingled system without water production.

Case 8: Actual field data, well C, with five-tank commingled system with water production from one tank.

4.2 Determination of Gas Critical (terminal) Velocity by Neural Network

Neural network (NN) is used to build the model to determine gas critical velocity and compare with result of Turner's gas critical loading velocity.

As mentioned Section 3.3, the knowledge or correlation of output and input parameters can be captured by the training process of multi-layer back propagation NN. The assumption for this study is that critical velocity is represented by gas rate in the well test record before the wells went to death. This database is called sudden death well database.

The sudden death well database stores gas rate of the last well test records before the wells went to no flow (by all means). Data of sudden death wells from the end of 2005 to the middle of 2007, about 200 records reside in this database. Some records were removed out from the database for neural network building because of the following reasons:

- 1) The flowing tubing pressure (FTP) when the well was loading up was higher than the FTP before the wells went to no flow (increased line pressure)
- 2) The choke size when the well was loading up was smaller than the previous well test (no flow because increased FTP)
- 3) The FTP when the well was loading up was higher than the previous test (the well was shut in or beamed down)
- 4) Doubtful records with excessive long time to die, > 40 days.

The total remaining of 116 records is kept in this database. This database should represent the wells that had no flow because of water (or liquid) load up, not by other causes. The records of the flow rate might not actually represent the critical rates as per Turner's definition but they should be similar. Some wells died suddenly right after the well test (WT) record. Some wells take more than 70 days before having no flow. The wells that took a long time to stop flowing perhaps are wells on the old platform that did not have automatic remote well testing facility or capability to monitor tubing head information (normally temperature) from the central processing platform (SCADA) and required production operators to visit the platform. This may

be the reason that well testing cannot be conducted frequently enough and the well may load up long before a subsequent platform visit to perform a well test.

The neural network software used for this project is “EasyNN Plus” from Neural Planner Software Ltd.

The neural network used to predict critical gas load up rate needs input and output as follows;

- 1) Difference between FTP and separator pressure which represents outgoing line pressure, psi
- 2) Condensate gas ratio (CGR), BBL/MMSCF
- 3) Water gas ratio (WGR), BBL/MMSCF
- 4) Shut in tubing pressure (SITP), psi
- 5) Measured depth in feet to the deepest flowing sand. If there is no MPLT on the bottom hole pressure (BHP) survey data, the deepest sand with porosity of more than 18% is used as the datum depth.
- 6) True vertical depth subsea (TVDSS), ft
- 7) BHT, deg Fahrenheit
- 8) The only output is gas rate before the well went to no flow, MMSCFPD

Since all tubing is 2 7/8” monobore, tubing diameter was not selected as input parameter.

This set of input parameters can be compared with the set of input required by a software called Olga2000. Olga2000 is the transient wellbore simulator. The following are the input parameters required for gas well load up modeling by Olga 2000.

- 1) Reservoir simulation results, such as "well block" pressure and PI changing with time, layer positions, types (oil/water/gas)
- 2) PVT compositions for reservoir fluids

- 3) Well trajectory and pipeline / riser surface system elevation profile, ID and insulation, and ambient temperature
- 4) Well structure includes tubing ID, casing ID / OD, casing layers, cement return height, annulus fluids, etc.
- 5) Separator pressure and size

The parameters needed to be determined by trial and error in building the best neural network are as follows:

- 1) Learning rate
- 2) Momentum
- 3) Number of hidden layers
- 4) Number of nodes in the hidden layer(s)

The number of total connection of all nodes must be kept lower than the number of training records.

One hundred and sixteen records of data were split into 4:1:1 proportion for training, validating, and testing. Therefore, seventy-eight data sets were allocated for training, seventeen sets for validating, and seventeen sets for testing. Various training parameters were tried to get the best network that has the least validation error and acceptable training error (not to be too low to prevent overfitting) and finally tested for fitness with the testing data set. All records that contain the maximum and minimum value of each parameter will only be selected for training.

Turner's gas well loading velocity model as described by Equations 2.12 and 2.13 in Section 2.2 are also used to calculate this velocity to compare with actual gas rate record in the sudden death well database and at the end compare with the prediction result from the neural network model.

CHAPTER V

RESULT AND DISCUSSION

The content in this chapter is divided into two parts. The first part begins with the investigation of the effect of water aquifer on determination of OGIP in a commingle system from water production and the commingle model with and without pressure drop calculation between sands. Also included in the first part is multi-tank model construction, history matching and testing of automatic history matching spreadsheet on many scenarios both with simulated and field data. The second part of the chapter is about the process of building Neural Network and testing it for critical gas loading velocity from sudden death well database.

5.1 Determination of OGIP and Aquifer Size

Case 1: Effect of Water on Gas Production

A commingled two-tank system was created for this investigation with MBAL; hence, there is no consideration of pressure drop between these reservoirs along the wellbore and these two reservoirs were assumed to be at the same datum. The reservoir depth is 8482' MD, TVD 7020'

Both tanks have the following PVT properties: gas specific gravity of 0.8, 15% CO₂, CGR = 50 STB/MMSCF, condensate density = 45 API, separator pressure 150 psi.

Table 5.1 Two-Tank commingle system reservoir property data

	Tank : 70-2	Tank : 77-5
Temperature (deg F)	315	332
Porosity	0.19	0.19
Initial Pressure (PSI)	3100	3600
Connate Water Saturation	0.35	0.5
OGIP (Bscf)	0.8	1
Well Performance Index C (Mscf/day/PSI ²)	0.0057	0.8039
Well Performance Index N	0.8753	0.5532

Relative permeability data for tank 77-5 was built with Corey function.

Water: end point = 0.8 and exponent = 1.

Gas: end point = 0.05 and exponent = 1.

The sweep efficiency was assumed to be 100%. This assumption is taken for demonstration to ensure water production in this case. It might not represent actual properties of the reservoir in the Gulf of Thailand. Tank 70-2 is depletion drive for all cases.

The simulation starting date is October 11, 2006 and end date is June 21, 2007.

Tank 77-5 was experimented under three scenarios.

- 1) No water influx, volumetric drive
- 2) Water influx = 50 MMRB of pot aquifer model
- 3) Water influx = 25 MMRB of pot aquifer model

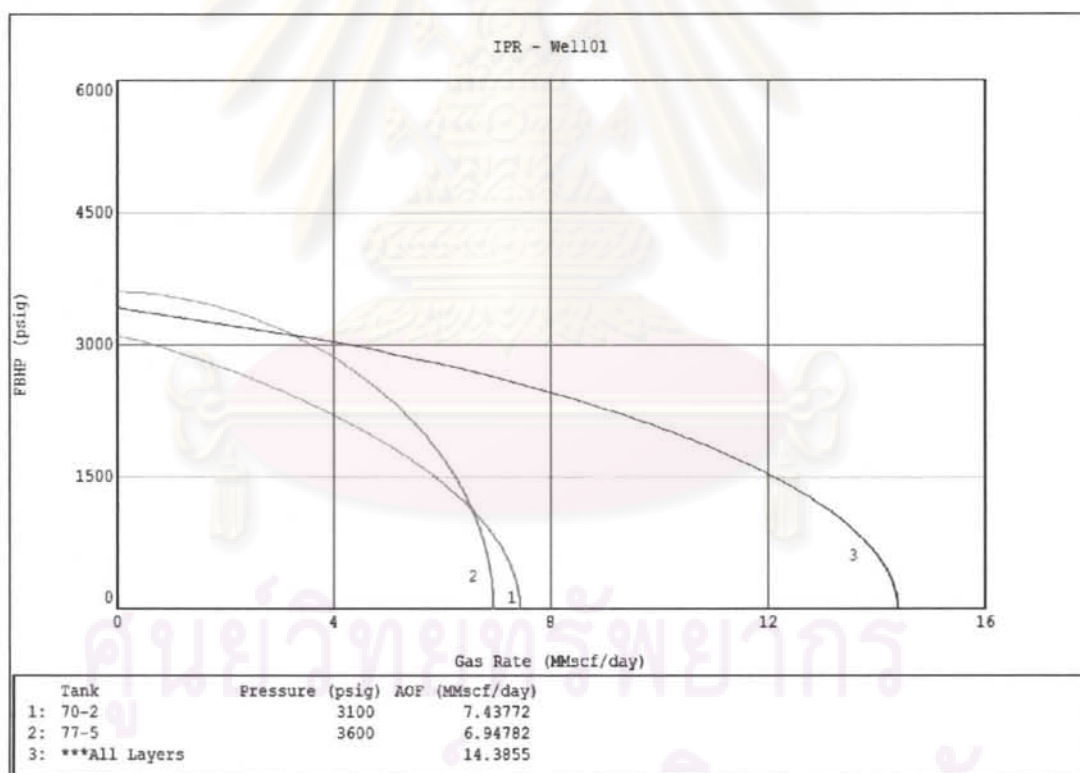


Figure 5.1 IPR of each tank and composite IPR

Figure 5.1 shows IPR curves of both tanks and composite IPR of the commingled system.

The result of simulation is presented in the following figures and discussed below:

Case 1.1 is the comparison of the commingled system with 25 MMrb aquifer drive on tank 77-5 compared with volumetric drive on both tanks.

Case 1.2 is the comparison of the commingle system with 50 MMrb aquifer drive on tank 77-5 compared with volumetric drive on both tanks.

Case 1.1 : 25 MMrb aquifer vs volumetric drive on tank 77-5

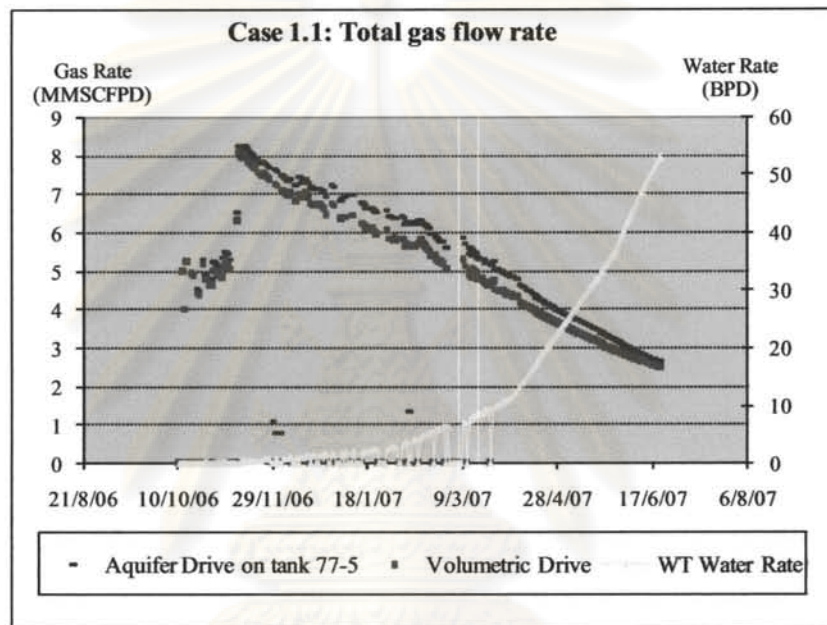


Figure 5.2 Comparison of total gas rate (Case 1.1)

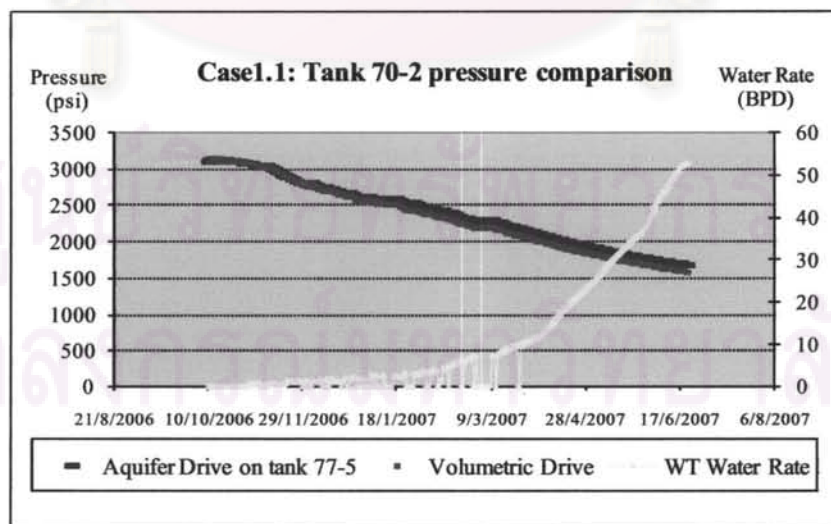


Figure 5.3 Comparison of pressure of tank 70-2 (Case 1.1)

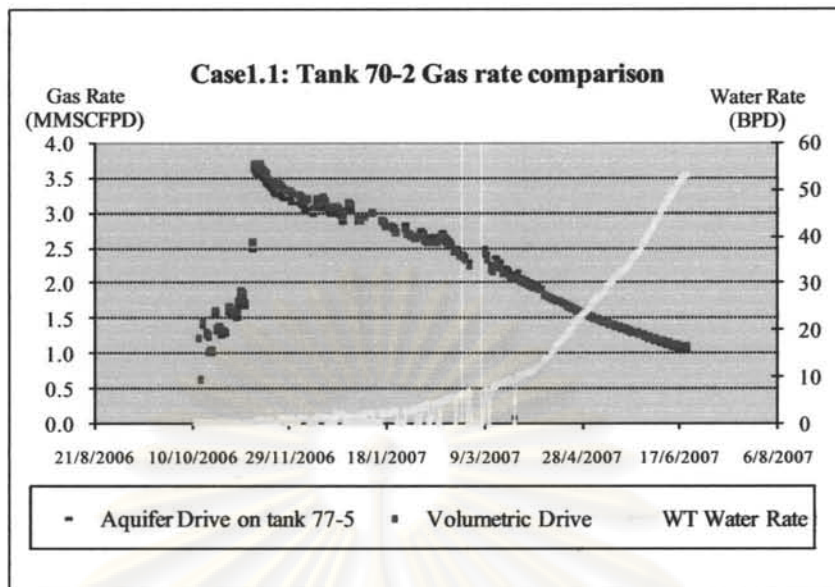


Figure 5.4 Comparison of gas rate of tank 70-2 (Case1.1)

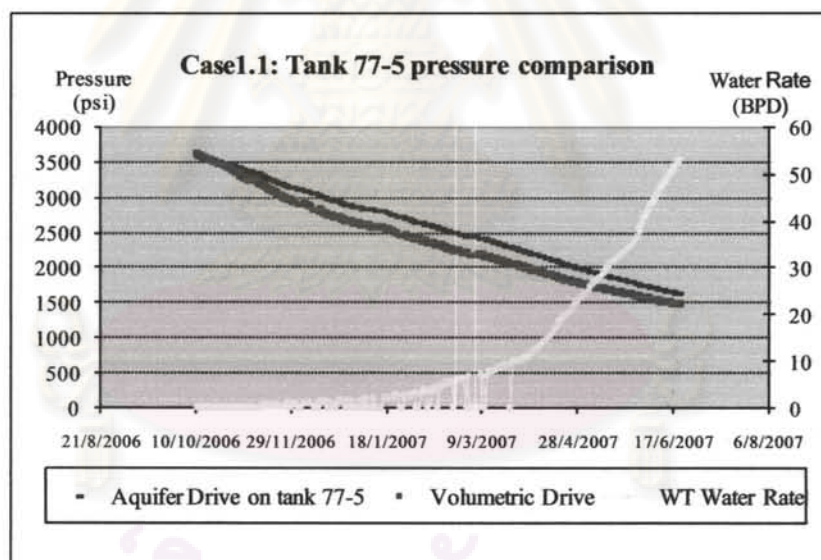


Figure 5.5 Comparison of pressure of tank 77-5 (Case1.1)

ศูนย์วิทยุทรัพยากร
จุฬาลงกรณ์มหาวิทยาลัย

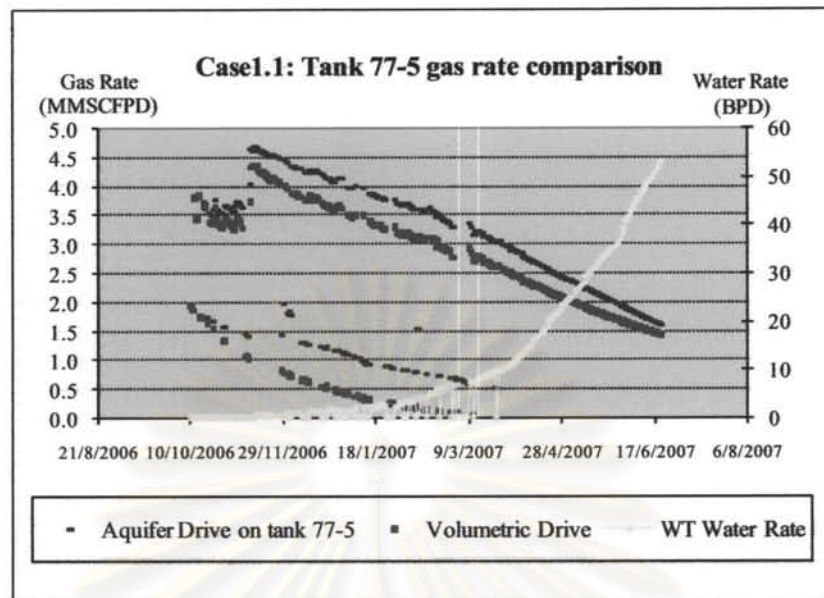


Figure 5.6 Comparison of gas rate of tank 77-5 (Case1.1)

Result discussion

Figure 5.2 indicates that total gas production is approximately 0.6-0.4 MMSCFPD more when there is a 25 MMrb aquifer drive on tank 77-5. The performance gap of aquifer drive becomes smaller towards the end of the simulation period due to an increase in the fractional flow of water from tank 77-5. Figure 5.3 indicates that the pressure depletion of tank 70-2 is only a little less when there is an aquifer support on tank 77-5 compared with volumetric depletion. Figure 5.4 shows that the gas rate produced from tank 70-2 in both scenarios are almost the same. Figure 5.5 shows that the pressure of tank 77-5 depletes about 250 psi less when there is a 25 MMrb aquifer support on the tank, compared with volumetric depletion. Figure 5.6 shows that the gas production from tank 77-5 becomes higher when there is an aquifer supporting the tank while the pressure is maintained at a higher value.

Case 1.2: 50 MMrb aquifer vs volumetric drive on tank 77-5

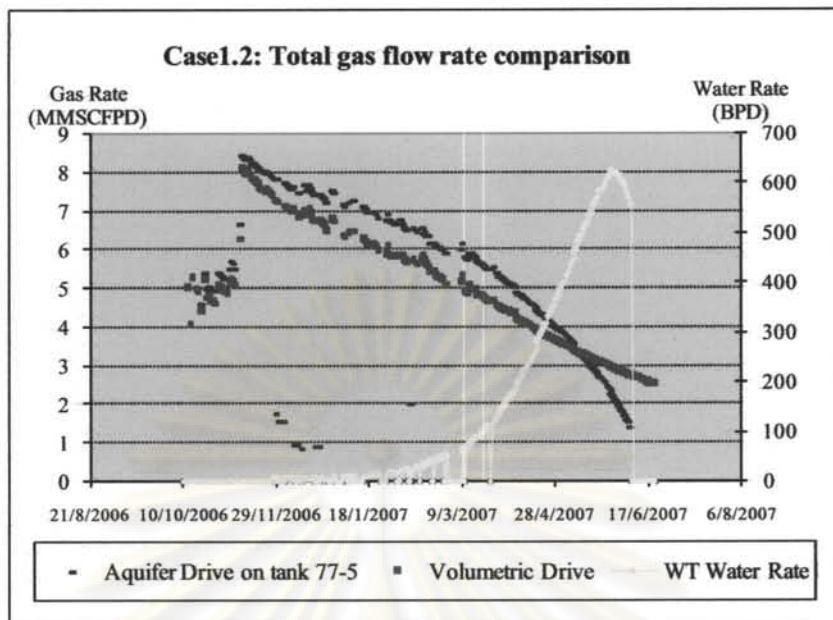


Figure 5.7 Comparison of total gas rate (Case1.2)

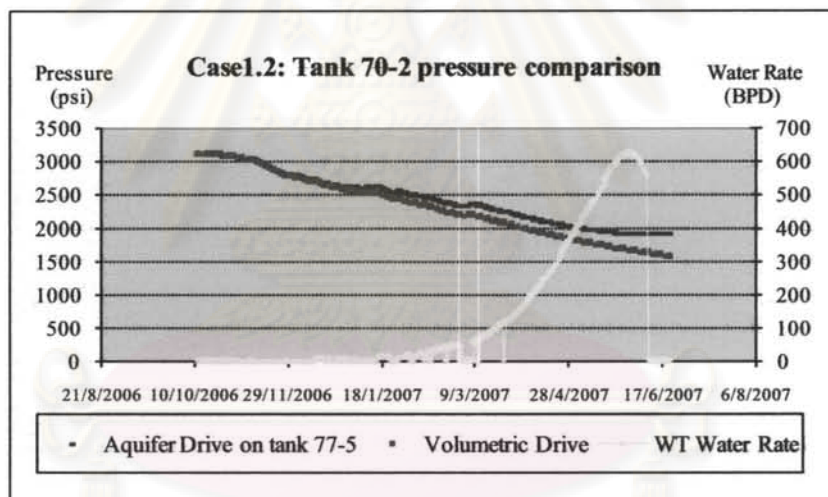


Figure 5.8 Comparison of pressure of tank 70-2 (Case1.2)

ศูนย์วิทยทรัพยากร
จุฬาลงกรณ์มหาวิทยาลัย

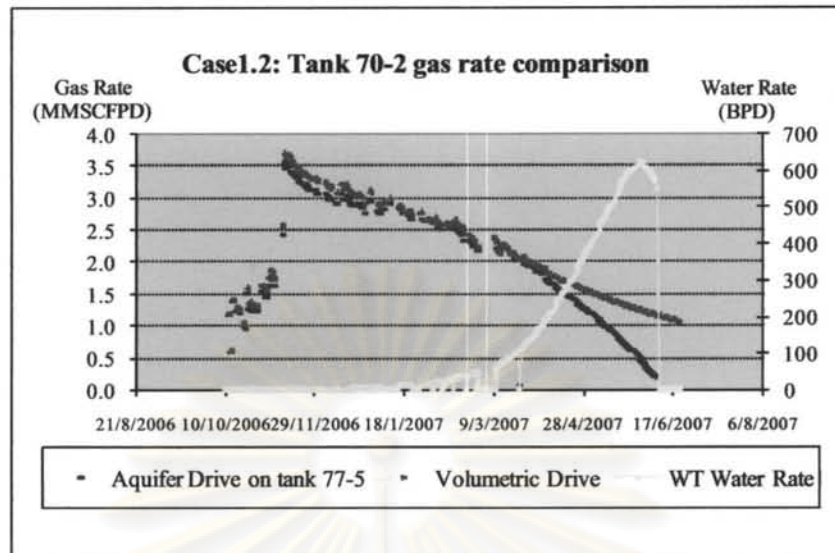


Figure 5.9 Comparison of gas rate of tank 70-2 (Case1.2)

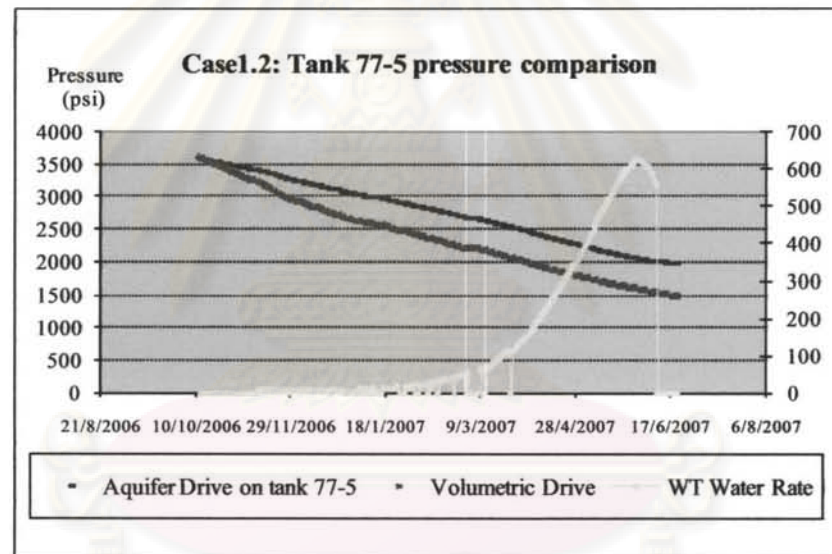


Figure 5.10 Comparison of pressure of tank 77-5 (Case1.2)

ศูนย์วิทยทรัพยากร
 จุฬาลงกรณ์มหาวิทยาลัย

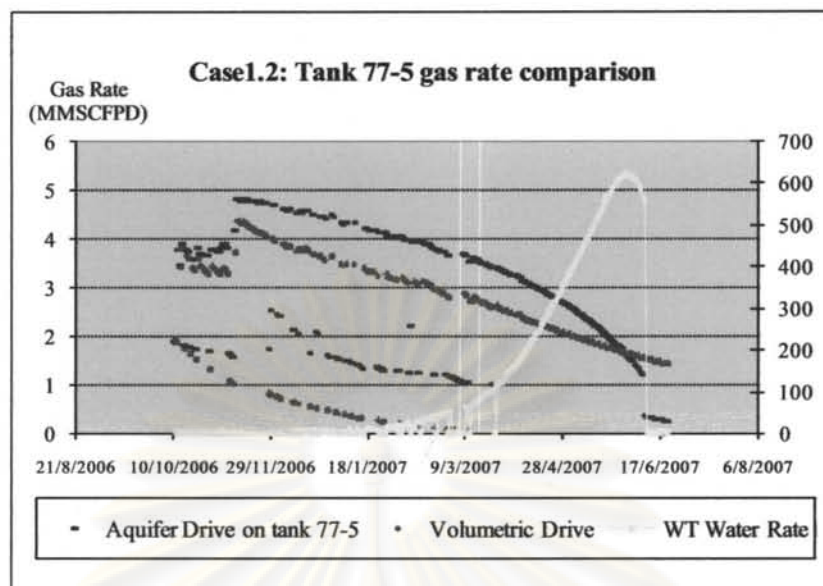


Figure 5.11 Comparison of gas rate of tank 77-5 (Case 1.2)

Result discussion of case 1.2

Figure 5.7 shows that the total gas rate production with an aquifer in the system is better than all-depletion drive system until the water rate reaches 500 bpd. The gas rate declines while the water rate increases until the water rate reaches a peak at 620 bpd then start dropping, and suddenly the well went to no flow. The pressure of tank 70-2 becomes relatively stable after water rate is 400 bpd as seen in Figure 5.8. The reason that the total gas rate declines is firstly due to an increase in hydrostatic pressure drop because of increased WGR which has large effect on gas production from tank 70-2. This effect is shown in Figure 5.9 that the gas rate of tank 70-2 which is similar in both systems until the water rate in the wellbore (from 77-5) increases to 200 bpd on April 10th. After that the gas rate from 70-2 drops quickly until the well becomes no flow. In case of aquifer drive, the pressure of tank 77-5 is higher despite the higher gas production rate due to the effect of water influx which helps maintain the pressure as seen in Figure 5.10. From Figure 5.11, the gas rate from 77-5 drops at higher rate after April 28th due to increased fractional flow of water from tank 77-5 because of water influx which increases the tank water saturation and decreases the relative permeability to gas (the water rate is still increasing while the gas rate is decreasing).

Result discussion of case 1.1 and 1.2

Another implication of this case is that we may be able to use the volumetric model to model and history match commingled system that has a certain degree of aquifer support while the water has not broken through the wellbore. The degree of error depends on the aquifer size. Small differences in the pressure and production profile were observed on tank 77-5 in case 1 (Figures 5.5 and 5.6). There are no significant differences in the pressure and production profile of tank 70-2 (Figures 5.3 and 5.4). Certainly, if the aquifer is big such as in case of 50 MMrb on 77-5, high degree of error on OGIP of tank 77-5 will occur if using depletion model for history matching as seen in Figures 5.7 to 5.11

Table 5.2 discusses the different characteristics of each tank and total system when there is either 50 MMrb or 25 MMrb aquifer on tank 77-5

Table 5.2 Summary of commingle multi-tank model study

	50 MMRB Pot Aquifer : 77-5	25 MMRB Pot Aquifer : 77-5
Total gas production	Close to volumetric drive until water produced to around 300 bpd	Profile similar to volumetric drive
Total water production	Increase to maximum of 620 bpd on May 29th	Increase to maximum of 53 bbl to last day of simulation period
Gas rate of tank 70-2	Close to volumetric drive until water increase to 200 bpd	Very close to volumetric drive
Pressure of tank 70-2	Less than 50 psi different from volumetric drive until 2 months after production	100 psi different at the end of simulation period
Gas rate of tank 77-5	0.5 MMSCFPD different from volumetric drive observed after a month of production	Only 0.2 MMSCFPD different from volumetric drive observed at the end of simulation period
Pressure of tank 77-5	About 500 psi different from volumetric drive observed at the end of simulation period	Close to volumetric drive

Case 2: Effect of Model with and without pressure drop between reservoirs

Case 2.1: All reservoirs are depletion drive

A two-tank commingled system was constructed with the first tank, 59-1 above the second tank, 78-6. Properties of both tank 59-1 and 78-6 displayed in Table 5.3 were used for simulation in both GAP and MBAL.

Table 5.3 Reservoir properties used in case 2.1

	Tank 59-1	Tank 78-6
Temperature (°F)	267	328
Porosity	0.22	0.17
Initial Pressure (psi)	2549	3682
Connate Water Saturation	0.45	0.43
OGIP (Bscf)	1	3

PVT properties of all reservoirs:

Gas specific gravity = 0.878, separator pressure = 750 psi, condensate gravity = 55° API, CGR = 12 BBL/MMSCF, water salinity = 100,000 ppm, CO₂ 15% by mole.

GAP model was built with the same data except the difference in the datum level of the two tanks as shown in Table 5.4.

Table 5.4 Depth data of two different reservoirs in case 2.1

	Tank 59-1	Tank 78-6
MD (ft)	9,680	11,954
VD (ft)	5,910	7,860

The same VLP and IPR (Figure 5.12) was used for calculating the pressure drop above the top tank in both GAP and MBAL. Petroleum Expert 2 Correlation was used to calculate the pressure drop between the two tanks in GAP.

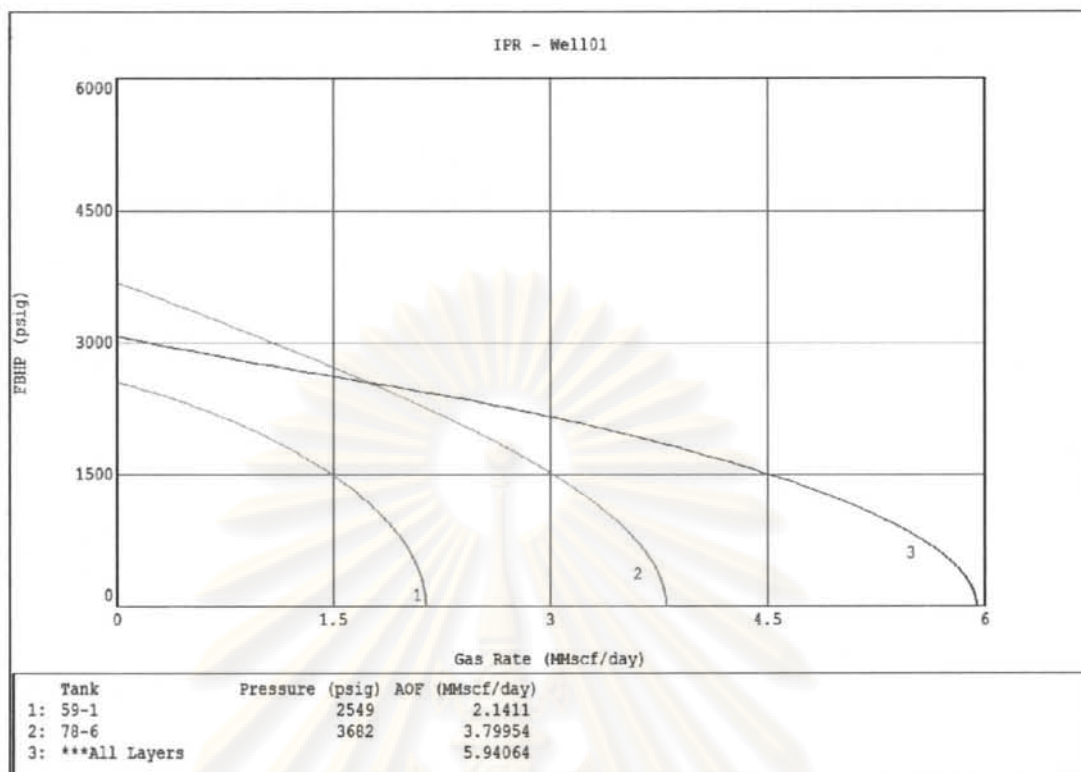


Figure 5.12 IPR of all reservoirs in the system for this case study

Result of simulation

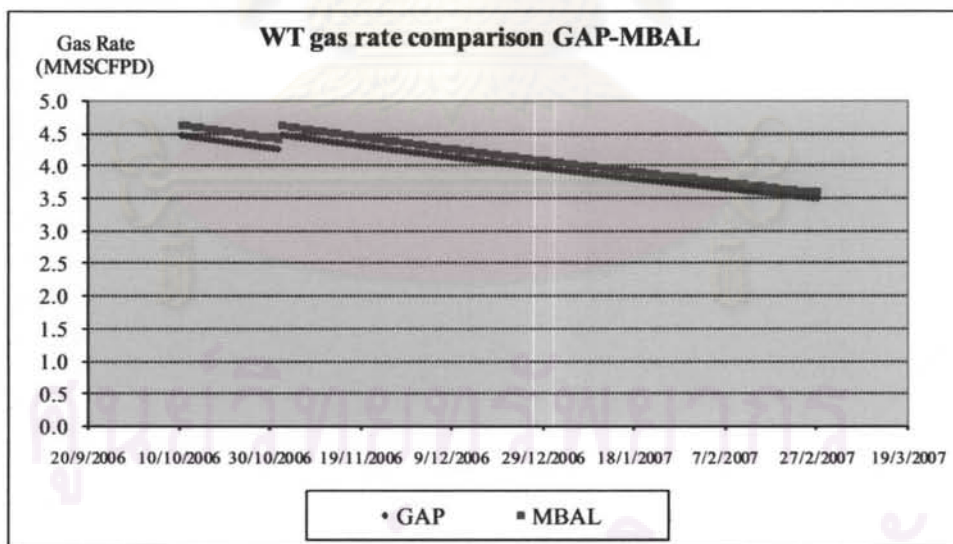


Figure 5.13 Plot of difference in total gas production between GAP and MBAL, all tanks having depletion drive

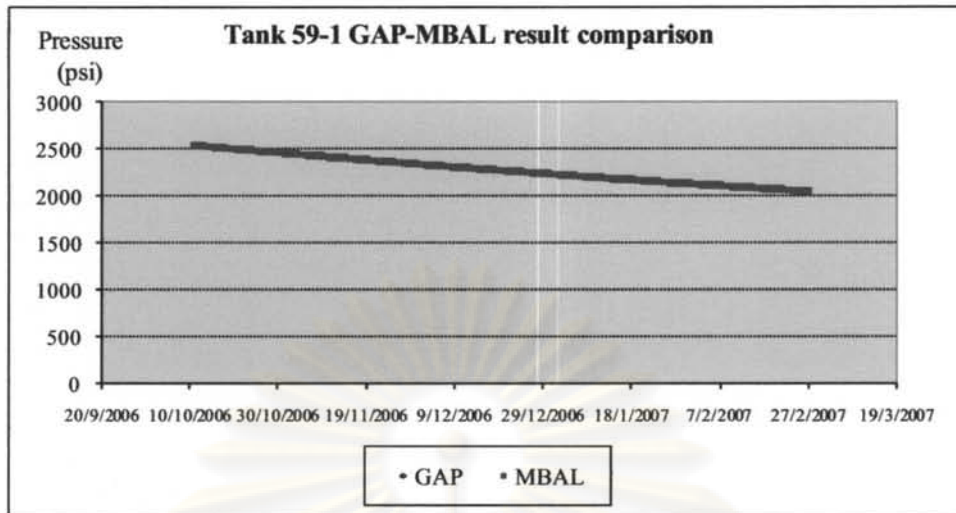


Figure 5.14 Difference in tank 59-1 pressure profile between GAP and MBAL, all tanks having depletion drive

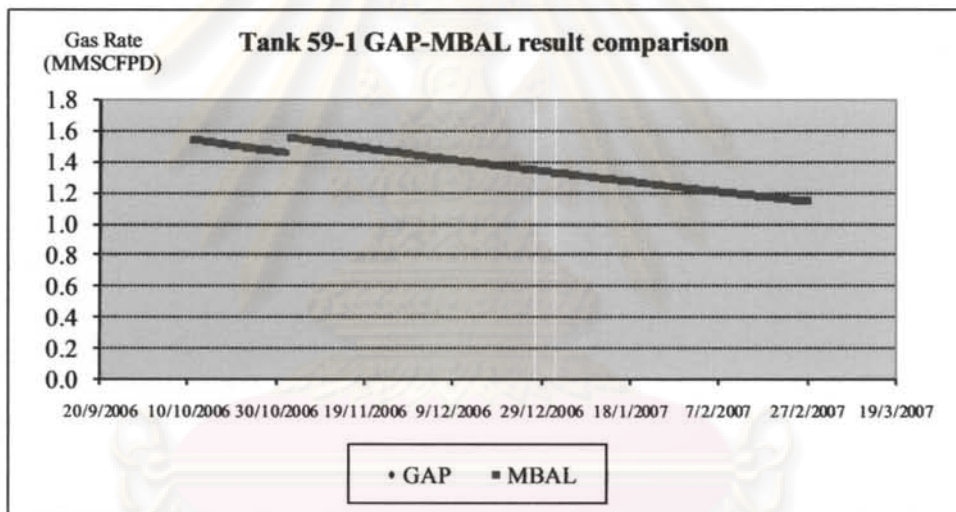


Figure 5.15 Difference in tank 59-1 gas rate profile between GAP and MBAL, all tanks having depletion drive

ศูนย์วิทยทรัพยากร
จุฬาลงกรณ์มหาวิทยาลัย

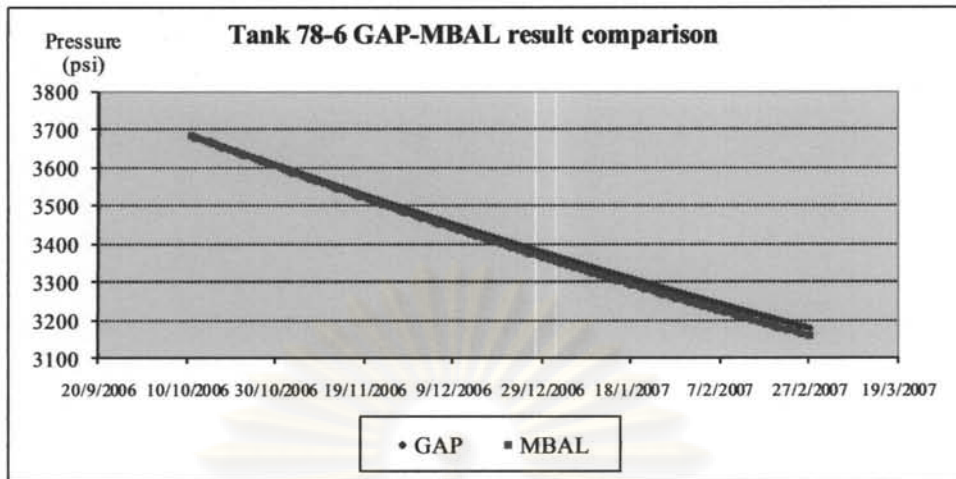


Figure 5.16 Difference in tank 78-6 pressure profile between GAP and MBAL, all tanks having depletion drive

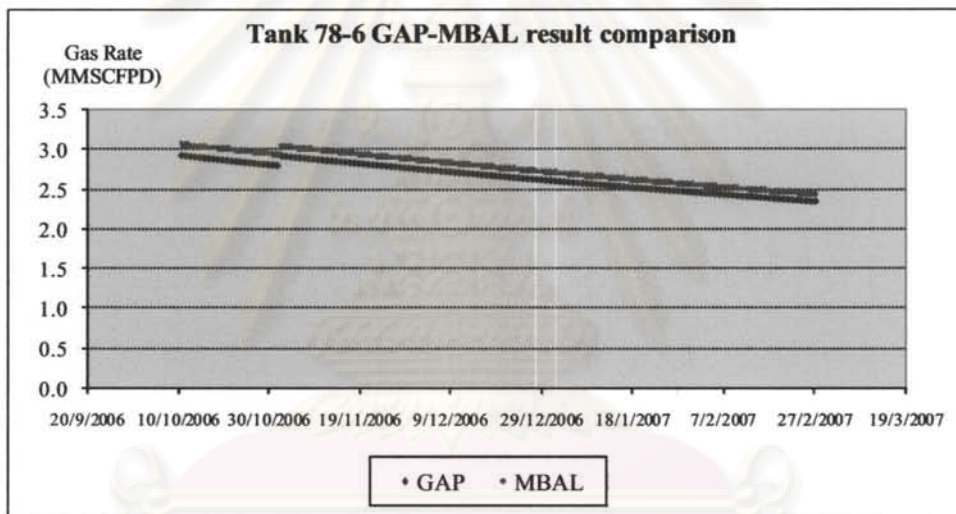


Figure 5.17 Difference in tank 78-6 gas production rate between GAP and MBAL, all tanks having depletion drive

Result discussion

Smaller production rate in the production profile simulated by GAP compared with MBAL was observed in Figures 5.13. From Figures 5.14 and 5.15, there is no difference between the production profiles of the top sand, 59-1, generated by GAP and MBAL. However, the result of the bottom sand, 78-6 shown in Figures 5.16 and 5.17 shows small difference in production profile with GAP model yielding lower gas rates and slower depletion rate than MBAL model due to the effect of pressure drop between the two sands.

Case 2.2: Tank 78-6 is water drive

The properties of both tanks are the same as in case 2.1 except there is an addition of aquifer of size 500 MMrb on tank 78-6. Two different scenarios were investigated:

- 1) Tank 78-6 is at the bottom with the same datum depth as in scenario 1.
- 2) Datum depth of tank 78-6 and tank 59-1 is switched, i.e., tank 59-1 becomes the deeper tank at the depth of tank 78-6 and tank 78-6 becomes the shallower tank at the depth of tank 59-1.

Result of simulation

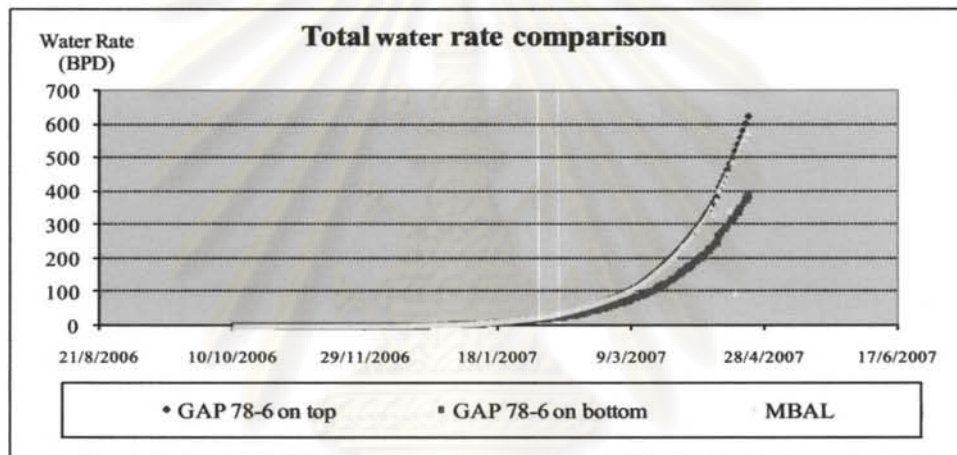


Figure 5.18 Difference in total water production profile between MBAL and GAP (scenario 1 and 2)

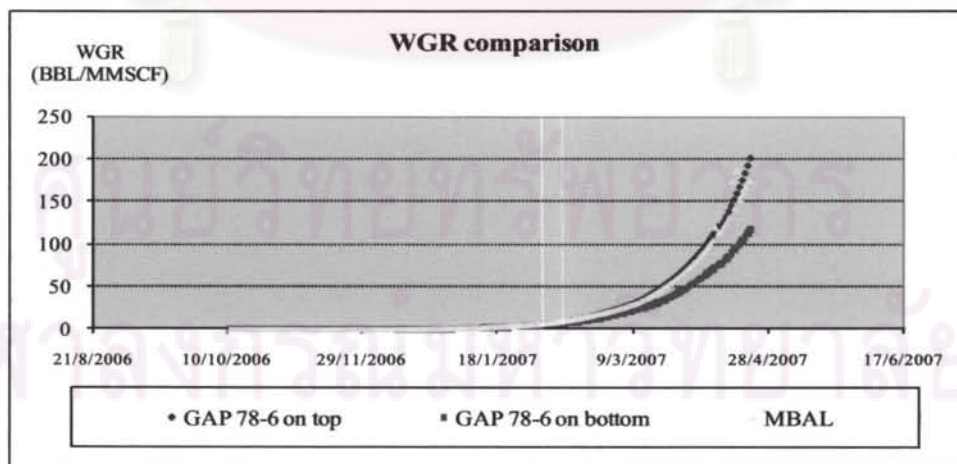


Figure 5.19 Difference in total WGR profile between MBAL and GAP (scenario 1 and 2)

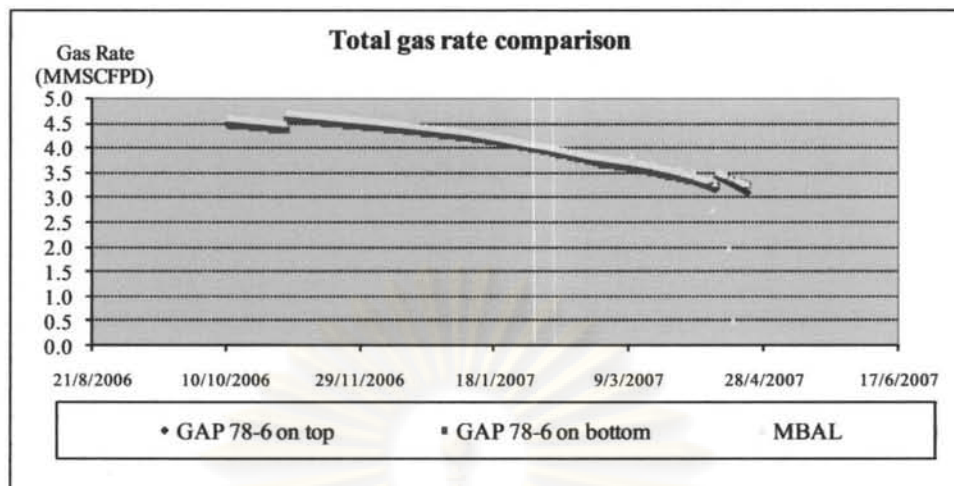


Figure 5.20 Difference in total gas production profile between MBAL and GAP (scenario 1 and 2)

Result discussion

From Figures 5.18 to 5.20, it is shown that the results from MBAL and GAP with tank 78-6 on the top were very close. Result of GAP with tank 78-6 at the bottom is much different from the other two cases (MBAL and GAP with 78-6 on the top), especially the result of water production rate and WGR.

Summary of discussion

- 1) In the scenario where the water producing tank is on the top, MBAL and GAP model shows small difference in the result. Multi-tank MBAL could be used to model commingle system with water production from the top most tank with insignificant error.
- 2) On the contrary, if the water producing tank is below the top most tank, MBAL multi-tank model may not correctly model the flow with acceptable error since the pressure drop between the tanks due to hydrostatic head is significant and affects the production of all tanks. Therefore, this pressure loss may not be neglected and MBAL multi-tank model may not be used. The degree of inaccuracy of MBAL model depends on WGR and TVD difference between the top most tank and the water producing tank.
- 3) Characteristic of simulated data are all the same for 3 cases when WGR is low.

Case 3 History matching two-tank commingle model with water drive

This is the reverse case study of case 1. Automatic history matching spread sheet was used to history match the model to determine OGIP from the simulated data from commingled multi-tank MBAL model built with an aquifer on tank 77-5 and depletion drive on tank 70-2. All the properties are the same as in case 1 except the aquifer size on tank 77-5. Since it is the model built with MBAL, both tanks were assumed to have the same datum without pressure loss between them. Table 5.5 shows the reservoir properties used in the modeling the two tanks.

Table 5.5 Reservoir properties used in case 3

	Tank	
	70-2	77-5
Temperature (F)	315	332
Initial Pressure	3,100	3,600
Porosity	0.19	0.19
Connate Water Saturation	0.35	0.5
OGIP (Bscf)	0.8	1
Aquifer Volume (MMRB)	-	50 (before water out) 30 (after water out)

To reflect the actual situation that happens in the field, we divided the scenario into two cases. Different parameters used in the optimization algorithm were tried to evaluate if different answers or convergence could be obtained

Case 3.1: Using depletion drive model to history match simulated data

Actual aquifer strength (size) in small compartmentalized and highly faulted gas reservoirs in the Gulf of Thailand won't allow the detection of water drive from non-straight line characteristic of P/Z plot. In addition, the quality and availability of average reservoir pressure prevents us to use Cole plot to detect the existing of non-depletion drive on the multi-reservoirs interested by the well. Even though we have some means to identify water drive before water breaks through, it is normally determined for the entire well unless we have geological data of the location of aquifer and which reservoir is connected to it. This is not always the case for highly faulted and complex geology as in gas reservoirs in Pattani basin, GOT. For these reasons, depletion drive model was assumed to all tanks for initial model building and

calibrating for the period that only gas production is observed in the well test and PLT.

For this case, simulated production data from commingle model that has an aquifer on tank 77-5 with 11 sample points of simulation data represents well test data for history matching. There is no water production until the end of simulation date. Therefore, only the gas rate is used for matching. One sample point of simulated result from each tank on 1/30/2007 is used to represent PLT data which is also used in the history matching. The automatic-history matching process started with an initial guess of OGIP in each tank of 0.5 Bscf. After running the regression, the result was summarized in table 5.6.

Summary of result of automatic history match

Table 5.6 Result of automatic history match with depletion drive model

Case #	Weight Factor	PLT	Lamda	Initial Guess OGIP		Converge	Converge Type	Last Iteration OGIP		Last Iteration #
				70-2	77-5			70-2	77-5	
1	1 all	Yes	0.001	0.5	0.5	Yes	3	0.7649	2.1478	24
2	1 on gas, 10 on PLT	Yes	0.001	0.5	0.5	Yes	3	0.771	2.091	37

Table 5.7 Result of automatic history matching of case 3.1#1

Residual type	Observed	Calculated	Residual
WT Date: Gas 10/14/2006	4.08	4.08	0.0050
WT Date: Gas 10/27/2006	4.93	4.89	0.0414
WT Date: Gas 11/6/2006	5.66	5.59	0.0657
WT Date: Gas 12/1/2006	7.81	7.73	0.0825
WT Date: Gas 12/9/2006	7.64	7.56	0.0823
WT Date: Gas 12/21/2006	7.44	7.36	0.0787
WT Date: Gas 1/20/2007	6.96	6.94	0.0204
WT Date: Gas 1/30/2007	6.78	6.80	-0.0138
WT Date: Gas 2/6/2007	6.69	6.76	-0.0705
WT Date: Gas 2/16/2007	6.59	6.76	-0.1654
Tank Pressure of 70-2 f/PLT Survey on 1/30/2007	2544	2521	23.0000
Tank Pressure of 77-5 f/PLT Survey on 1/30/2007	2905	2883	22.0000
Gas rate of 70-2 f/PLT Survey on 1/30/2007	2.69	2.70	-0.0116
Gas rate of 77-5 f/PLT Survey on 1/30/2007	4.09	4.09	-0.0022

Result discussion

From Table 5.7 and Figures 5.21-5.23, the automatic history matching routine converged and found the solution with a very small residual for both cases. All trials give a good answer for OGIP on tank 70-2 but not for tank 77-5 which actually has the water drive but was assumed to be depletion drive due to lack of indication of water production. Such answer has 100% error. Thus, we may not apply this algorithm to such a case.

Result of case 3.1#1

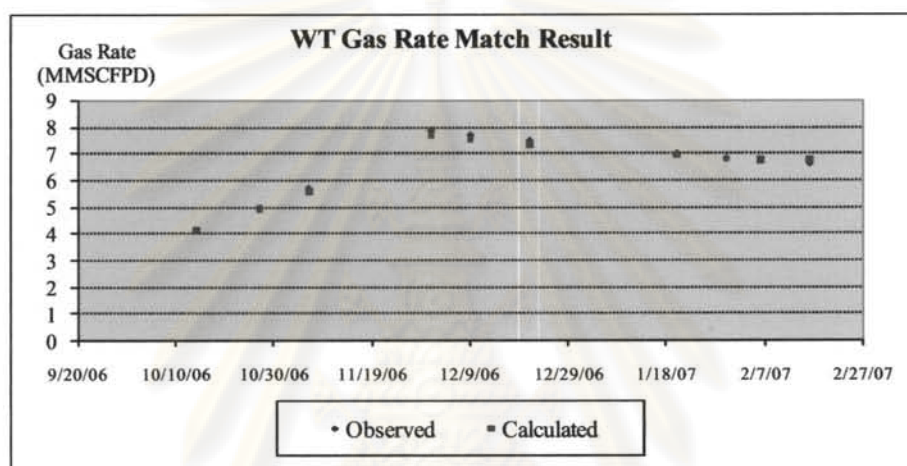


Figure 5.21 Result of automatic history matching of well gas rate

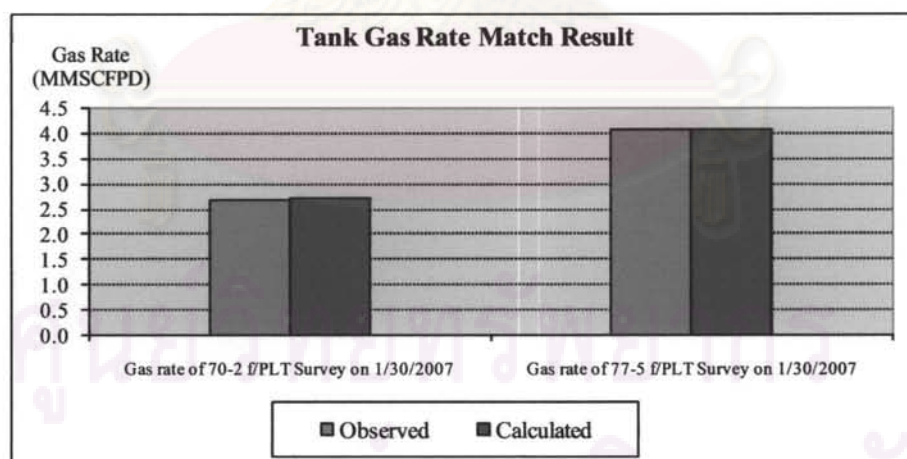


Figure 5.22 Result of automatic history matching of tank gas rate

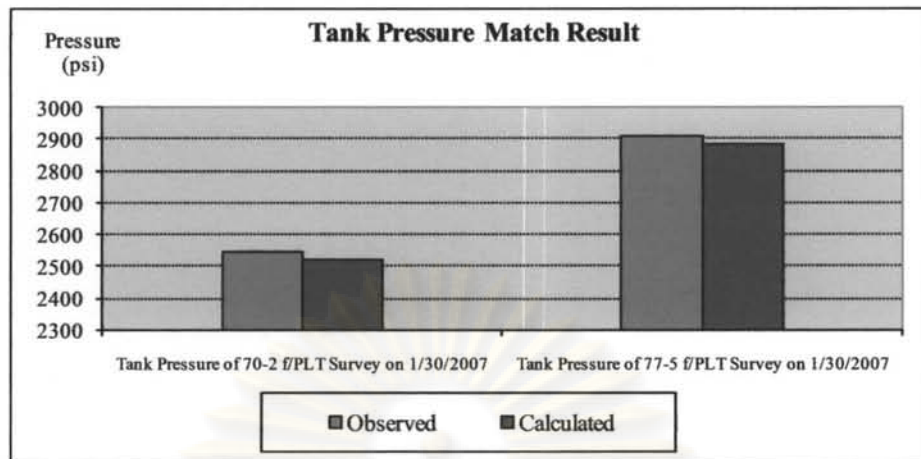


Figure 5.23 Result of automatic history matching of tank pressure

Case 3.2 Perform history matching after water breakthrough using water drive model

After the water production is observed at the surface, PLT will normally be run to identify water producing sand(s). Aquifer model would be certainly incorporated to the sand that produced water, and we would attempt to history match all observed parameters such as WT gas rate, WT water rate, PLT gas, water, pressure of each tank to determine OGIP of each tank and aquifer size of the water producing tank(s).

In addition to the usual and expected cause for automatic history matching routine to stop running when convergence criteria is met, this routine was sometime terminated manually when the solution of many iterations were repeat and oscillated around certain value. Sometime automatic history matching routine gave exaggerated value of matching parameter(s) which causes the simulation period ended before desired simulation ended, the automatic history matching routine would stop running even though convergence criteria was not met. These were noted with “Manually” and “MBAL Terminated” in Case of End column of table 5.8 respectively.

จุฬาลงกรณ์มหาวิทยาลัย

Table 5.8 Summary of automatic history matching on simulated data of Multi-tank Model with Aquifer on tank 77-5

Trial#	Weighing Factor	Lamda	Initial Guess OGIP		Initial Guess Aquifer 77-5	Convergence Type	Last Iteration OGIP		Last Initial Aquifer 77-5	Last Iteration #	Cause of End
			70-2	77-5			70-2	77-5			
1	1	0.001	0.5	0.5	10	No	0.01	3.4496	183.40	35	Manually
2	1 on all WT, 10 on PLT	0.01	0.5	0.5	10	No	0.01	0.0100	14.00	1	MBAL Terminated
3	1 on all WT, 10 on PLT	0.01	0.8	1	10	No	0.01	0.0100	1,394.00	3	MBAL Terminated
4	1 on all WT, 10 on PLT	0.01	0.77	2.09	10	No	0.02	0.0100	20,244.00	4	MBAL Terminated
5*	1	0.01	0.8	1	25	No	0.48	1.0400	30.00	48	Manually
6*	1 on all WT, 10 on PLT	0.01	0.8	1	25	No	0.48	1.0400	32.51	28	Manually
7	1	0.01	0.8	1	10	No	31.99	0.0100	10.00	35	Manually
8	1	0.001	0.77	2.09	10	No	92.58	0.0061	838.00	29	Manually
9*	10	0.00001	0.8	1	25	No	0.80	0.9900	29.81	23	Manually
10*	10	0.001	0.8	1	25	No	0.80	0.9900	29.75	7	Manually
11	10	0.001	0.5	0.5	25	No	0.42	0.5000	10.81	14	Manually
12	100	0.001	0.5	0.5	25	No	0.55	0.4100	9.06	13	Manually
13	1 on all WT, 10 on PLT	0.001	0.8	1	10	No	1.95	0.0100	2,094.00	7	Manually
14	(normalized#13)	0.001	0.8	1	10	No	1.56	0.0100	210.00	9	Manually

Result discussion

Various different combination of parameters such as weighing factors, Lamda, initial guess values, were tried in each trial with automatic history matching spread sheet. The result of each trial is shown in table 5.8.

From Table 5.8, the result can be summarized as follows:

- 1) Different value of Lamda has little effect. It may cause converge sooner with lower value (in orders of magnitude) as in trial # 9 and 10.
- 2) Initial guesses that are far from the correct answers may never bring the answers to the correct ones or even cause the program to terminate. However, it also depends on the weighing factors. Initial guesses that are far from the correct values could bring the solutions to correct answers with proper weighing factors. Examples are trial #11 & 12 which seems to oscillate around a local minimum which is wrong solutions.
- 3) Weighing factors have an effect on convergence as seen in the case of high weighing factors (weighing factors = 10). The weighing factors help bringing the solutions closer to the correct ones or converge despite the fact that initial guesses are far from the solutions. Examples are trial case # 9 and #10. When compared to same initial guess values but with lower weighing factor as in trial case # 5 (equal to 1) and trial case # 6 (1 on WT and 10 on PLT data), trial case #9 and #10 could find the solutions. Having different weighing factors 1 on WT and 10 on PLT in this case did not make a difference from having weighing factors = 1 as seen in trial case # 5 compared to trial case # 6.
- 4) Local trap minima may be the cause for solutions not to converge when initial guesses are far from the correct solutions. A global minimum search will help search for converged and correct solutions.
- 5) Using equal weighing factor got the solutions closer to actual solutions than unequal weight factor in this case. Optimization program can continue running despite being unable to find converged solutions, because the global minimum is not found, but the predicted intermediate values are not too exaggerated that cause overflow or simulation date ends before specified end simulation period.

- 6) Using normalized combination weight (trial case #14) gives error as much as normal combination weight (trial case #13).

Case 4: History Matching simulated data incorporated with pressure drop between reservoirs

To evaluate the performance of multi-tank model built with MBAL which does not take into account the pressure drop between multiple reservoirs, result of simulation with GAP, which takes into account the pressure drop between multiple reservoirs, was used for automatic history matching with multi-tank model built with MBAL. Two scenarios were investigated. Simulated data generated by GAP and MBAL in case 2.1 are used as historical data in this case.

Case 4.1 Two tanks commingle. Both tanks are depletion drive.

Data from same reservoir model as in case 2.1 was generated by GAP. Tank A refers to tank 59-1 and tank B refers to tank 78-6 in case 2.1. MBAL Multi-tank commingle model was used for history matching with automatic history matching spreadsheet with various trial parameters as the result shown in Table 5.9.

Table 5.9 Summary of automatic history matching result of case 4.1

Case	Weight Factor	PLT	Lam da	Initial Guess OGIP		Converge	Converge Type	Last Iteration OGIP		Last Iteration #
				59-1	78-6			59-1	78-6	
1	10	Yes	0.001	1	1	Yes	3	0.6339	1.3669	8
2	10	No	0.001	1	1	Yes	1	1	1	11
3	1	Yes	0.01	1	2.5	Yes	1 & 3	1.32	2	22
4	1	Yes	0.01	1	1	Yes	1 & 3	1.12	2.55	22
5	1	No	0.01	1	1	Yes	1	7.45	1.45	8

Result discussion

With different weighing factors and initial guesses of OGIP for each tank, different answers were observed from different trials (cases). Even though all trials show convergence but only trial #3 and trial #4 show good answers. Using all weighing factors equal to one for all residuals obtained the closed solution to actual ones. Trial #4 which has far initial guesses from correct answer gave a close solution to the actual OGIP of tank 78-6 but the answer is still lower than the correct value by 0.45 Bcf.

This is due to the effect of commingled model which does not calculate the pressure drop between sands. Table 5.10 and Figures 5.24 to 5.26 show the result of history match for case (trial) #3

Table 5.10 Result of history match of case 4.1#3

Date Number	Residual type	Observed	Calculated	Residual
1	WT Date: Gas 10/14/2006	4.45	4.58	-0.1238
2	WT Date: Gas 10/27/2006	4.32	4.42	-0.1022
3	WT Date: Gas 11/6/2006	4.45	4.52	-0.0715
4	WT Date: Gas 12/1/2006	4.22	4.25	-0.0323
5	WT Date: Gas 12/9/2006	4.15	4.17	-0.0211
6	WT Date: Gas 12/21/2006	4.04	4.05	-0.0055
7	WT Date: Gas 1/20/2007	3.80	3.77	0.0285
8	WT Date: Gas 1/30/2007	3.72	3.68	0.0374
9	WT Date: Gas 2/6/2007	3.66	3.62	0.0450
10	WT Date: Gas 2/16/2007	3.59	3.53	0.0531
NA	Tank Pressure of 59-1 f/PLT Survey on 1/30/2007	2148	2234	-86.0000
NA	Tank Pressure of 78-6 f/PLT Survey on 1/30/2007	3268	3091	177.0000
NA	Gas rate of 59-1 f/PLT Survey on 1/30/2007	1.24	1.34	-0.1087
NA	Gas rate of 78-6 f/PLT Survey on 1/30/2007	2.48	2.33	0.1471

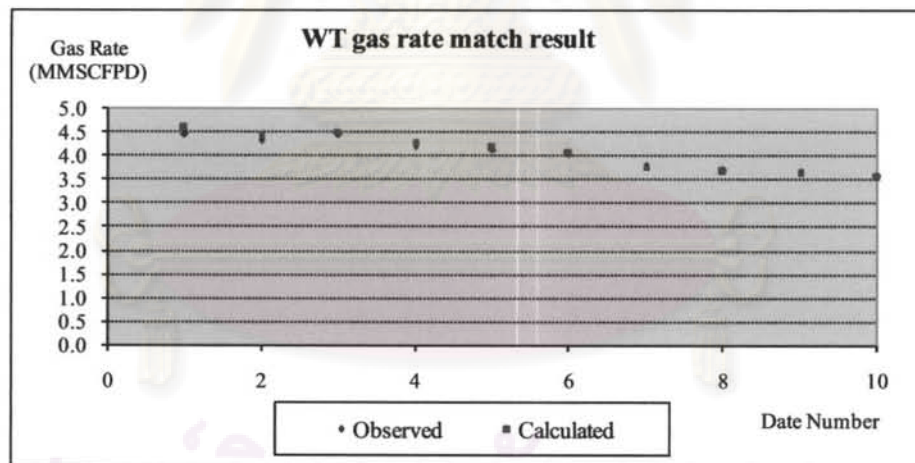


Figure 5.24 Plot of gas WT history match result of case 4.1#3

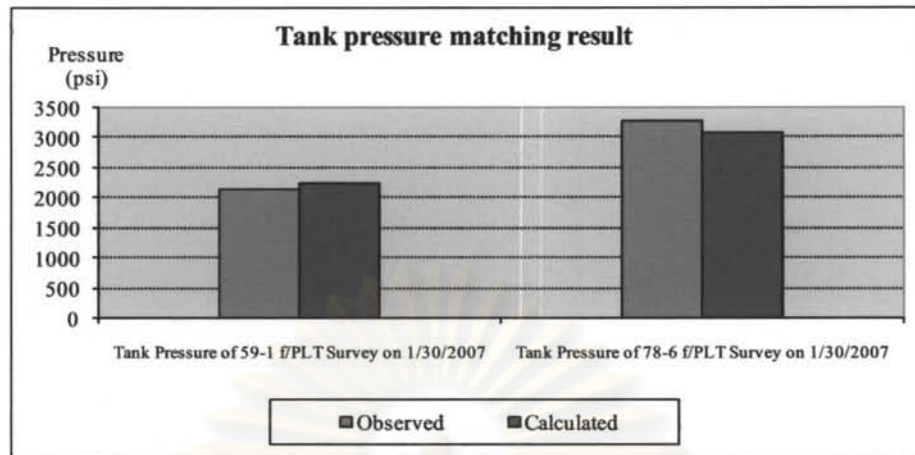


Figure 5.25 Chart of tank Pressure history match result of case 4.1#3

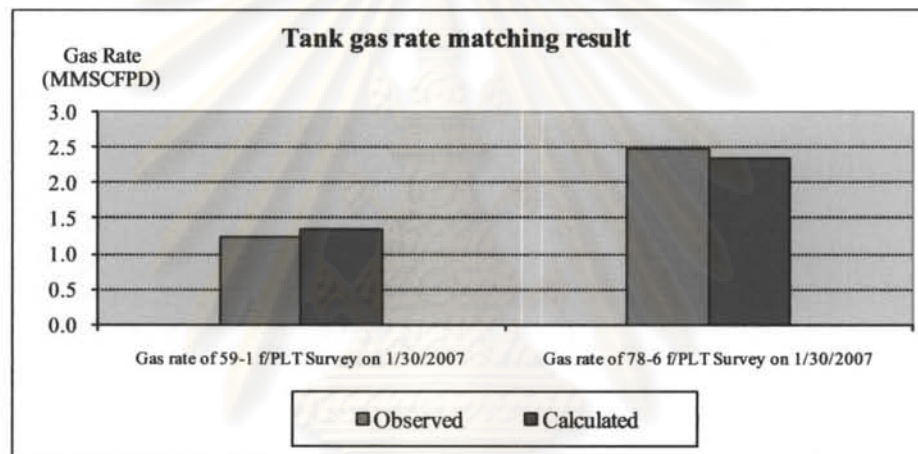


Figure 5.26 Chart of tank gas rate history matching result of case 4.1#3

Case 4.2 Two tanks commingle system. The bottom tank (78-6) has an aquifer support built with a small pot aquifer model.

The same reservoir properties, IPR and VLP as in case 2.1 were used as input except the following:

OGIP of tank 59-1 = 0.8 Bscf, OGIP of tank 78-6 = 1 Bscf, Aquifer Volume on tank 78-6 = 500 MMRB

Tank 59-1 is on the top and tank 78-6 is at the bottom with datum data shown in Table 5.4.

The methodology is similar to case 3.2. The simulation result obtained from GAP, such as total gas rate, water rate, individual tank pressure, gas rate, water rate (simulated PLT data) were history matched by the multi-tank model built with MBAL with a small pot aquifer model attached to tank 78-6.

All cases use OGIP of 0.5 Bscf and aquifer size of 500 MMRB as initial guess. The result of automatic history matching is in Table 5.11.

Result discussion

From Table 5.11, the automatic history matching spreadsheet neither had the converged solutions on any cases (trials) nor had any solution in any iteration close to the actual solutions. It is suspected that because GAP takes into account the pressure drop between sands, the effect of high WGR in the last portion of WT data and PLT data cannot be fitted into the model built by MBAL since it does not take into account the pressure drop between sands. Had tank 78-6 which has an aquifer attached to is the top most tank above any sands, MBAL and GAP result should be similar and MBAL should be able to match GAP data. The comparison run of MBAL and GAP with different positions of aquifer tank shown in case 2.2 indicates that the result of MBAL and GAP is very close if the water producing sand is on the top above other sands. Therefore, MBAL should be able to match water production in this case if the water sand is above or are almost at the top of any sands below.

Summary of trials in case 4.2

- 1) Only one trial has converged solutions with weighing factor equal to 0.001 but the answers are still far from the correct answers.
- 2) Despite using the correct aquifer size in autohistory match, correct OGIP cannot be achieved.
- 3) It may be due to the fact that MBAL model did not consider the pressure drop between sands. Hence, when high water production and WGR simulated by GAP causes a high pressure drop between sands, the history matching routine cannot match the data. As discussed in case 2.2 that the simulation results from GAP and MBAL are similar when the water producing sand is the top most or when WGR

is still low, the automatic history matching algorithm based on MBAL does not work in this case since the water producing sand is at the bottom.

Table 5.11 Summary of automatic history matching of case 4.2

Case	Weighing Factor	Lamda	Initial Guess OGIP		Initial Guess Aquifer Tank 78-6	Converge	Converge Type	Last Iteration OGIP		Aquifer on 78-6	Last Iteration #
			59-1	78-6				59-1	78-6		
1	10	0.001	0.5	0.5	500	No	-	0.0017	505	0.000001	8
2	1	0.001	0.5	0.5	500	No	-	0.0145	11	0.000001	11
3	0.1	0.001	0.5	0.5	500	No	-	0.0134	0.5251	0.000001	22
4	0.01	0.001	0.5	0.5	500	No	-	0.8165	0.2926	9.1516	22
5	0.001	0.001	0.5	0.5	500	Yes	2	0.6265	0.396	496.699	8
6	0.01	0.001	0.7	0.7	500	No	-	0.4283	1.09	1423	18
7	1	1	0.7	0.7	500	No	-	10.41	0.8059	66	98

Case 5: History match simulated data three-layer system

A three tank commingled model in this case is composed of tanks 76-7, 75-3 and 75-6. The individual tank properties in Table 5.12 were used for building multi-tank model with MBAL. The gas rate data and one point individual data of tank gas rate and pressure (representing PLT) was generated and used for testing the automatic history matching spreadsheet. Since the model was built with MBAL, all tanks were assumed to have the same datum depth at 9624' MD or 6,320'TVD. The VLP curves was generated by PROSPER.

The PVT data of all three tanks are shown below:

Gas specific gravity = 1.15, separator pressure = 614 psi, condensate gravity = 55 API, CGR = 9 BBL/MMSCF, water salinity = 100,000 ppm, CO₂ = 47% by mole.

The IPR of the system is shown in Figure 5.27.

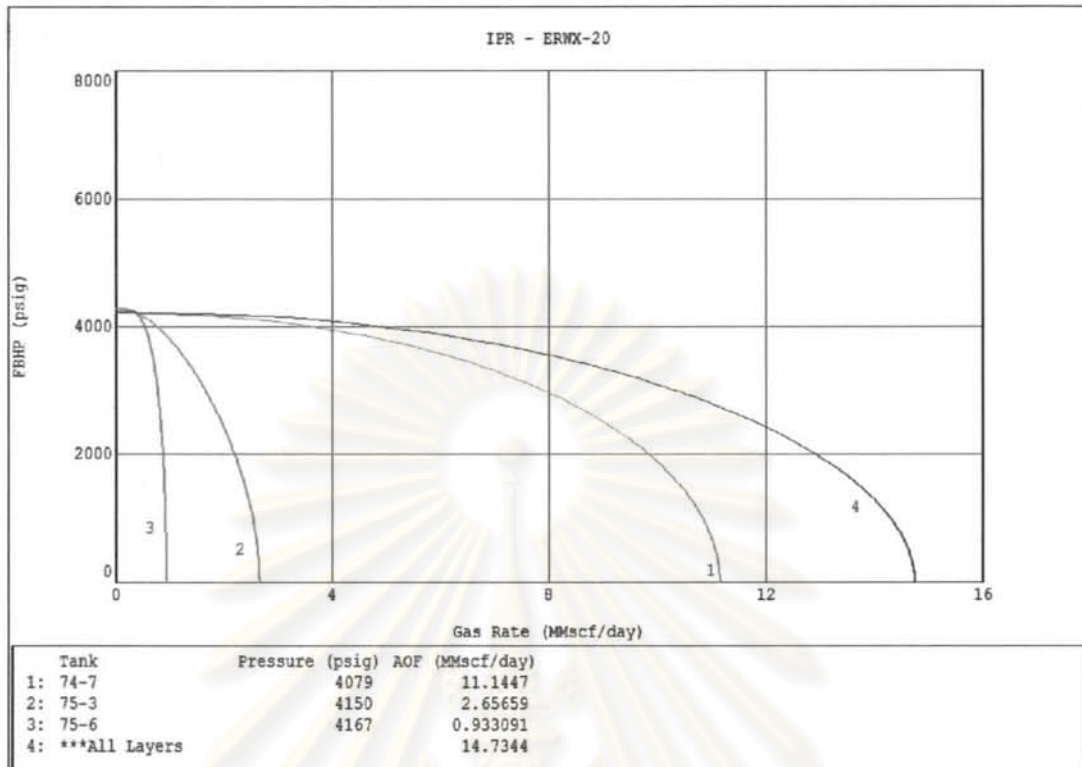


Figure 5.27 System and individual IPR for case 5

Table 5.12 Reservoir data of three-tank commingled system

	Tank : 76-7	Tank : 75-3	Tank : 75-6
Temperature (deg F)	300	300	300
Initial Pressure (PSI)	4,079	4,150	4,167
Porosity	0.2	0.18	0.18
Connate Water Saturation	0.33	0.52	0.54
OGIP (Bscf)	6	0.2	0.8
Well Performance Index C (Mscf/day/PSI ²)	3.437	-	-
Well Performance Index N	0.4841	-	-
Well Performance Index A (PSI ² /CP/Mscf/day)	-	153,302	326,998
Well Performance Index B (PSI ² /CP(Mscf/day) ²)	-	2.936	37.43

Table 5.13 shows the parameters used in the automatic history matching of WT gas rate with one point PLT individual gas rate and tank pressure. Also shown in the table are the results of the regression run.

Table 5.13 Result of automatic history matching of case 5

Case	Weighing Factor	λ	Initial Guess OGIP			Converge	Converge Type	Last Iteration OGIP			Last Iteration #
			74-7	75-3	75-6			74-7	75-3	75-6	
1	1 on all	1E-03	1	1	1	Yes	3	5.22	0.39	1.74	31
2	10 on all	1E-03	1	1	1	No	NA	0.0079	0.9762	1.9646	15
3	1 on all WT, 10 on PLT	1E-03	1	1	1	Yes	3	6	0.1963	0.8019	22*
4	same as 3 but normalized	1E-03	1	1	1	Yes	1 & 3	0.99	1.027	0.9736	9
5	Same as 3	1E03	1	1	1	Yes	3	1.0093	1.0285	1.0043	9
6	Same as 3	1E-05	1	1	1	Yes	3	5.85	0.2048	0.8347	19*

Remarks

- 1) In case # 2, the automatic history match macro stopped running since MBAL terminated simulation before the simulation end date.
- 2) Only Case # 2 did not have converged simulations.

Table 5.14 Comparison of various normalized Σ R2 from converged solution

Case #	Normalized R2
1	0.1998
3	0.0001
4	12.48
5	12.23
6	0.0041

**Table 5.15 Result of history matching from case 5#4, normalized weighing factor
10 times on PLT data**

Date Number	Residual type	Observed	Calculated	Residual
1	WT Date: Gas 3/28/2006	7.10	7.02	0.0738
2	WT Date: Gas 4/4/2006	7.56	6.90	0.6550
3	WT Date: Gas 5/6/2006	10.50	8.83	1.6753
4	WT Date: Gas 5/12/2006	9.37	7.25	2.1172
5	WT Date: Gas 5/15/2006	10.61	8.72	1.8889
6	WT Date: Gas 6/7/2006	9.63	7.05	2.5729
7	WT Date: Gas 6/22/2006	9.67	7.00	2.6689
8	WT Date: Gas 7/5/2006	9.25	6.31	2.9358
9	WT Date: Gas 7/22/2006	8.95	5.82	3.1279
10	WT Date: Gas 8/5/2006	8.83	5.60	3.2351
11	WT Date: Gas 8/15/2006	8.70	5.37	3.3295
12	WT Date: Gas 9/13/2006	8.38	4.98	3.4046
13	WT Date: Gas 10/12/2006	8.00	4.43	3.5726
14	WT Date: Gas 10/30/2006	7.81	4.15	3.6574
15	WT Date: Gas 11/8/2006	7.63	3.85	3.7743
16	WT Date: Gas 11/15/2006	7.51	3.69	3.8161
17	WT Date: Gas 11/29/2006	6.79	0.84	5.9591
18	WT Date: Gas 12/5/2006	6.72	0.16	6.5537
19	WT Date: Gas 12/21/2006	3.28	0.00	3.2837
20	WT Date: Gas 12/27/2006	5.73	0.00	5.7341
21	WT Date: Gas 1/8/2007	7.39	3.79	3.5966
22	WT Date: Gas 1/22/2007	7.12	3.47	3.6510
23	WT Date: Gas 2/13/2007	7.13	3.26	3.8752
24	WT Date: Gas 2/20/2007	7.07	3.33	3.7331
25	WT Date: Gas 3/3/2007	6.91	3.10	3.8083
26	WT Date: Gas 3/19/2007	6.58	2.57	4.0098
27	WT Date: Gas 4/8/2007	6.27	1.50	4.7707
28	WT Date: Gas 4/9/2007	6.29	2.18	4.1044
29	WT Date: Gas 4/29/2007	6.12	1.66	4.4595
30	WT Date: Gas 6/13/2007	6.24	2.93	3.3128
31	WT Date: Gas 6/21/2007	5.99	2.29	3.6981
32	WT Date: Gas 6/29/2007	5.74	0.00	5.7359
NA	Tank Pressure of 74-7 f/PLT Survey on 6/1/2007	2219	959	12600.0000
NA	Tank Pressure of 75-3 f/PLT Survey on 6/1/2007	1511	1531	-200.0000
NA	Tank Pressure of 75-6 f/PLT Survey on 6/1/2007	2510	2665	-1550.0000
NA	Gas rate of 74-7 f/PLT Survey on 6/1/2007	4.97	0.35	46.2000
NA	Gas rate of 75-3 f/PLT Survey on 6/1/2007	0.51	0.93	-4.1799
NA	Gas rate of 75-6 f/PLT Survey on 6/1/2007	0.64	0.70	-0.6154

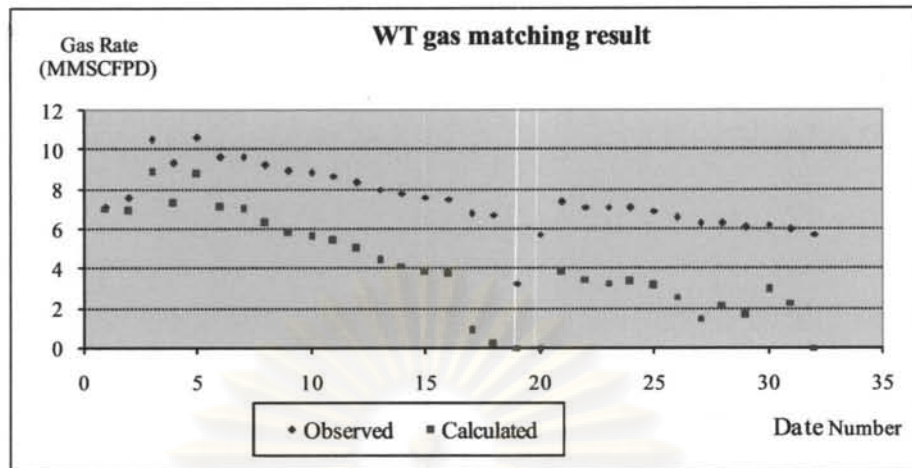


Figure 5.28 Gas WT matching result of case 5#4

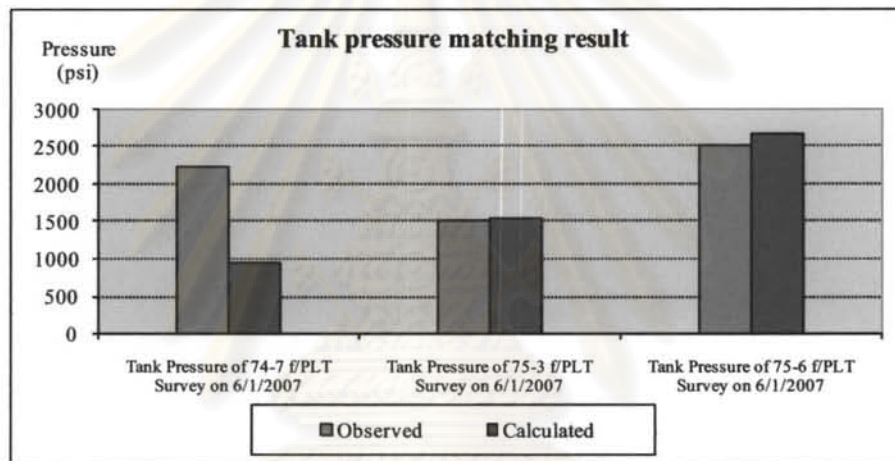


Figure 5.29 Chart of tank pressure history matching result of case 5#4

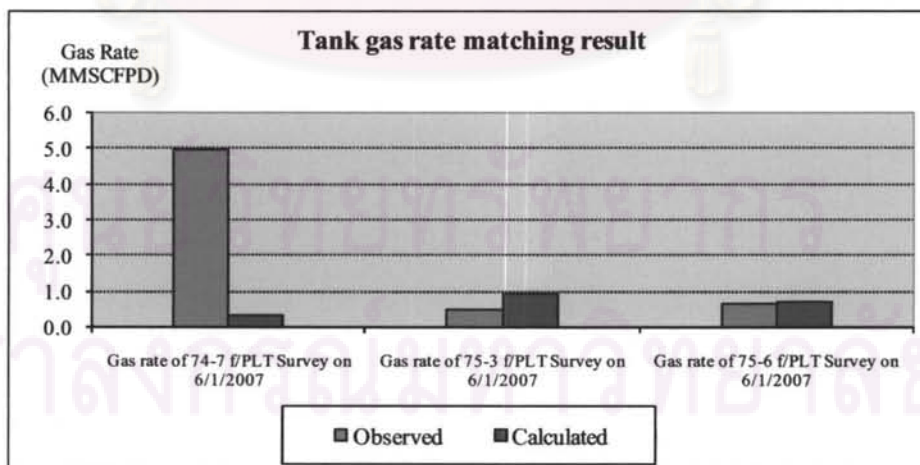


Figure 5.30 Chart of tank gas rate history matching result of case 5#4

Result Discussion

All trials as seen in Table 5.13 reached convergence solutions except case #2 although it has the same initial guess values. Each trial started with different weight factors and/or Lamda (λ). From Table 5.14, case #3 has most correct solutions with the least normalized sigma squares error (error is almost null). From the results, we can extract several observations as follows:

- 1) The weighing factor has the most effect to make the solutions converge to the correct answers. Case #1 with weight factor equal to 1 on all residual can lead to converged solution but the result is not as good as using weighing factor of 10 on PLT data and 1 on WT data as in case # 6 while both cases used the same initial guess values.
- 2) When using a high order of magnitude of Lamda (λ) than the default value (0.001), as in case #5, the convergence was achieved with a little change in OGIP. The effect is similar to the case of using normalized weights.
- 3) When using too much weights in all the residuals as in case#2, the optimization routine stopped prematurely since changes in OGIP are exaggerated which caused the simulation to end before a specified simulation ending period.
- 4) When using normalized weights (all weights summed up to 1) as in case # 4, converged solutions were found but with they were wrong. The answers were found to be very near initial guesses with little changes despite using the same value for other parameters as in the case of least normalized error, case #3. Table 5.15 and Figures 5.28 to 5.30 show the error of history match from case #4 with normalized weighing factors. WT gas rate, tank gas rate and tank pressure from of tank 74-7 are far off from actual value despite converged criteria was achieved in this case #4.

Case 6 to 8: Field example

Example data from gas wells in the GOT (Gulf of Thailand) with production/PLT data were used in cases 6 to 8. Three wells were selected for building the model and testing the automatic history matching spreadsheet.

Case 6: Well A – two-tank commingle model

Four reservoirs are penetrated by well A but from the PLT survey, only two reservoirs (tanks) were flowing namely 70-2 (actual datum of 8,484' MD/7,020' VD) and 77-5 (actual datum of 9,278' MD/7,750' VD). Therefore, a two- tank commingle model was constructed for this well. There was no significant water production observed in this well, thus WT gas rate, individual tank gas rate and pressure were used for history matching with the automatic history matching spreadsheet. The data from the PLT was used for IPR determination with result of well performance index calculated and shown in Table 5.16, and the IPR is plotted in Figure 5.31. PROSPER was used for VLP curve generation.

Table 5.16 Reservoir properties for well A

	Tank : 70-2	Tank : 77-5
Temperature (deg F)	315	332
Initial Pressure (psi)	3100	3600
Porosity	0.19	0.19
Connate Water Saturation	0.35	0.5
Well Performance Index C (Mscf/day/psi ²)	0.0057	0.8039
Well Performance Index n	0.8753	0.5532

The PVT properties were input for both tanks as follows: gas specific gravity = 1.15, separator pressure = 614 psi, condensate gravity = 55 API, CGR = 9 BBL/MMSCF, water salinity = 100,000 ppm, CO₂ = 47% by mole.

The reservoir datum (assumed for all tanks) is 8484'MD or 7020'TVD.

ศูนย์วิทยทรัพยากร
จุฬาลงกรณ์มหาวิทยาลัย

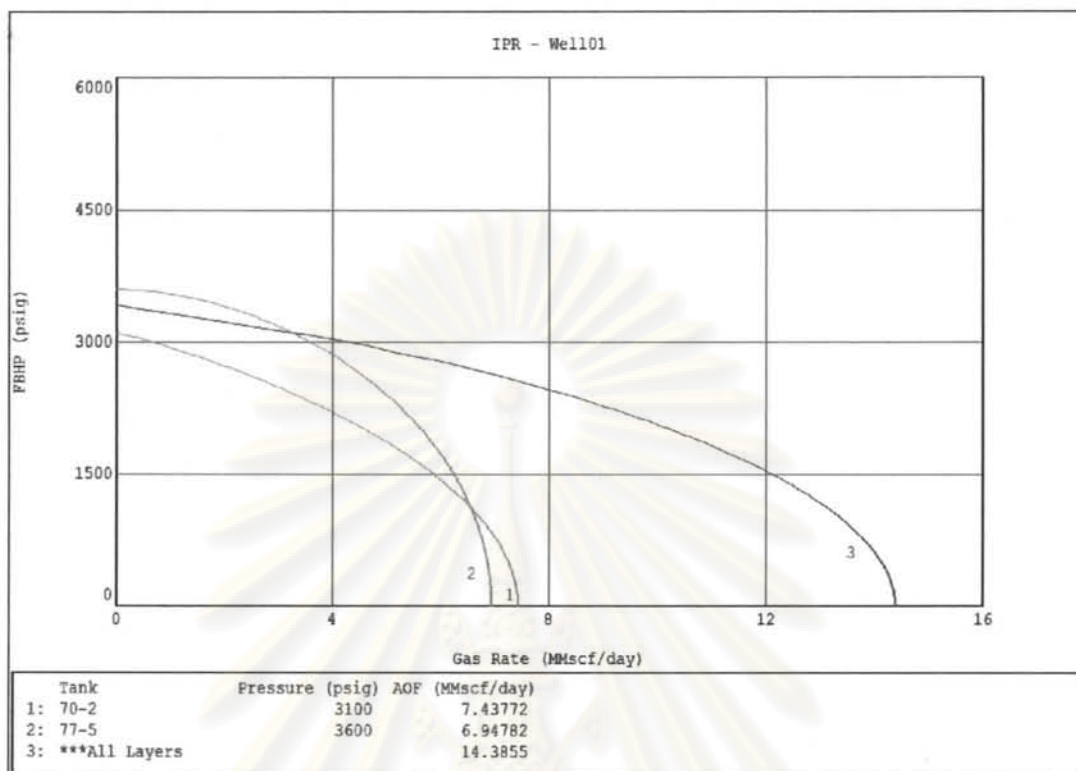


Figure 5.31 IPR of commingle system – well A

The well was perforated first batch in October 2006 for all the four sands. The well has been operated as a swing well (open to supply gas if gas is short of. Choked down or shut in if the gas is more than needed). Therefore, several periods of shut in were observed and entered into tubing head pressure schedule. A MPLT survey was conducted on April 8th, 2007. The history matching period is from the initial perforation date until the day that the MPLT was performed because the 2nd batch of perforation was done on April 14th, 2007. During this period, 16 WT data are available for history matching. No water break through was observed during this period. Therefore, the depletion drive model was used for both tanks in the system. The initial guesses for OGIP of the two tanks were calculated from the volumetric method with inferred areas.

Table 5.17 Result of trial of automatic history matching parameters on well A

Case	Weighing Factor	Lamda	Initial Guess OGIP		Converge	Converge Type	Last Iteration OGIP		Last Iteration #
			70-2	77-5			70-2	77-5	
1	1	0.01	0.9	1	Yes	1 & 3	0.98	1.07	14
2	1 on WT, 0.1 on PLT	0.01	0.9	1	Yes	1 & 3	0.88	1.2	17
3	1 on WT data, 12/06/2006 to 03/10/2007 0.1 on the rest	0.01	0.9	1	Yes	1 & 3	0.9	0.99	13
4	1	0.01	0.5	0.5	Yes	1 & 3	0.99	0.76	31

Table 5.18 Comparison of various normalized $\Sigma R2$ from converged solution

Case #	Normalized $\Sigma R2$
1	0.4843
2	0.5594
3	0.3895
4	0.3727

ศูนย์วิทยทรัพยากร
จุฬาลงกรณ์มหาวิทยาลัย

Table 5.19 Result of automatic history match case 6#4

Date Number	Residual type	Observed	Calculated	Residual
1	WT Date: Gas 10/14/2006	4.11	3.72	0.3944
2	WT Date: Gas 10/27/2006	4.53	4.27	0.2554
3	WT Date: Gas 11/6/2006	4.94	4.85	0.0879
4	WT Date: Gas 12/1/2006	5.82	6.96	-1.1363
5	WT Date: Gas 12/9/2006	5.97	6.72	-0.7485
6	WT Date: Gas 12/21/2006	5.66	6.42	-0.7586
7	WT Date: Gas 1/20/2007	5.37	5.72	-0.3521
8	WT Date: Gas 1/30/2007	5.05	5.50	-0.4539
9	WT Date: Gas 2/6/2007	5.30	5.44	-0.1415
10	WT Date: Gas 2/16/2007	4.10	5.43	-1.3327
11	WT Date: Gas 3/10/2007	4.62	4.81	-0.1856
12	WT Date: Gas 3/18/2007	4.86	4.46	0.4014
13	WT Date: Gas 3/28/2007	4.53	4.21	0.3195
14	WT Date: Gas 4/2/2007	4.41	4.04	0.3673
15	WT Date: Gas 4/8/2007	4.14	3.84	0.3018
16	WT Date: Gas 4/9/2007	3.45	2.63	0.8233
NA	Tank Pressure of 70-2 f/PLT Survey on 4/8/2007	2251	2015	236.0000
NA	Tank Pressure of 77-5 f/PLT Survey on 4/8/2007	2000	1796	204.0000
NA	Gas rate of 70-2 f/PLT Survey on 4/8/2007	2.35	1.94	0.4085
NA	Gas rate of 77-5 f/PLT Survey on 4/8/2007	2.33	1.90	0.4323

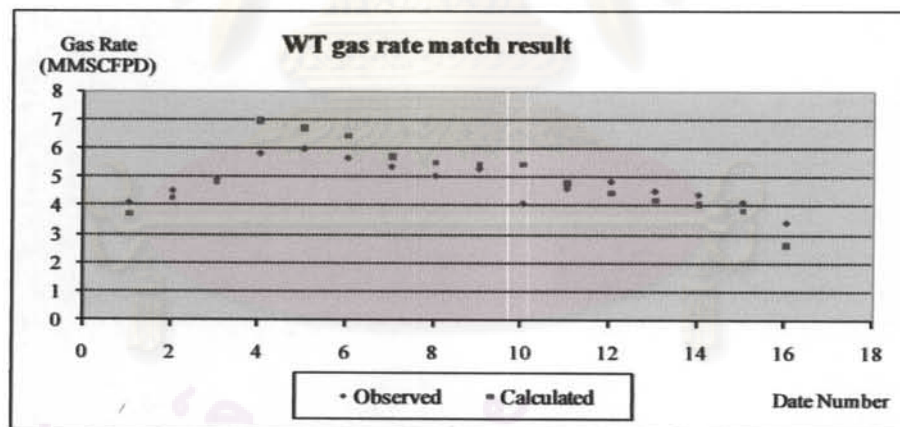


Figure 5.32 Well test automatic history matching result of case 6#4

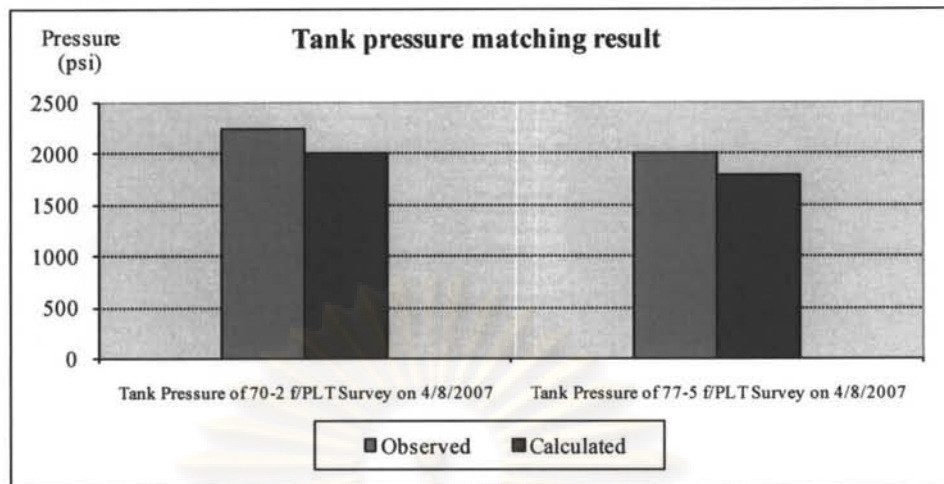


Figure 5.33 Tank pressure matching result of case 6#4

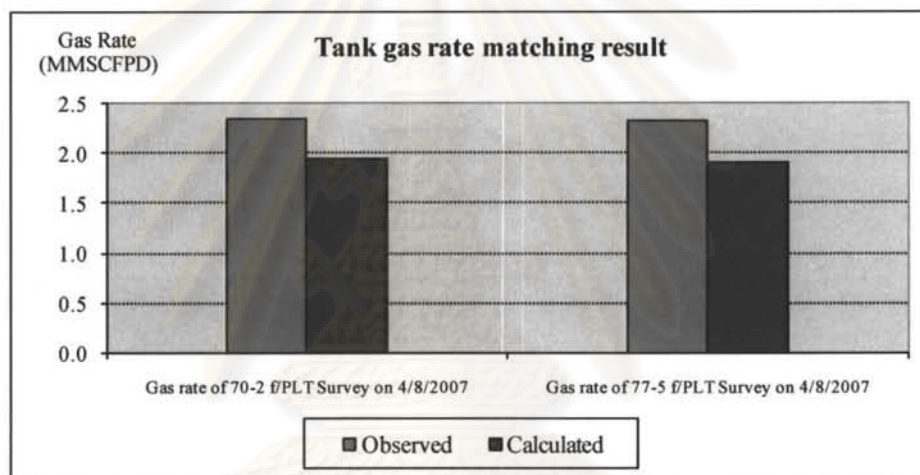


Figure 5.34 Tank gas rate matching result of case 6#4

Table 5.20 OGIP of individual layer of well A compared with various methods

	OGIP from MBAL & automatic history match	OGIP from CWM
Tank 70-2, Bscf	0.99	0.92
Tank 77-5, Bscf	0.76	0.96

Result Discussion

- 1) From Table 5.17, OGIP of tank 70-2 seems to be consistent in all trial cases at around 0.88-0.99 Bscf.
- 2) From Table 5.18, result of matching showed that trial case # 4 has the lowest normalized $\Sigma R2$ which should reflect the most correct solutions. Table 5.19 and Figure 5.32 to 5.34 show the result of history matching of trial case #4. From table 5.19, we can see the total gas rate matches quite well except between the period of 12/1/2006 until 2/16/2006. Individual gas rate of both tank are lower than actual value but pressure of both tanks matches quite well
- 3) From Figure 5.32, WT gas rate between 12/1/2006 to 03/10/2006 cannot be matched very well in this trial case #4 which has the least normalized $\Sigma R2$ as well as case trial #3 which has more weight in this WT residual interval.
- 4) From Table 5.20, OGIPs from the trial case with the least normalized $\Sigma R2$ are a bit different from OGIPs calculated by commingle wellbore model (CWM), proposed by Last^[1]. OGIPs calculated from CWM was close to the result of trial case #3 which has the second least normalized $\Sigma R2$.

Case 7: Well B – six-tank commingle model

In this trial case, eight reservoirs were penetrated by a single well but only six sands flow during a PLT survey, namely, 59-1 (formation top is at 9,680' MD and 5,910' VD), 63-4 (formation top is at 10,183' MD and 6,340' VD), 68-4 (formation top is at 10,770' MD and 6,840' VD), 69-6 (formation top is at 10,908' MD and 6,960' VD), 78-1 (formation top is at 11,902' MD and 7,810' VD), 78-6 (formation top is at 11,954' MD and 7,860' VD). The individual reservoir properties of each tank are shown in Table 5.21. The well started production on October 6th, 2006. WT history between October 6th, 2006 and January 25th, 2007 and one multi rate PLT data, run on January 27th, 2007, were used for history matching and constructing IPR of each tank. The IPR parameters are shown in table 5.21, and the IPR curve is shown in Figure 5.35. The reservoir top of the shallowest tank is at 9,680' MD or 5,910' TVD. This datum was assumed to be the datum point of other reservoirs due to MBAL limitation that it cannot account for the pressure drop between reservoirs.

Table 5.21 Reservoir properties for all sands in well B

	Tank					
	59-1	63-4	68-4	69-6	78-1	78-6
Temperature (deg F)	267	280	296	300	327	328
Initial Pressure (psi)	2,549	2,829	3,028	3,155	3,616	3,682
Porosity	0.22	0.22	0.22	0.22	0.18	0.17
Connate Water Saturation	0.45	0.49	0.46	0.41	0.49	0.43
Well Performance Index C (Mscf/day/psi ²)	-	0.000516	0.000179	0.0014	0.000891	-
Well Performance Index n	-	0.999	1	0.9346	0.8326	-
Well Performance Index A (psi ² /cp/Mscf/day)	120451	-	-	-	-	193353
Well Performance Index B (psi ² /cp(Mscf/day) ²)	35.99	-	-	-	-	0
OGIP from Volumetric Method (Bscf)	0.6	0.26	0.6	1.16	0.35	0.85

Remark: A = Darcy Coefficient and B = Non Darcy Coefficient in Forchheimer Pseudo pressure IPR equation

The PVT properties were input for both tanks as follows: gas specific gravity = 0.878, separator pressure = 750 psi, condensate gravity = 55 API, CGR = 12 BBL/MMSCF, water salinity = 100,000 ppm, CO₂ = 15% by mole.

The well was perforated second batch on February 6th, 2007. The history matching period started from October 10th, 2006 and ended on January 30th, 2007. A total of 9 WT data points and one PLT were used in the history matching. No water was observed during period of history matching, therefore, depletion drive model was used.

The initial guesses for all tank OGIPs were from the volumetric method calculated from inferred areas except trial case #4 that the initial guess of OGIP of tank 69-5 was found by trial and error.

ศูนย์วิทยทรัพยากร
จุฬาลงกรณ์มหาวิทยาลัย

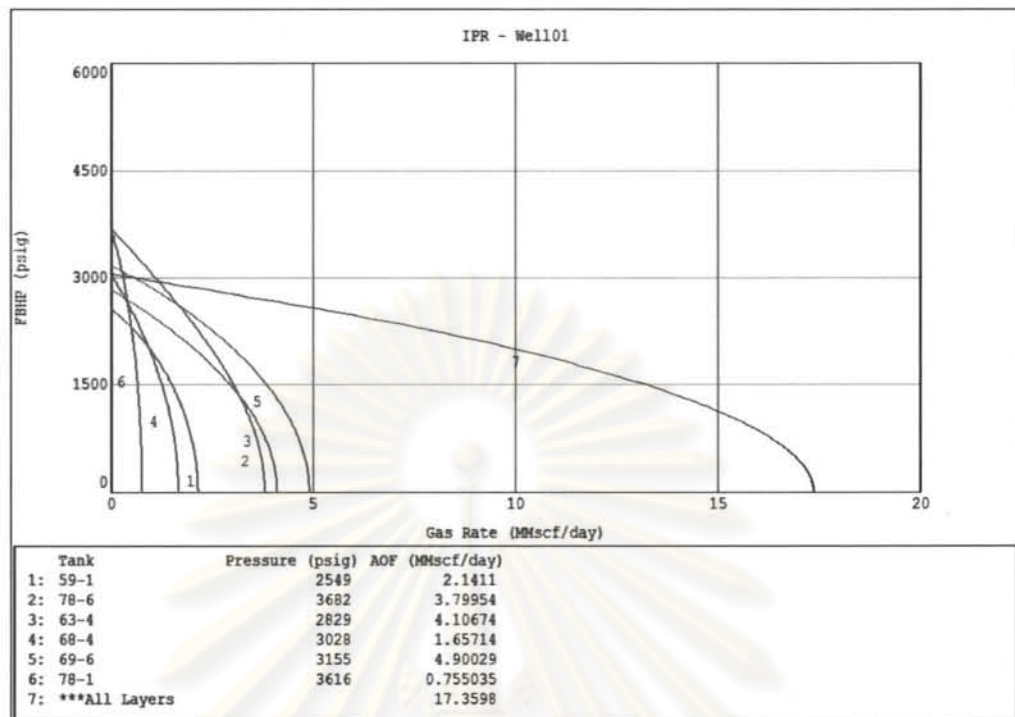


Figure 5.35 IPR of commingle system - well B

ศูนย์วิทยทรัพยากร
จุฬาลงกรณ์มหาวิทยาลัย

Table 5.22 Result of various trials of automatic history matching parameters

Case	Weighing Factor	Lamda	Initial OGIP						Con verge	Last Iteration OGIP						Last Iteration #
			59-1	63-4	68-4	69-6	78-1	78-6		59-1	63-4	68-4	69-6	78-1	78-6	
1	1	0.01	0.61	0.26	0.6	1.16	0.35	0.85	NA	0.34	0.01	0.62	1.08	0.37	0.63	4
2	10	0.01	0.61	0.26	0.6	1.16	0.35	0.85	3	0.61	0.26	0.6	1.16	0.35	0.85	9
3	1 on WT, 10 on PLT	0.01	0.6	0.26	0.6	1.16	0.35	0.85	3	0.2	0.12	0.58	1.36	0.43	0.45	25
4	1 on WT, 10 on PLT	0.01	0.6	0.26	0.6	0.5	0.35	0.85	3	0.55	0.23	0.58	0.57	0.4	0.55	

Table 5.23 Comparison of various normalized $\Sigma R2$ error from converged solution

Case #	Normalized $\Sigma R2$
2	3.278
3	2.3992
4	2.1567

Table 5.24 Comparison of OGIP of individual sands using different methods (software)

	OGIP from MBAL & automatic history match, case trial #4	OGIP from CWM
Tank 59-1, Bscf	0.55	0.07
Tank 63-4, Bscf	0.23	0.079
Tank 68-4, Bscf	0.58	1.062
Tank 69-6, Bscf	0.57	0.873
Tank 78-1, Bscf	0.4	0.268
Tank 78-6, Bscf	0.55	0.241
Total, Bscf	2.88	2.593

ศูนย์วิทยทรัพยากร
จุฬาลงกรณ์มหาวิทยาลัย

Table 5.25 Result of automatic history matching case 7 #4

Date Number	Residual type	Observed	Calculated	Residual
1	WT Date: Gas 10/6/2006	2.40	4.96	-2.5630
2	WT Date: Gas 10/18/2006	3.62	4.74	-1.1227
3	WT Date: Gas 10/30/2006	3.35	5.08	-1.7330
4	WT Date: Gas 11/11/2006	3.25	4.47	-1.2170
5	WT Date: Gas 12/4/2006	3.09	3.81	-0.7197
6	WT Date: Gas 12/20/2006	3.16	3.28	-0.1208
7	WT Date: Gas 1/21/2007	6.69	7.44	-0.7530
8	WT Date: Gas 1/24/2007	7.20	7.24	-0.0370
9	WT Date: Gas 1/25/2007	2.00	2.48	-0.4821
NA	Tank Pressure of 59-1 f/PLT Survey on 1/23/2007	2447.00	2449.00	-20.0000
NA	Tank Pressure of 63-4 f/PLT Survey on 1/23/2007	2436.00	2374.00	620.0000
NA	Tank Pressure of 68-4 f/PLT Survey on 1/23/2007	2809.00	2750.00	590.0000
NA	Tank Pressure of 69-6 f/PLT Survey on 1/23/2007	2600.00	2521.00	790.0000
NA	Tank Pressure of 78-1 f/PLT Survey on 1/23/2007	3075.00	3204.00	-1290.0000
NA	Tank Pressure of 78-6 f/PLT Survey on 1/23/2007	2683.00	2795.00	-1120.0000
NA	Gas rate of 59-1 f/PLT Survey on 1/23/2007	1.02	1.19	-1.7639
NA	Gas rate of 63-4 f/PLT Survey on 1/23/2007	1.03	1.45	-4.1591
NA	Gas rate of 68-4 f/PLT Survey on 1/23/2007	1.27	0.86	4.0933
NA	Gas rate of 69-6 f/PLT Survey on 1/23/2007	1.65	1.87	-2.1832
NA	Gas rate of 78-1 f/PLT Survey on 1/23/2007	0.62	0.47	1.4360
NA	Gas rate of 78-6 f/PLT Survey on 1/23/2007	1.31	1.45	-1.3933

ศูนย์วิทยทรัพยากร
จุฬาลงกรณ์มหาวิทยาลัย

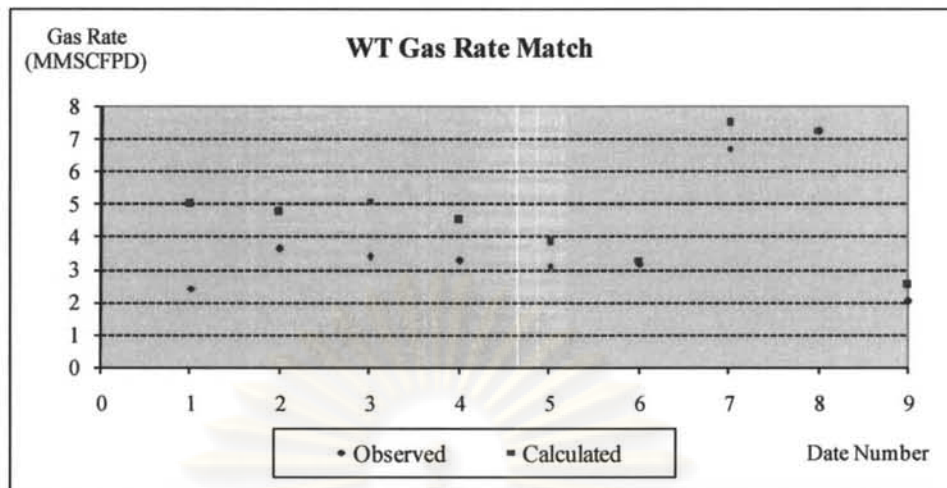


Figure 5.36 WT gas rate matching result of case 7#4

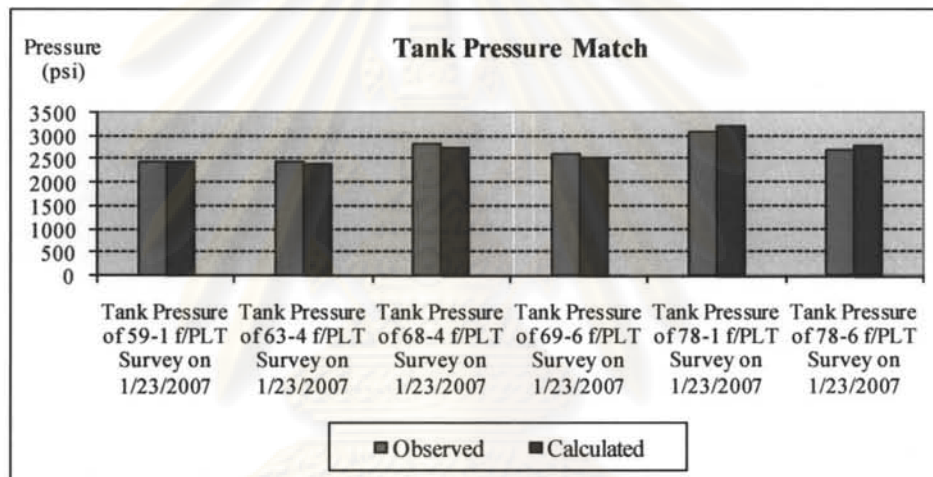


Figure 5.37 Tank pressure matching result of case 7#4

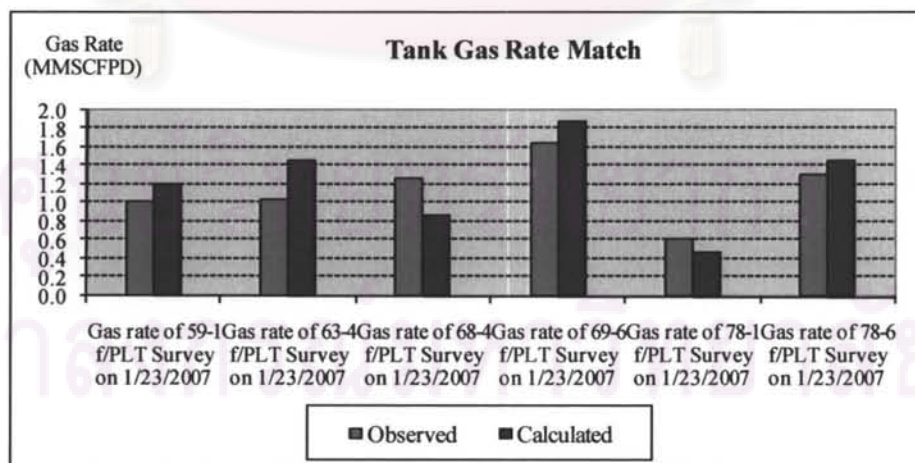


Figure 5.38 Tank gas rate matching result of case 7#4

Result Discussion

From Table 5.22, the following points can be observed:

- 1) When using weighting factors = 1, the optimization routine was prematurely terminated as in case #1.
- 2) When using weighing factors = 10, the optimization routine had the solutions equal to the guess values in iteration # 9 as in case #2.
- 3) When using weighting factor = 1 on WT and 10 on PLT data, the optimization routine converged with a lower normalized $\Sigma R2$ error.
- 4) When performing history matching manually with OGIP = 0.5 Bcf on 69-6 (by trial and error) and kept OGIP of other tanks from original volumetric calculation with inferred area, the normalized $\Sigma R2$ error was lower. After using the same initial guess for OGIP on other tanks but changing the initial guess OGIP on 69-6 to 0.5 Bscf, the new solutions from the auto matching spreadsheet were obtained with a lower error and hence selected as the solution.

From the observation above, we can see that there is a limitation in the optimization algorithm used in the automatic history matching spreadsheet. There is the limitation of local minimum into which the solution can be trapped, especially when there were many variables to be determined, such as in this case of six commingled tanks.

From Table 5.23, it can be concluded that trial case # 4 had the lowest normalized $\Sigma R2$ error and should be closet to the actual solutions.

From Table 5.24, it was found that individual OGIP from the method proposed in this thesis and CWM have some discrepancy. Despite the fact that case #4 has lowest normalized $\Sigma R2$ error, the qualities of the match on WT gas rate and PLT gas rate (of individual tank) are not as good as in the other cases. The total well OGIP calculated with the P/Z plot for the well by the asset engineer is only 1.1 Bscf which is much less than the sum of individual zone OGIP determined by the two methods.

Case 8: Well C – five-tank commingled well with one watered-out layer.

In this case, fifteen reservoirs were penetrated by well C, and the production started in March 2006. Water production was observed since the first well test but the trend of water has been increasing only gradually during the period of history matching. A MPLT survey was conducted on June 15, 2007. Only 5 reservoirs were found producing; therefore, only 5 tanks were used in the multi-tank model, namely, 63-2 (formation top is at 9,624' MD and 6,320' VD), 69-4 (formation top is at 10,520' MD and 6,940' VD), 74-7 (formation top is at 11,290' MD and 7,470' VD), 75-3 (formation top is at 11,372' MD and 7,530' VD), 75-6 (formation top is at 11,422' MD and 7,560' VD). The IPR was determined from MPLT data as shown in Table 5.26 and Figure 5.40. The top most reservoir formation (63-2) is at 9,624 MD (6,320 TVD) which was used for VLP curve generation.

The PVT properties were input for all tanks as follows: gas specific gravity = 1.15, separator pressure = 614 psi, condensate gravity = 55 API, CGR = 9 BBL/MMSCF, water salinity = 100,000 ppm, CO₂ = 47% by mole. Properties of each layer are summarized in Table 5.26.

Table 5.26 Reservoir properties for all layers modeled in well C

	Tank				
	63-2	69-4	74-7	75-3	75-6
Temperature (deg F)	283	294	300	300	300
Initial Pressure (psi)	2,400	3,500	4,079	4,150	4,167
Porosity	0.26	0.17	0.20	0.18	0.18
Connate Water Saturation	0.33	0.36	0.33	0.52	0.54
Well Performance Index C (Mscf/day/psi ²)	0.000163	9	3.437	-	-
Well Performance Index n	0.998	0.2803	0.4841	-	-
Well Performance Index A (psi ² /cp/Mscf/day)	-	-	-	153,302	326,998
Well Performance Index B (psi ² /cp(Mscf/day) ²)	-	-	-	2.93689	37.43

Table 5.27 Relative permeability for well C from Boatman correlation

Sw	S*	Krw B	Krg B	Sg
0.36	0	0	1	0.64
0.389	0.1	0.0001	0.8019	0.611
0.418	0.2	0.0016	0.6144	0.582
0.447	0.3	0.0081	0.4459	0.553
0.476	0.4	0.0256	0.3024	0.524
0.505	0.5	0.0625	0.1875	0.495
0.563	0.7	0.2401	0.0459	0.437
0.534	0.6	0.1296	0.1024	0.466
0.592	0.8	0.4096	0.0144	0.408
0.621	0.9	0.6561	0.0019	0.379
0.65	1	1	0	0.35

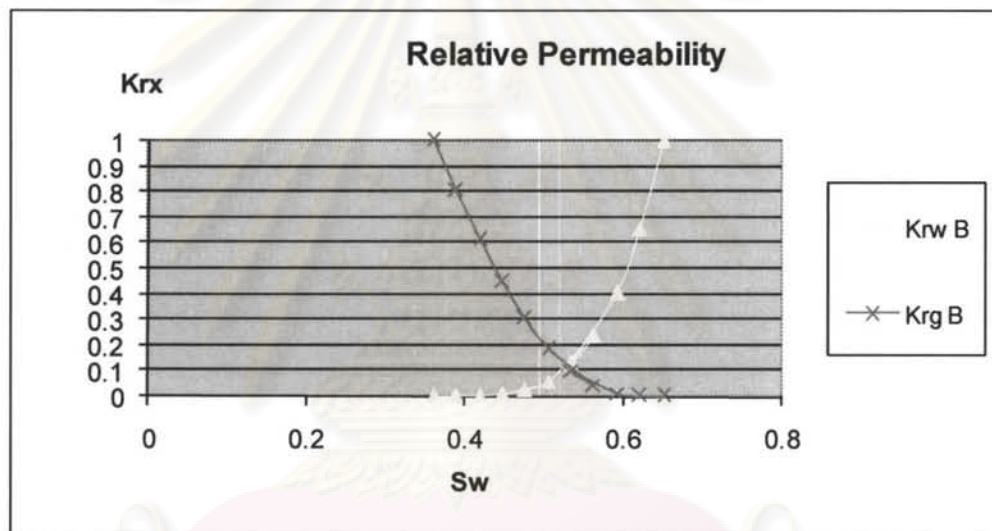
**Figure 5.39 Relative permeability curve calculated from Boatman correlation**

Table 5.27 and Figure 5.39 show the relative permeability data used for the watered-out tank, 69-4. Boatman correlation was used for constructing this relative permeability data. The following properties were used in Boatman correlation:

$$S_{wi} = 0.36$$

$$\phi = 0.17$$

$$S_{gr} = 0.35 (0.35 \phi)$$

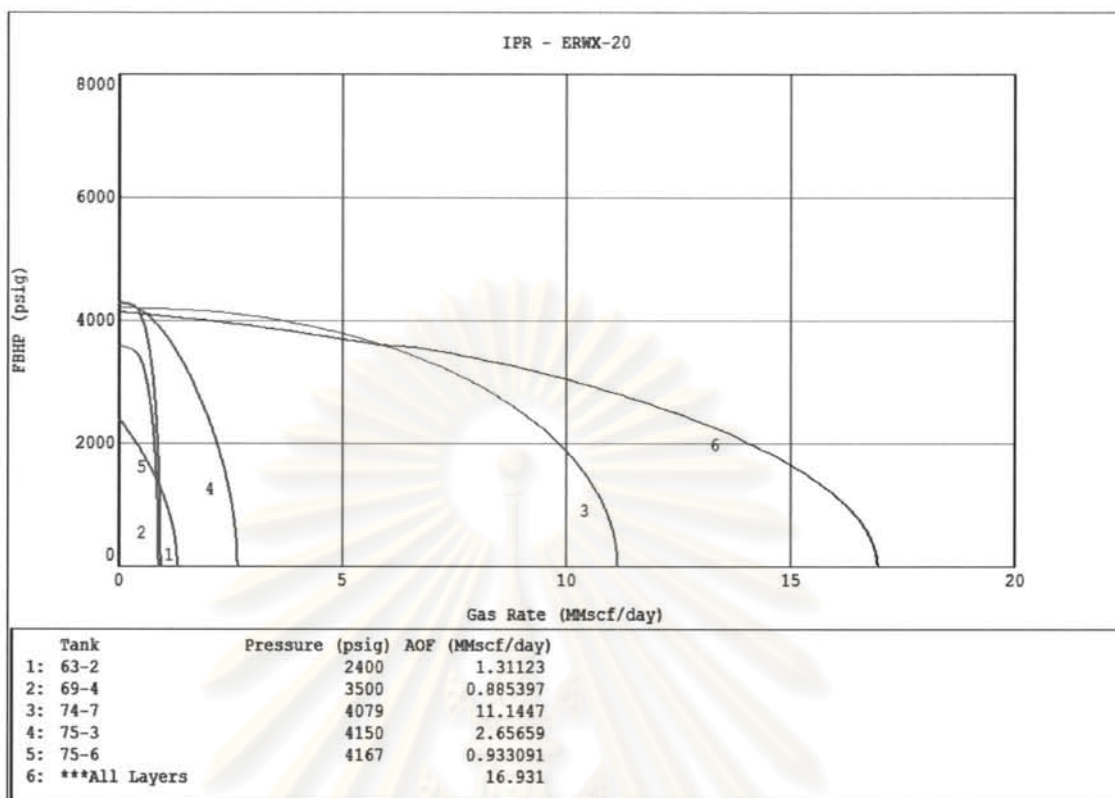


Figure 5.40 IPR of commingle system - well C

Initial guess of OGIP was from trial manually with “manual” worksheet in the automatic history matching spreadsheet since there was no OGIP calculated from the volumetric method with inferred area. From Table 5.28, only case #4, which used weighing factors = 1 on all residuals, had the converged solutions. Table 5.29 and Figures 5.41 to 5.45 show the result of history matching of case #4. Most of the historical data were matched quite well except WT water rate and water rate of tank 69-4.

ศูนย์วิทยทรัพยากร
จุฬาลงกรณ์มหาวิทยาลัย

Table 5.28 Result of various trials of automatic history matching parameters

Case	Weight Factor	Landa	Initial Guess OGIP					Initial Guess Aquifer 69-4	Convergence Type	Last Iteration OGIP					Last Initial Aquifer 69-4	Last Iteration #
			63-2	69-4	74-7	75-3	75-6			63-2	69-4	74-7	75-3	75-6		
1	1	0.001	0.1	0.1	6	0.1	0.1	70	NA	0.09	0.1	6.16	0.13	0.13	68.5	19
2	10	0.001	0.1	0.1	6	0.1	0.1	70	NA	0.68	0.12	15.68	0.01	4.72	0.0317	88
3	1 on all WT, 10 on PLT	0.001	0.1	0.1	6	0.1	0.1	70	NA	0.06	0.1	3.08	0.12	0	116	0
4	1	0.001	0.5	0.13	6.52	1.1	0.5	9	3	0.1	0.12	6.92	1.93	0.4	4.75	2

Only case# 4 had the converged solution. Normalized ΣR^2 error of converged solution trial case #4 is 24.84.

Table 5.29 Result of automatic history matching case 8#5

Date Number	Residual type	Observed	Calculated	Residual
1	WT Date: Gas 3/28/2006	3.62	6.04	-2.4185
2	WT Date: Gas 4/4/2006	4.29	7.57	-3.2771
3	WT Date: Gas 5/6/2006	15.82	11.84	3.9804
4	WT Date: Gas 5/12/2006	11.12	10.62	0.5039
5	WT Date: Gas 5/15/2006	11.34	12.17	-0.8344
6	WT Date: Gas 6/7/2006	9.61	11.29	-1.6760
7	WT Date: Gas 6/22/2006	10.34	11.44	-1.0953
8	WT Date: Gas 7/5/2006	10.42	11.05	-0.6285
9	WT Date: Gas 7/22/2006	9.56	10.65	-1.0931
10	WT Date: Gas 8/5/2006	9.92	10.37	-0.4464
11	WT Date: Gas 8/15/2006	9.72	10.17	-0.4477
12	WT Date: Gas 9/13/2006	9.48	9.58	-0.0998
13	WT Date: Gas 10/12/2006	8.81	9.28	-0.4733
14	WT Date: Gas 10/30/2006	8.43	9.12	-0.6885
15	WT Date: Gas 11/8/2006	8.32	9.00	-0.6770
16	WT Date: Gas 11/15/2006	8.01	8.93	-0.9175
17	WT Date: Gas 11/29/2006	7.50	8.72	-1.2180
18	WT Date: Gas 12/5/2006	7.49	8.59	-1.0975
19	WT Date: Gas 12/21/2006	4.30	5.06	-0.7564
20	WT Date: Gas 12/27/2006	7.33	7.41	-0.0756
21	WT Date: Gas 1/8/2007	7.68	8.63	-0.9490
22	WT Date: Gas 1/22/2007	7.30	8.26	-0.9637
23	WT Date: Gas 2/13/2007	8.86	8.52	0.3393
24	WT Date: Gas 2/20/2007	7.60	8.28	-0.6811
25	WT Date: Gas 3/3/2007	7.37	8.08	-0.7104
26	WT Date: Gas 3/19/2007	6.80	7.74	-0.9359
27	WT Date: Gas 4/8/2007	6.59	7.58	-0.9873
28	WT Date: Gas 4/9/2007	6.54	7.58	-1.0369
29	WT Date: Gas 4/29/2007	6.46	7.42	-0.9636
30	WT Date: Gas 6/13/2007	9.04	7.43	1.6098
31	WT Date: Gas 6/21/2007	6.27	7.11	-0.8390
32	WT Date: Gas 6/29/2007	6.16	6.91	-0.7493
1	WT Date: Water 3/28/2006	82	0	81.9862
2	WT Date: Water 4/4/2006	20	0	19.8236
3	WT Date: Water 5/6/2006	81	2	79.1420
4	WT Date: Water 5/12/2006	50	2	48.0759
5	WT Date: Water 5/15/2006	83	2	80.5548
6	WT Date: Water 6/7/2006	63	6	56.5803
7	WT Date: Water 6/22/2006	36	17	18.8665
8	WT Date: Water 7/5/2006	70	34	35.7404
9	WT Date: Water 7/22/2006	80	65	14.6018
10	WT Date: Water 8/5/2006	161	121	39.9131

Table 5.29 Result of automatic history matching case 8#5 (continued)

Date Number	Residual type	Observed	Calculated	Residual
11	WT Date: Water 8/15/2006	116	147	-31.0158
12	WT Date: Water 9/13/2006	90	191	100.7851
13	WT Date: Water 10/12/2006	132	166	-34.1494
14	WT Date: Water 10/30/2006	159	147	11.5652
15	WT Date: Water 11/8/2006	148	126	21.7973
16	WT Date: Water 11/15/2006	159	112	46.8744
17	WT Date: Water 11/29/2006	122	12	109.5859
18	WT Date: Water 12/5/2006	143	12	130.9939
19	WT Date: Water 12/21/2006	51	3	47.8491
20	WT Date: Water 12/27/2006	126	5	120.5975
21	WT Date: Water 1/8/2007	142	99	42.6479
22	WT Date: Water 1/22/2007	154	130	23.7901
23	WT Date: Water 2/13/2007	105	60	45.3533
24	WT Date: Water 2/20/2007	136	83	52.6730
25	WT Date: Water 3/3/2007	175	96	78.9408
26	WT Date: Water 3/19/2007	159	104	55.1001
27	WT Date: Water 4/8/2007	219	71	147.8636
28	WT Date: Water 4/9/2007	217	76	141.1182
29	WT Date: Water 4/29/2007	212	72	139.6445
30	WT Date: Water 6/13/2007	167	82	85.1181
31	WT Date: Water 6/21/2007	191	91	99.6269
32	WT Date: Water 6/29/2007	173	75	97.6149
NA	Tank Pressure of 63-2 f/PLT Survey on 6/1/2007	2237	2031	206.0000
NA	Tank Pressure of 69-4 f/PLT Survey on 6/1/2007	1613	1728	-115.0000
NA	Tank Pressure of 74-7 f/PLT Survey on 6/1/2007	2260	2448	-188.0000
NA	Tank Pressure of 75-3 f/PLT Survey on 6/1/2007	2160	2515	-355.0000
NA	Tank Pressure of 75-6 f/PLT Survey on 6/1/2007	2103	2064	39.0000
NA	Gas rate of 63-2 f/PLT Survey on 6/1/2007	0.24	0.18	0.0655
NA	Water rate of 63-2 f/PLT Survey on 6/1/2007	0	0	-0.0558
NA	Gas rate of 69-4 f/PLT Survey on 6/1/2007	0.28	0.28	0.0021
NA	Water rate of 69-4 f/PLT Survey on 6/1/2007	100	71	29.2443
NA	Gas rate of 74-7 f/PLT Survey on 6/1/2007	4.83	5.17	-0.3448
NA	Water rate of 74-7 f/PLT Survey on 6/1/2007	0	3	-2.9177
NA	Gas rate of 75-3 f/PLT Survey on 6/1/2007	1.13	1.39	-0.2588
NA	Water rate of 75-3 f/PLT Survey on 6/1/2007	0	3	-3.1372
NA	Gas rate of 75-6 f/PLT Survey on 6/1/2007	0.53	0.31	0.2160
NA	Water rate of 75-6 f/PLT Survey on 6/1/2007	0	1	-1.0429

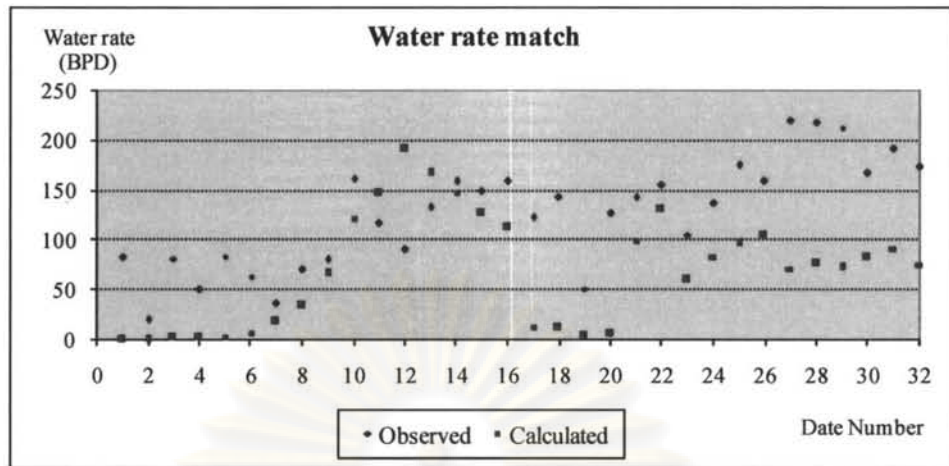


Figure 5.41 WT water rate match result of case 8#5

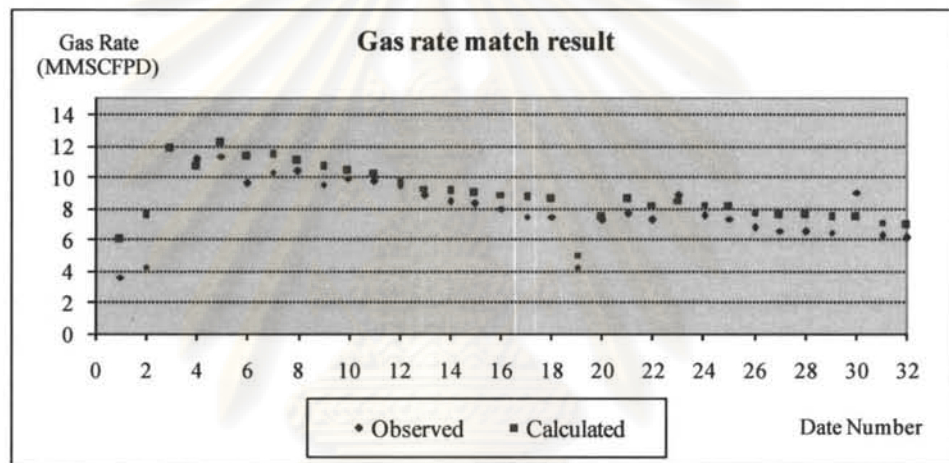


Figure 5.42 WT gas rate match result of case 8#5

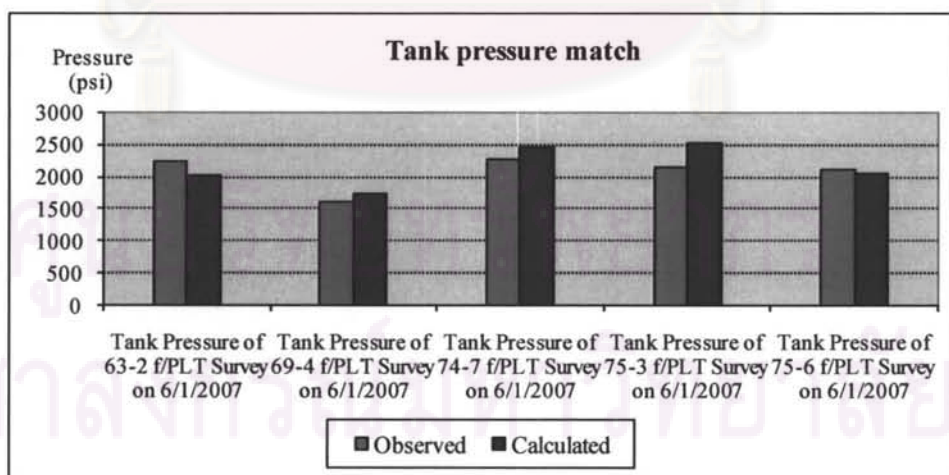


Figure 5.43 Tank pressure matching result of case 8#5

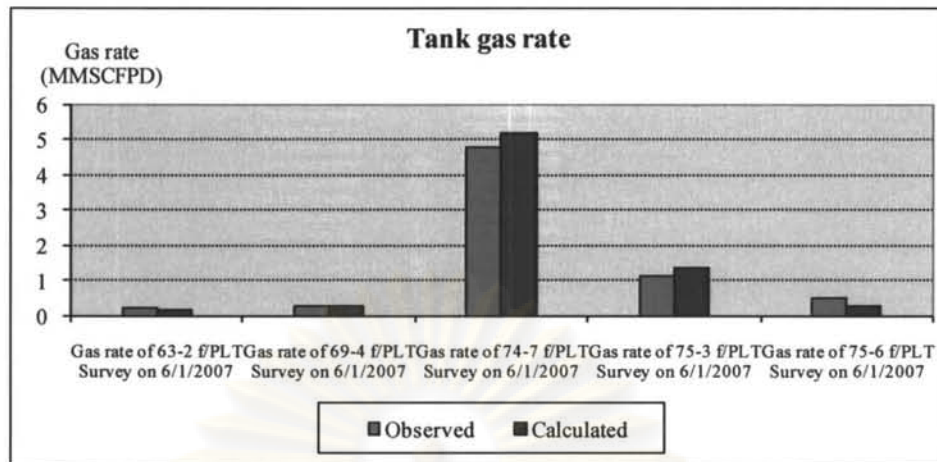


Figure 5.44 Tank gas rate matching result of case 8#5

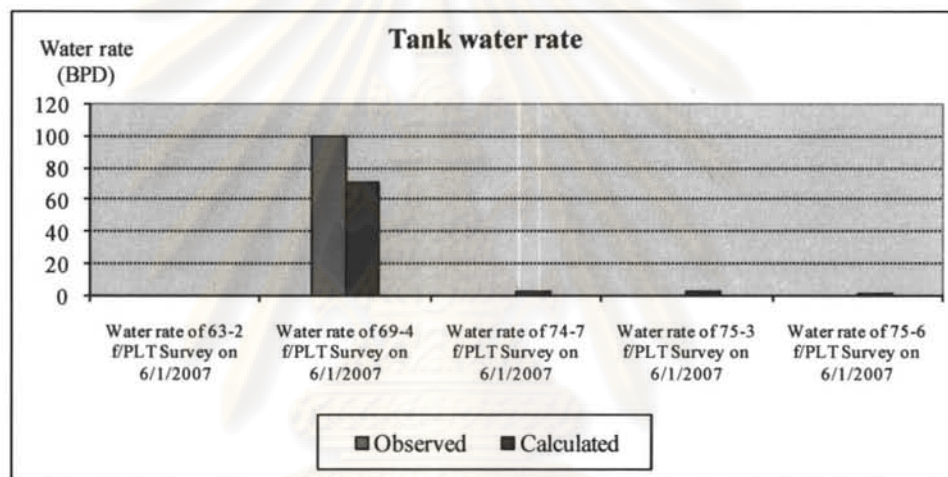


Figure 5.45 Tank water rate matching result of case8#5

Only one convergence was obtained from the history matching as seen in Table 5.28. Up to this point, the algorithm is reviewed. The new idea to use normalized error function instead of Equation 3.1 came up.

$$E(\bar{p}) = \sum_{m=1}^{Nr} W_m^2 \left[\frac{H_m^c(\bar{p}) - H_m^{obs}}{H_m^{obs}} \right]^2 \quad (4.1)$$

Table 5.30 Result of new trials performed with normalized error in the algorithm

Case	Weighing Factor	Lamda	Initial Guess OGIP					Initial Guess Aquifer 69-4	Convergence Type	Last Iteration OGIP					Last Initial Aquifer 69-4	Last Iteration #
			63-2	69-4	74-7	75-3	75-6			63-2	69-4	74-7	75-3	75-6		
1	1	0.001	0.5	0.5	4	0.5	0.5	5	NA	0.01	0.03	83.02	0.00	0.00	130.930	12
2	1 on all WT, 10 on PLT	0.001	0.5	0.5	4	0.5	0.5	5	NA	0.95	70.51	0.01	0.07	0.97	82.230	54
3	1 on all WT, 10 on PLT	0.001	0.5	0.5	4	0.5	0.5	5	2	0.21	0.36	4.06	0.22	1.11	5.010	1
4*	1	0.001	0.5	0.13	6.52	1.1	0.5	9	3	0.01	0.11	7.04	2.38	0.04	4.773	2
5	1 on all WT, 10 on PLT	0.001	0.5	0.13	6.52	1.1	0.5	4.773	NA	0.68	0.02	2.71	0.70	0.56	0.000	17
6	1 on all WT, 10 on PLT Normalized	0.001	0.5	0.13	6.52	1.1	0.5	4.773	3	0.50	0.13	6.52	1.10	0.50	6.773	0
7	1 on all WT, 10 on PLT	0.001	0.5	0.5	4	0.5	0.5	5	2	0.21	0.36	4.06	0.22	1.11	5.010	1

Table 5.31 Comparison of various normalized $\Sigma R2$ from converged solution

Case #	Normalized $\Sigma R2$
3	40.52
4	24.13
6	29.89
7	40.5

After running a new history matching process with normalized error functions using different regression parameters, the results are summarized in Table 5.30.

From Table 5.30, it can be observed that there are four trial cases that reaches converged solutions. Of all the four cases, case #4 has the lowest $\Sigma R2$ and should be closet to the actual answers.

When comparing the solutions case 4 when the normalized error and original error definition were used, the solutions in the case of normalized error has a lower $\Sigma R2$ error (24.13 vs 24.84). Hence solution of case 4 with normalized error should be the closet solutions. Table 5.32 and Figures 5.46 to 5.50 show the result of history matching of this least $\Sigma R2$ error of trial case #4. Total gas rate in Figures 5.47 matches quite well but total water rate in Figures 5.46 and tank water rate of tank 69-4 in Figures 5.50 do not match well. This may be due to incorrect relative permeability parameters. Tank gas rate in Figure 5.49 shows good match except tank 75-3 as well as its tank pressure rate in Figure 5.48 which shows bigger discrepancy than other tanks.

The OGIP for this well was only calculated with the well P/Z plot (without water influx taken into account). It was calculated to be about 9 Bscf. Summation of individual OGIP solution from trial case # 4 is about 9.58 Bscf which is a bit higher than the one obtained from conventional P/Z plot.

It looks as if the automatic history matching algorithm with normalized error function finds better solutions than the algorithm with un-normalized error function since the

lowest ΣR^2 error of the trial cases with this normalized error algorithm is lower than ΣR^2 error of the trial cases of algorithm with conventional error definition.

Table 5.32 Result of automatic history matching case 8#4 normalized error

Date Number	Residual type	Observed	Calculated	Residual
1	WT Date: Gas 3/28/2006	3.62	6.04	-2.4208
2	WT Date: Gas 4/4/2006	4.29	7.48	-3.1866
3	WT Date: Gas 5/6/2006	15.82	11.04	4.7752
4	WT Date: Gas 5/12/2006	11.12	9.53	1.5945
5	WT Date: Gas 5/15/2006	11.34	11.35	-0.0121
6	WT Date: Gas 6/7/2006	9.61	10.19	-0.5804
7	WT Date: Gas 6/22/2006	10.34	10.44	-0.1026
8	WT Date: Gas 7/5/2006	10.42	10.27	0.1544
9	WT Date: Gas 7/22/2006	9.56	9.85	-0.2907
10	WT Date: Gas 8/5/2006	9.92	9.63	0.2852
11	WT Date: Gas 8/15/2006	9.72	9.54	0.1815
12	WT Date: Gas 9/13/2006	9.48	8.99	0.4875
13	WT Date: Gas 10/12/2006	8.81	8.91	-0.1047
14	WT Date: Gas 10/30/2006	8.43	8.77	-0.3353
15	WT Date: Gas 11/8/2006	8.32	8.50	-0.1770
16	WT Date: Gas 11/15/2006	8.01	8.43	-0.4201
17	WT Date: Gas 11/29/2006	7.50	8.30	-0.8018
18	WT Date: Gas 12/5/2006	7.49	8.24	-0.7503
19	WT Date: Gas 12/21/2006	4.30	4.93	-0.6294
20	WT Date: Gas 12/27/2006	7.33	7.43	-0.1025
21	WT Date: Gas 1/8/2007	7.68	8.66	-0.9784
22	WT Date: Gas 1/22/2007	7.30	7.94	-0.6356
23	WT Date: Gas 2/13/2007	8.86	8.69	0.1660
24	WT Date: Gas 2/20/2007	7.60	8.31	-0.7051
25	WT Date: Gas 3/3/2007	7.37	8.09	-0.7162
26	WT Date: Gas 3/19/2007	6.80	7.59	-0.7884
27	WT Date: Gas 4/8/2007	6.59	7.51	-0.9228
28	WT Date: Gas 4/9/2007	6.54	7.30	-0.7607
29	WT Date: Gas 4/29/2007	6.46	7.36	-0.9026
30	WT Date: Gas 6/13/2007	9.04	7.59	1.4458
31	WT Date: Gas 6/21/2007	6.27	7.02	-0.7480
32	WT Date: Gas 6/29/2007	6.16	6.88	-0.7180
1	WT Date: Water 3/28/2006	82	0	81.9324
2	WT Date: Water 4/4/2006	20	0	19.5241
3	WT Date: Water 5/6/2006	81	3	78.3236
4	WT Date: Water 5/12/2006	50	2	47.6181
5	WT Date: Water 5/15/2006	83	4	78.7121
6	WT Date: Water 6/7/2006	63	12	50.9268
7	WT Date: Water 6/22/2006	36	29	6.8813
8	WT Date: Water 7/5/2006	70	56	14.2590
9	WT Date: Water 7/22/2006	80	97	-16.6268
10	WT Date: Water 8/5/2006	161	168	-6.8533

**Table 5.32 result of automatic history matching case8#4 normalized error
(continued)**

Date Number	Residual type	Observed	Calculated	Residual
11	WT Date: Water 8/15/2006	116	182	-66.3059
12	WT Date: Water 9/13/2006	90	199	-109.4381
13	WT Date: Water 10/12/2006	132	144	-11.7408
14	WT Date: Water 10/30/2006	159	132	27.0459
15	WT Date: Water 11/8/2006	148	130	18.0542
16	WT Date: Water 11/15/2006	159	115	43.7313
17	WT Date: Water 11/29/2006	122	5	117.0962
18	WT Date: Water 12/5/2006	143	5	137.9661
19	WT Date: Water 12/21/2006	51	3	48.1188
20	WT Date: Water 12/27/2006	126	5	120.9667
21	WT Date: Water 1/8/2007	142	77	64.8227
22	WT Date: Water 1/22/2007	154	128	25.8546
23	WT Date: Water 2/13/2007	105	49	55.7960
24	WT Date: Water 2/20/2007	136	71	65.3498
25	WT Date: Water 3/3/2007	175	82	92.8914
26	WT Date: Water 3/19/2007	159	93	65.5497
27	WT Date: Water 4/8/2007	219	47	171.7961
28	WT Date: Water 4/9/2007	217	81	135.5367
29	WT Date: Water 4/29/2007	212	59	153.3657
30	WT Date: Water 6/13/2007	167	71	95.6698
31	WT Date: Water 6/21/2007	191	90	101.4754
32	WT Date: Water 6/29/2007	173	71	102.2853
NA	Tank Pressure of 63-2 f/PLT Survey on 6/1/2007	2237	2016	221.0000
NA	Tank Pressure of 69-4 f/PLT Survey on 6/1/2007	1613	1732	-119.0000
NA	Tank Pressure of 74-7 f/PLT Survey on 6/1/2007	2260	2450	-190.0000
NA	Tank Pressure of 75-3 f/PLT Survey on 6/1/2007	2160	2825	-665.0000
NA	Tank Pressure of 75-6 f/PLT Survey on 6/1/2007	2103	1803	300.0000
NA	Gas rate of 63-2 f/PLT Survey on 6/1/2007	0.24	0.22	0.0245
NA	Water rate of 63-2 f/PLT Survey on 6/1/2007	1	0	0.9099
NA	Gas rate of 69-4 f/PLT Survey on 6/1/2007	0.28	0.26	0.0212
NA	Water rate of 69-4 f/PLT Survey on 6/1/2007	100	58	42.2111
NA	Gas rate of 74-7 f/PLT Survey on 6/1/2007	4.83	5.14	-0.3096
NA	Water rate of 74-7 f/PLT Survey on 6/1/2007	1	3	-1.8938
NA	Gas rate of 75-3 f/PLT Survey on 6/1/2007	1.13	1.56	-0.4245
NA	Water rate of 75-3 f/PLT Survey on 6/1/2007	1	3	-1.7950
NA	Gas rate of 75-6 f/PLT Survey on 6/1/2007	0.53	0.36	0.1629
NA	Water rate of 75-6 f/PLT Survey on 6/1/2007	1	1	-0.3201

จุฬาลงกรณ์มหาวิทยาลัย

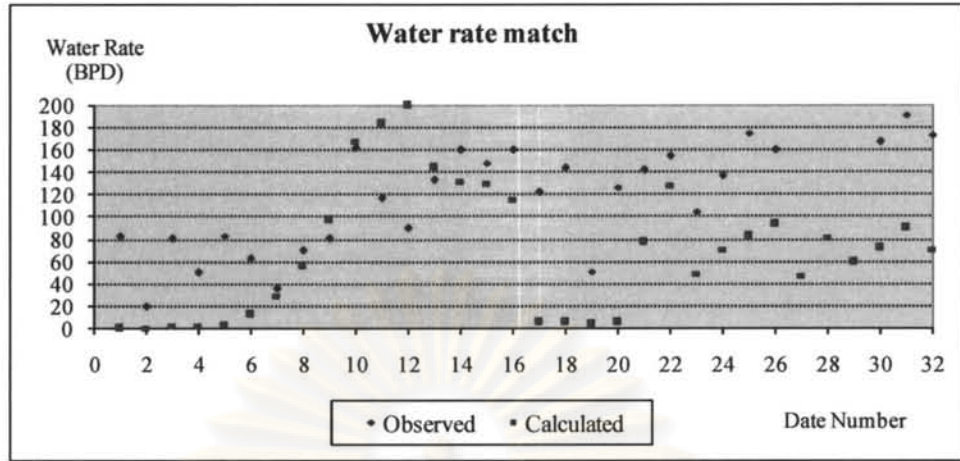


Figure 5.46 WT water rate matching result of case8#4 normalized error

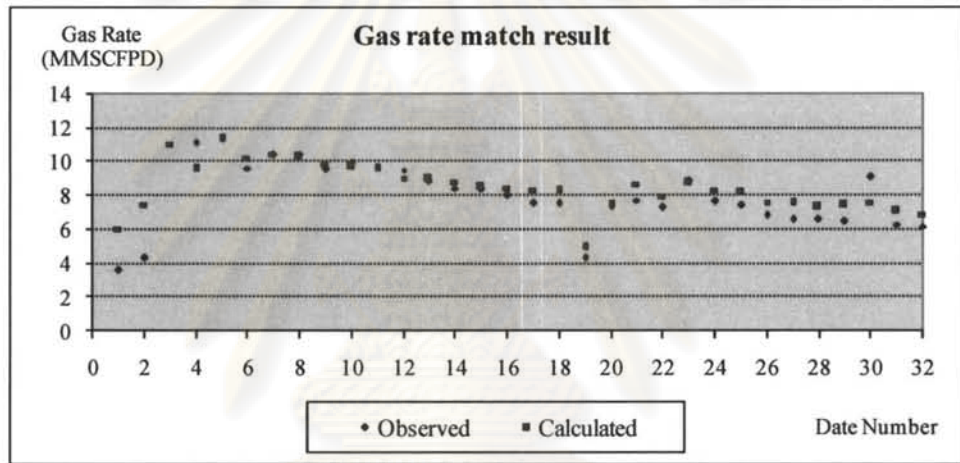


Figure 5.47 Result of WT water matching result case 8#4 normalized error

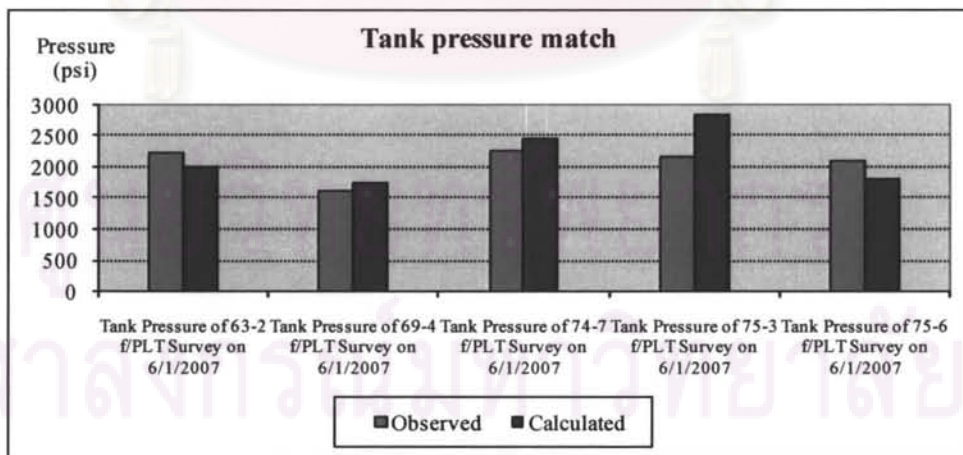


Figure 5.48 Result of tank pressure matching result case case 8#4 normalized error

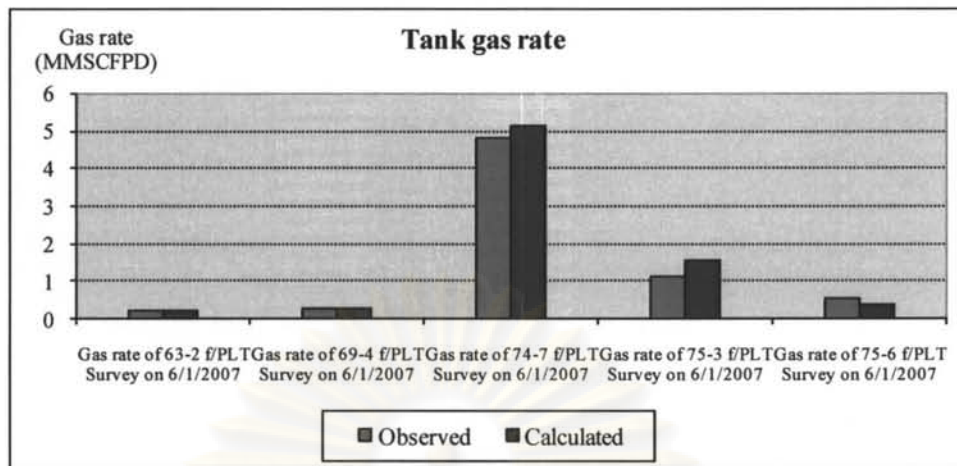


Figure 5.49 Result of tank gas rate matching result of case case 8#4 normalized error

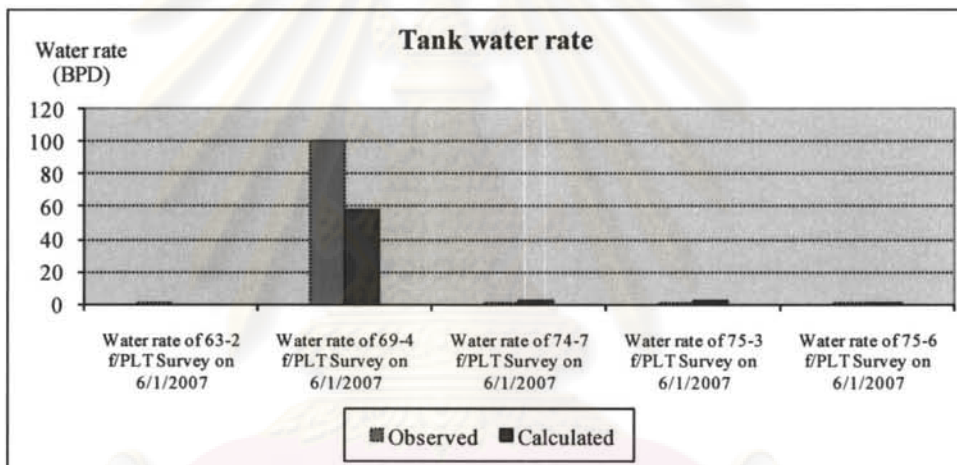


Figure 5.50 Result of tank water rate matching result of case 8#4 normalized error

5.2 Construction and Testing of Neural Network for Gas Well Critical Loading Velocity Determination

5.2.1 Turner Critical Rate

Calculation of Turner's critical velocity and gas rate is performed using Equation 2.11 mentioned in Chapter 2. Assuming gas specific gravity of 0.85, 15% CO₂ and Dranchuk et al. correlation to compute the Z factor, Turner critical velocities calculated at respective wellhead conditions are compared with actual latest gas rates shown in Table 5.33.

The result in Table 5.33 shows that all wells were still flowing above Turner's critical rate before the latest well test. This could have two different meanings, i.e., Turner's velocity equation might not be applicable to our well conditions (commingled production) or the wells were very sensitive to line pressure that when the line pressure swung up to the value close to FTP, the wells went to no flow for this reason, not because of liquid loading.

Table 5.33 Turner's critical gas loading velocity and rate

Actual Data	Input Parameters		Turner's Parameters				Last Gas Rate higher than Qg?
	FTP psig	TEMP deg F.	Z	Gas Density (lb/ft ³)	Turner Vg (ft/sec)	Turner Qg (MMscf/day)	
1.730	300	130	0.954	1.246	14.338	0.760	Yes
2.600	530	179	0.930	2.185	10.787	0.957	Yes
3.490	489	200	0.935	2.005	11.270	0.888	Yes
1.920	516	205	0.952	1.874	11.663	0.945	Yes
2.420	640	165	0.917	2.540	9.992	1.109	Yes
2.390	432	123	0.936	1.820	11.837	0.931	Yes
1.810	427	134	0.943	1.750	12.074	0.915	Yes
2.137	405	189	0.949	1.497	13.068	0.854	Yes
2.940	440	149	0.944	1.760	12.041	0.916	Yes
2.137	405	189	0.959	1.497	13.068	0.845	Yes
1.781	455	201	0.939	1.857	11.717	0.854	Yes
1.781	455	201	0.939	1.857	11.716	0.853	yes
3.319	531	166	0.939	2.077	11.070	0.994	yes
1.865	406	170	0.954	1.553	12.826	0.861	yes
3.375	452	199	0.957	1.649	12.444	0.887	yes
3.171	574	164	0.934	2.265	10.591	1.037	yes
2.230	580	157	0.930	2.324	10.455	1.050	yes
2.040	522	154	0.936	2.029	11.202	1.011	yes
2.075	414	135	0.943	1.697	12.265	0.899	yes
2.230	580	157	0.930	2.324	10.455	1.050	yes
3.384	580	154	0.978	0.690	19.312	1.855	yes
1.617	409	225	0.966	1.422	13.411	0.824	yes
1.697	225	179	0.975	0.830	17.593	0.631	yes
1.634	390	126	0.943	1.622	12.547	0.880	yes
1.862	433	151	0.946	1.723	12.169	0.906	yes
1.616	410	168	0.953	1.575	12.736	0.867	yes
1.690	436	156	0.947	1.719	12.184	0.905	yes
2.191	483	164	0.944	1.886	11.625	0.948	yes
1.796	543	142	0.929	2.335	10.429	1.007	Yes
2.077	416	192	0.958	1.531	12.920	0.855	Yes
1.860	490	118	0.926	2.106	10.991	1.001	Yes
1.977	416	189	0.958	1.539	12.885	0.857	Yes
1.819	404	169	0.954	1.548	12.847	0.860	Yes

Table 5.33 Turner's critical gas loading velocity and rate (continued)

Actual Data	Input Parameters		Turner's Parameters				
	FTP psig	TEMP deg F.	Z	Gas Density (lb/ft ³)	Turner Vg (ft/sec)	Turner Qg (MMscf/day)	Last Gas Rate higher than Qg?
1.900	405	178	0.956	1.527	12.938	0.854	Yes
1.860	490	118	0.926	2.106	10.991	1.001	Yes
1.790	406	173	0.955	1.545	12.862	0.859	Yes
1.872	446	174	0.951	1.701	12.249	0.901	Yes
3.760	700	188	0.930	2.670	9.740	1.124	Yes
1.860	490	118	0.926	2.106	10.991	1.001	Yes
3.610	616	144	0.920	2.548	9.976	1.099	Yes
3.515	277	195	0.972	1.001	16.010	0.692	Yes
1.872	446	174	0.951	1.701	12.249	0.901	Yes
1.848	465	152	0.942	1.855	11.724	0.940	Yes
2.027	541	172	0.940	2.094	11.024	0.998	Yes
1.670	410	163	0.952	1.590	12.675	0.871	Yes
1.790	406	173	0.955	1.545	12.862	0.859	Yes
2.270	520	203	0.951	1.896	11.595	0.950	Yes
4.470	869	199	0.921	3.294	8.748	1.246	Yes
2.320	533	187	0.946	2.003	11.275	0.976	Yes
2.770	360	135	0.950	1.464	13.215	0.836	Yes
1.720	524	207	0.952	1.897	11.589	0.950	Yes
4.974	604	204	0.944	2.215	10.713	1.026	Yes
1.630	390	129	0.944	1.612	12.586	0.877	Yes
2.522	582	153	0.928	2.352	10.392	1.056	Yes
1.630	390	129	0.944	1.612	12.586	0.877	Yes
2.020	193	200	0.981	0.685	19.372	0.574	Yes
1.681	419	165	0.951	1.621	12.554	0.879	Yes
1.800	573	163	0.933	2.266	10.590	1.037	Yes
1.540	549	156	0.934	2.195	10.762	1.021	Yes
1.553	401	150	0.949	1.592	12.665	0.872	Yes
1.864	401	169	0.954	1.536	12.898	0.856	Yes
2.830	280	190	0.971	1.020	15.861	0.699	Yes
2.450	570	125	0.917	2.443	10.193	1.076	Yes
3.760	700	240	0.948	2.426	10.227	1.073	Yes
3.480	550	160	0.935	2.182	10.795	1.018	Yes
3.589	280	253	0.979	0.922	16.685	0.665	Yes
1.610	550	190	0.945	2.059	11.118	0.989	Yes
1.630	209	198	0.970	0.746	18.566	0.604	Yes
2.819	443	177	0.952	1.680	12.327	0.895	yes
1.929	205	199	0.980	0.730	18.767	0.592	yes
3.310	262	225	0.978	0.900	16.894	0.657	yes
1.878	201	191	0.979	0.725	18.834	0.590	yes
1.913	194	177	0.799	0.716	18.956	0.719	yes
1.941	192	184	0.980	0.700	19.169	0.580	yes
2.210	522	158	0.937	2.072	11.083	0.993	yes
2.300	765	261	0.950	2.570	9.933	1.103	yes

5.2.2 Neural Network for Critical Gas Rate and its prediction result

After going through these sudden death well records as described in the methodology in Section 4.2, chapter 4, these records were used for building a neural network for future prediction of critical rate in the field. All the records for training and validating are shown in Table 5.34. All records for testing were shown in table 5.35. The histogram which shows the distribution of data for training/validating compared with that of the data used in the testing are shown in Figure 5.51. Similar distribution between the two groups can be observed for all parameters.

Training and validating data set

Table 5.34 Training and validated data set records

Record #	Pressure Difference (psi)	CGR (bbl/MMscf)	WGR (bbl/MMscf)	SITP (psig)	MD (ft)	TVDSS (ft)	BHT (deg F)	GAS (MMscfd)
1	13	5.846	137.049	1,366	9,672	8,150	346	1.540
2	61	24.419	469.186	1,200	13,158	8,080	321	1.720
3	25	39.910	17.738	1,196	12,041	9,320	377	1.804
4	16	1.610	14.488	757	12,425	9,630	375	1.864
5	14	1.676	13.967	757	12,425	9,630	375	1.790
6	16	26.535	21.662	2,284	11,834	8,030	310	1.847
7	22	4.338	39.041	1,311	11,061	8,320	363	2.075
8	13	21.812	11.104	632	10,335	8,170	322	2.522
9	54	21.972	30.141	490	12,240	9,320	331	3.550
10	29	14.730	71.384	963	12,294	9,220	391	1.765
11	16	1.610	14.488	757	12,425	9,630	375	1.864
12	32	68.201	10.879	1,709	10,600	8,870	376	2.390
13	211	4.007	70.517	1,099	11,789	9,250	370	2.496
14	67	6.877	19.484	1,040	10,444	7,450	307	3.490
15	93	0.711	152.533	1,444	11,433	8,530	340	4.222
16	24	40.331	34.254	1,246	11,129	9,150	352	1.810
17	22	10.215	37.097	1,178	10,963	9,830	408	1.860
18	17	36.053	20.677	928	14,230	8,890	345	1.886
19	21	1.508	11.059	1,944	14,355	9,510	383	1.989
20	16	6.441	32.850	879	13,340	9,450	380	1.553
21	19	5.390	31.142	879	13,340	9,450	380	1.670
22	29	3.540	33.377	1,499	12,424	8,650	348	1.977
23	19	1.981	10.401	1,944	14,355	9,510	383	2.019
24	71	4.950	40.099	1,177	12,438	10,170	388	2.020
25	70	35.242	339.648	1,200	13,158	8,080	321	2.270
26	14	1.676	13.967	757	12,425	9,630	375	1.790
27	20	38.548	29.043	996	13,700	9,510	360	1.894
28	15	9.979	9.453	2,284	11,834	8,030	310	1.904
29	16	12.464	14.022	2,649	13,036	8,470	290	1.925
30	73	23.323	68.415	641	14,429	9,580	390	1.929

Table 5.34 Training and validated data set records (continued)

Record #	Pressure Difference (psi)	CGR (bbl/MMscf)	WGR (bbl/MMscf)	SITP (psig)	MD (ft)	TVDSS (ft)	BHT (deg F)	GAS (MMscfd)
31	26	2.941	28.922	1,044	11,625	8,240	330	2.040
32	19	6.429	19.931	1,802	14,600	9,090	370	1.555
33	22	8.318	67.138	1,458	13,196	9,690	390	1.683
34	20	4.947	48.368	1,090	14,720	9,670	380	1.819
35	17	21.899	26.171	1,139	12,041	9,320	377	1.872
36	22	10.000	72.308	1,065	10,015	8,490	299	2.600
37	21	46.111	21.111	2,284	11,834	8,030	310	1.800
38	55	2.130	63.364	1,226	12,438	10,170	388	1.878
39	32	68.201	10.879	1,709	10,600	8,870	376	2.390
40	16	10.577	28.948	1,044	11,625	8,240	330	1.796
41	17	21.899	26.171	1,139	12,041	9,320	377	1.872
42	16	35.031	20.722	2,284	11,834	8,030	310	2.027
43	17	1.224	6.733	1,592	14,355	9,510	383	1.634
44	26	7.303	174.719	1,081	12,527	9,710	392	1.780
45	28	25.650	18.810	1,196	12,041	9,320	377	2.339
46	70	2.394	135.638	1,600	8,738	6,740	300	3.760
47	18	46.805	24.291	1,246	11,129	9,150	352	1.688
48	13	38.124	68.193	996	13,700	9,510	360	1.862
49	87	4.532	112.689	1,200	10,692	6,810	280	3.310
50	58	12.506	61.212	412	13,370	9,410	384	3.039
51	82	8.889	44.446	1,079	13,099	9,360	368	3.375
52	22	10.215	37.097	1,178	10,963	9,830	408	1.860
53	26	40.833	27.691	876	13,664	9,250	374	2.131
54	38	0.591	8.570	632	10,335	8,170	322	3.384
55	99	100.204	189.208	1,211	11,902	9,180	350	1.697
56	94	36.390	17.089	1,237	11,346	8,990	376	4.974
57	22	10.215	37.097	1,178	10,963	9,830	408	1.860
58	69	40.104	425.000	1,200	13,158	8,080	321	1.920
59	30	77.978	6.498	750	9,758	8,300	307	2.770
60	36	38.046	52.159	1,161	11,129	9,150	352	1.630
61	39	32.328	320.259	1,200	13,158	8,080	321	2.320
62	57	14.694	268.980	1,200	13,158	8,080	321	2.450
63	63	7.420	158.657	1,160	6,759	6,100	274	2.830
64	53	0.936	23.783	725	10,840	9,470	395	5.340
65	20	9.829	191.897	1,515	12,885	9,600	392	2.137
66	20	9.829	191.897	1,515	12,885	9,600	392	2.137
67	10	35.632	91.667	1,000	12,225	9,070	312	3.480
68	3	7.389	1.478	490	12,521	9,180	350	2.030
69	362	73.602	200.671	1,560	9,700	7,480	315	4.470
70	13	0.000	3.023		10,335	8,170	322	1.985
71	13	0.000	3.023		10,335	8,170	322	1.985
72	16	0.000	0.000	1,592	14,355	9,510	383	1.630
73	16	0.000	0.000	1,592	14,355	9,510	383	1.630
74	23	0.000	19.863	723	11,656	9,660	392	2.819
75	71	277.686	317.355	1,330	11,820	8,020	297	2.420
76	80	34.441	3.625	1,250	6,594	4,450	300	3.310
77	224	60.001	0.000		11,524	8,800	364	2.300
78	104	17.729	79.780	292	12,240	8,750	373	3.610
79	36	12.219	119.021		12,607	10,090	410	2.210
80	140	8.251	35.848	404	10,949	9,480	372	3.515

Table 5.34 Training and validated data set records (continued)

Record #	Pressure Difference (psi)	CGR (bbl/MMscf)	WGR (bbl/MMscf)	SITP (psig)	MD (ft)	TVDSS (ft)	BHT (deg F)	GAS (MMscfd)
81	157	4.737	39.008	404	10,949	9,480	372	3.589
82	23	5.202	109.249	440	5,806	3,730	298	1.730
83	70	19.086	78.807	1,350	14,884	10,440	412	3.248
84	315	58.165	114.774	1,900	6,296	5,680	272	6.430
85	67	1.568	63.769	1,226	12,438	10,170	388	1.913
86	45	0.603	34.950	2,149	10,330	6,490	250	3.319
87	24	71.644	20.991	1,836	12,240	9,320	423	2.191
88	17	21.901	16.591		12,810	9,200	397	1.507
89	53	0.936	23.783	725	10,840	9,470	395	5.340
90	16	6.441	32.850	879	13,340	9,450	380	1.553
91	19	12.378	63.748	1,458	13,196	9,690	390	1.616
92	33	6.804	64.947	809	11,552	9,480	372	1.617
93	14	32.396	18.949	1,139	12,041	9,320	377	1.636
94	22	8.133	87.716	1,458	13,196	9,690	390	1.721
95	21	46.111	21.111	2,284	11,834	8,030	310	1.800
96	28	22.981	45.342	780	7,621	6,850	306	1.610
97	70	2.394	135.638	1,580	8,738	6,740	300	3.760

Table 5.35 Testing data set records

Record #	Pressure Difference (psi)	CGR (bbl/MMscf)	WGR (bbl/MMscf)	SITP (psig)	MD (ft)	TVDSS (ft)	BHT (deg F)	GAS (MMscfd)
1	60	11.229	113.976	1,099	11,789	9,250	370	1.781
2	22	10.215	37.097	1,178	10,963	9,830	408	1.860
3	15	26.768	22.604	1,139	12,041	9,320	377	1.681
4	189	3.750	76.667	1,099	11,789	9,250	370	2.400
5	22	9.484	33.472	1,802	14,600	9,090	370	1.793
6	28	2.889	34.181	1,499	12,424	8,650	348	2.077
7	53	0.936	23.783	725	10,840	9,470	395	5.340
8	21	31.924	75.210	978	11,346	8,990	376	1.848
9	27	7.883	16.713	989	12,000	8,130	355	3.171
10	60	11.229	113.976	1,099	11,789	9,250	370	1.781
11	20	1.579	14.737	757	12,425	9,630	375	1.900
12	17	1.576	7.354	1,944	14,355	9,510	383	1.904
13	19	13.095	85.117	0	12,607	10,090	410	1.527
14	20	8.520	12.108	1,334	9,800	7,850	290	2.230
15	20	8.520	12.108	1,334	9,800	7,850	290	2.230
16	17	50.891	55.625	1,382	12,605	9,100	371	1.690
17	22	11.257	49.317	1,152	14,116	9,170	374	1.865
18	67	5.152	54.100	1,226	12,438	10,170	388	1.941
19	0	32.653	43.537	0	13,193	9,200	390	2.940

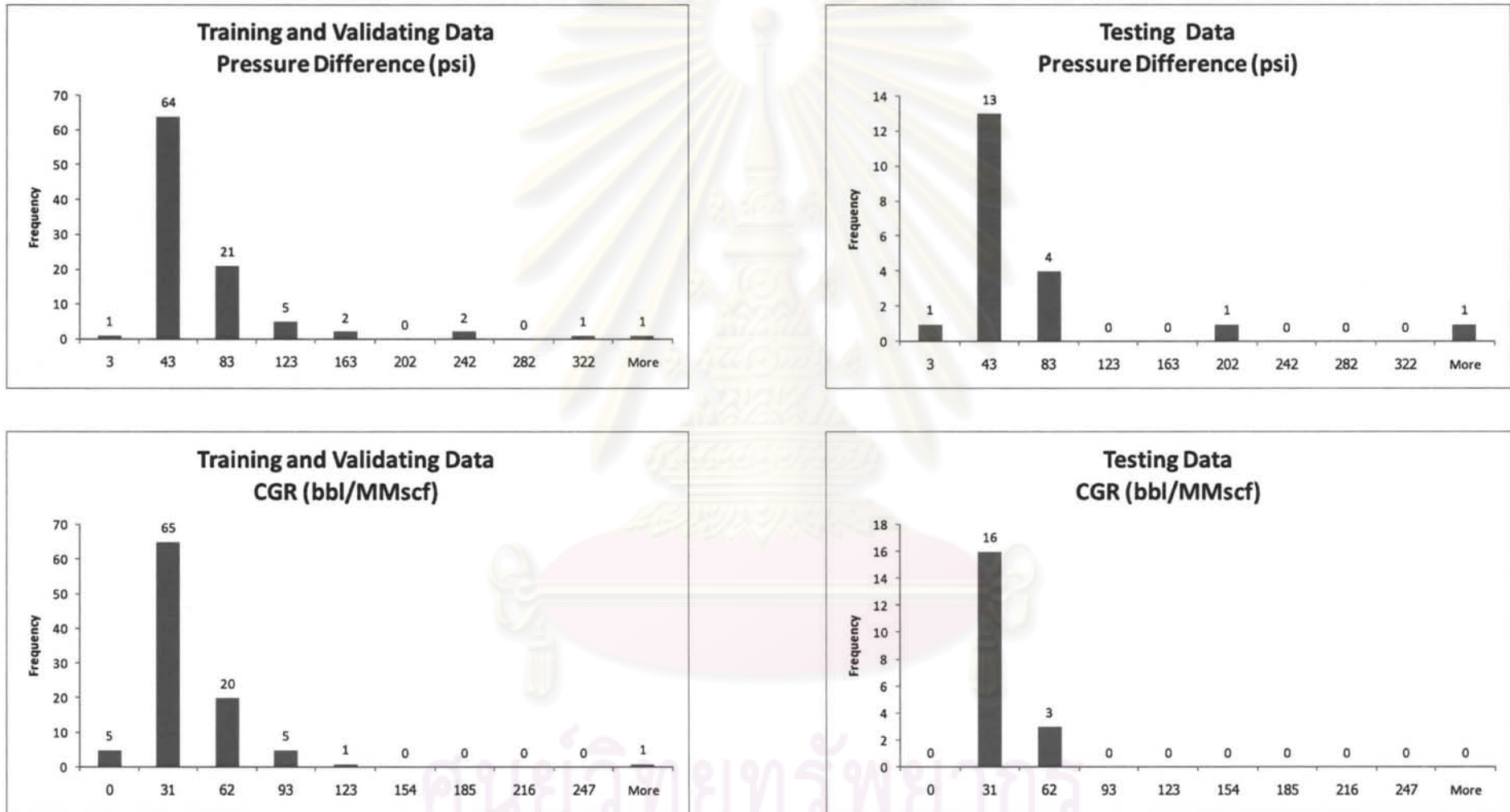


Figure 5.51 Data distribution histogram

จุฬาลงกรณ์มหาวิทยาลัย

Data distribution histogram

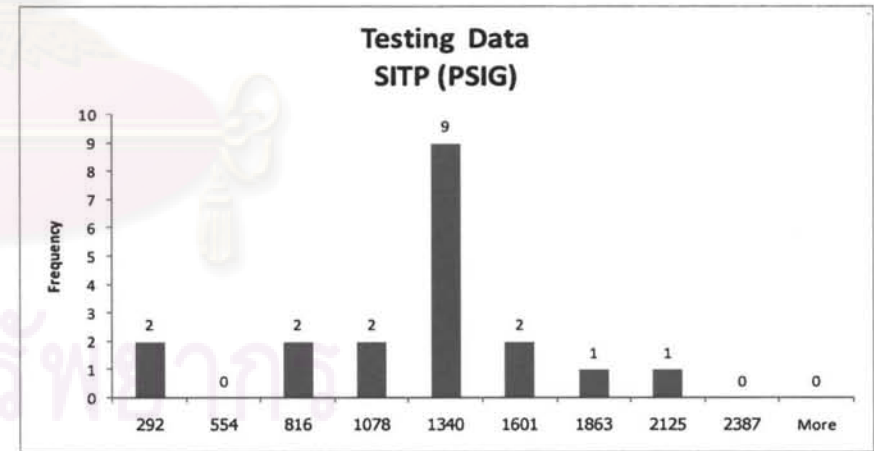
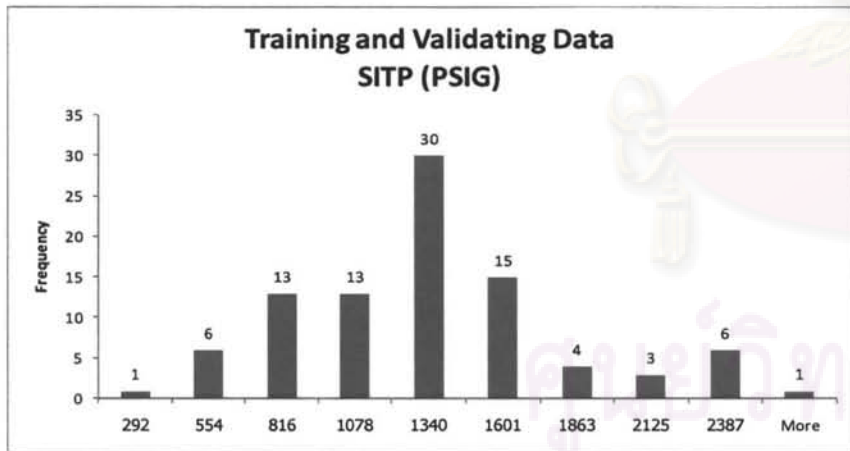
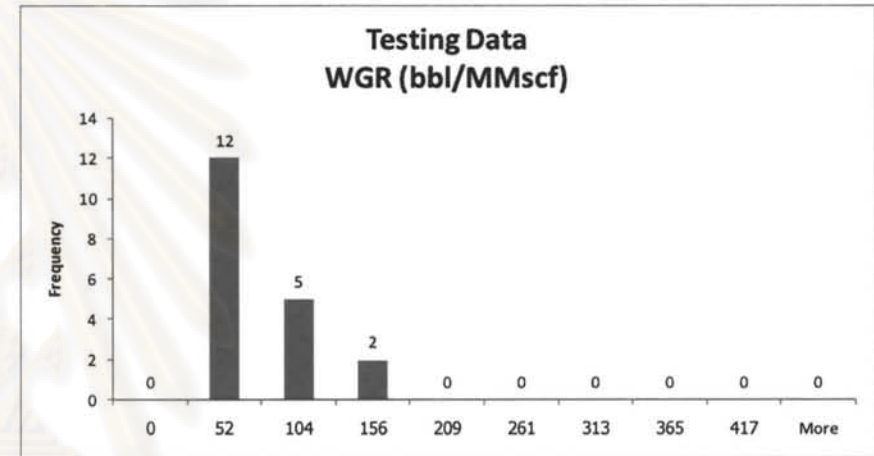
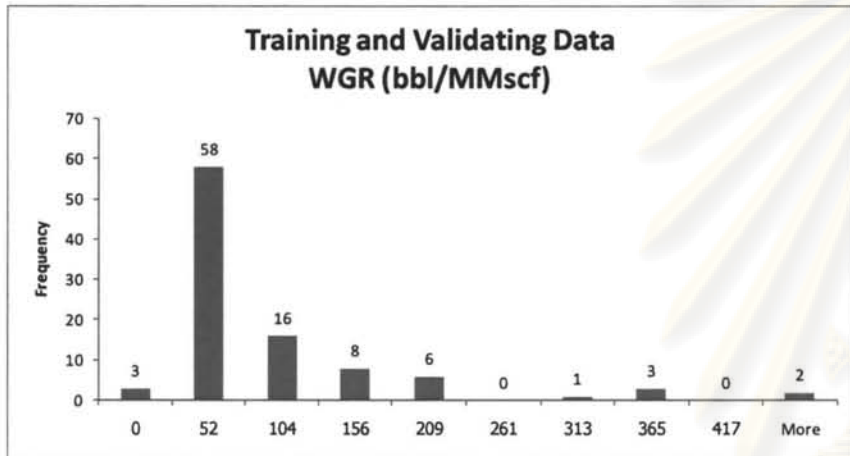


Figure 5.51 Data distribution histogram (continued)

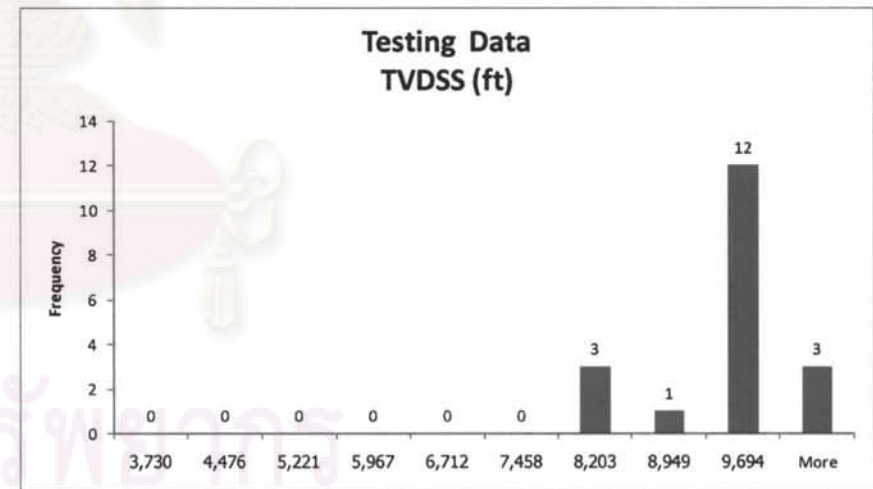
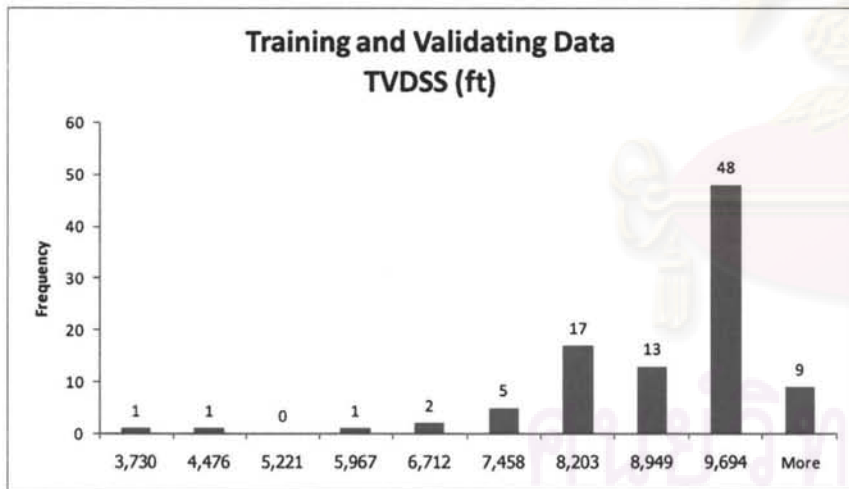
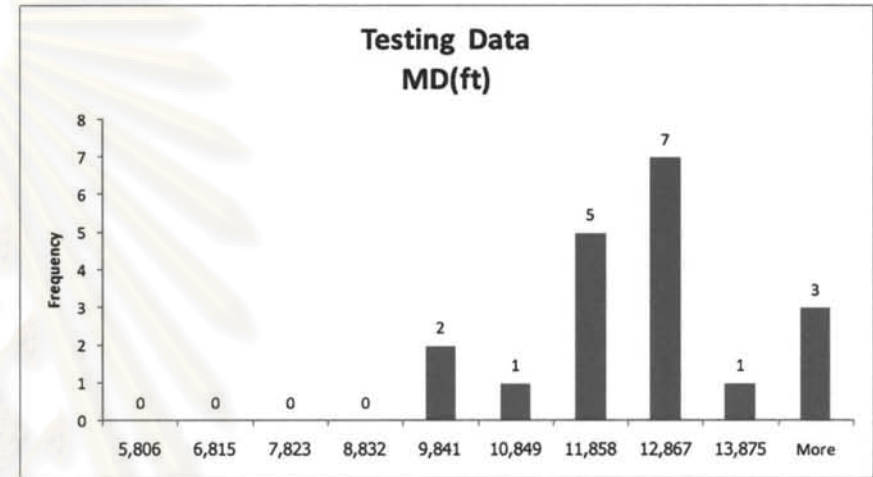
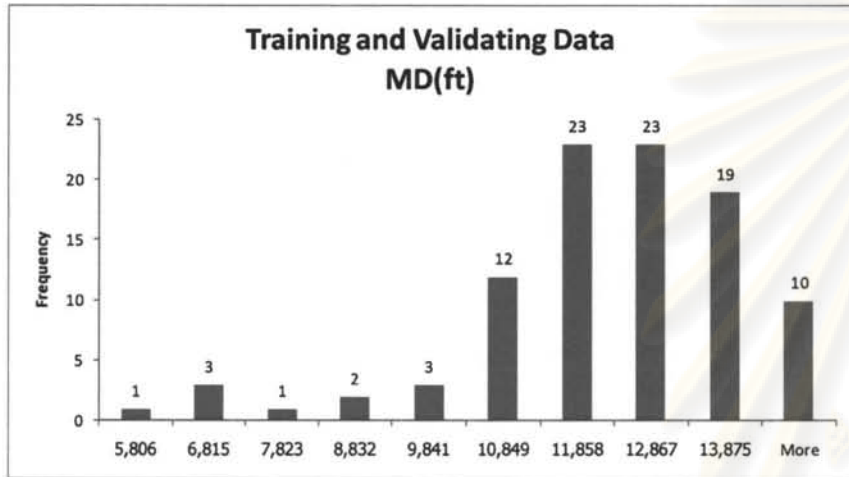


Figure 5.51 Data distribution histogram (continued)

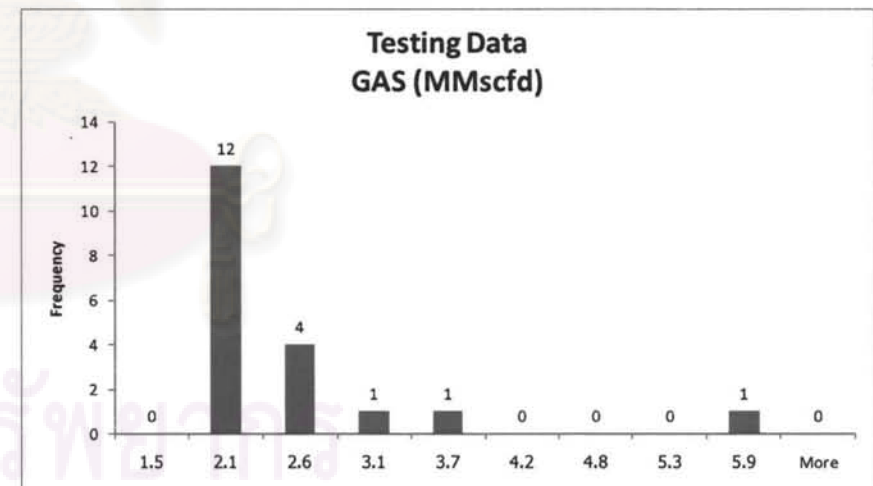
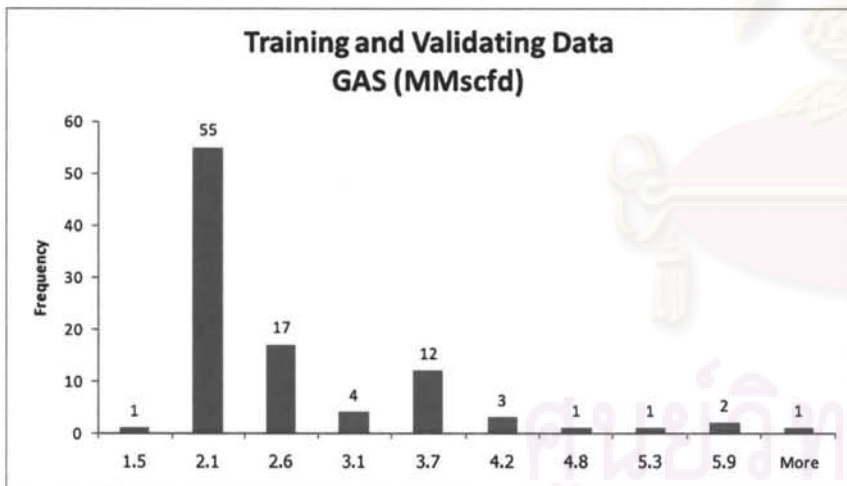
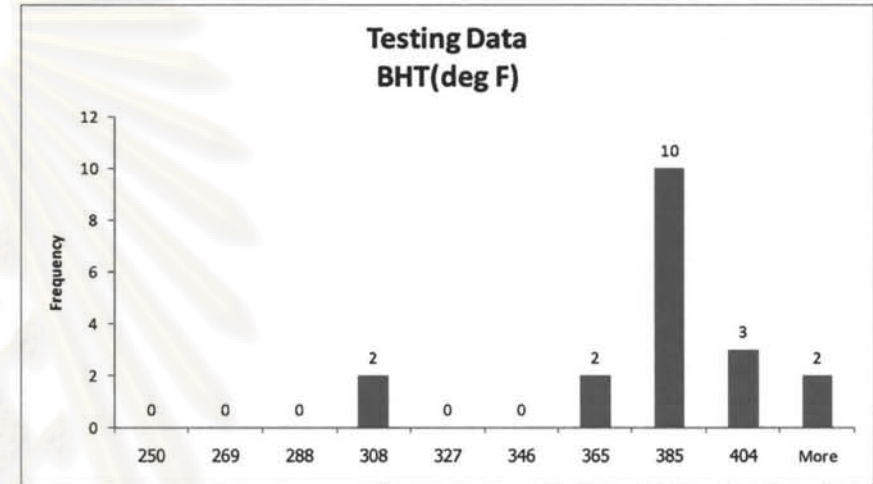
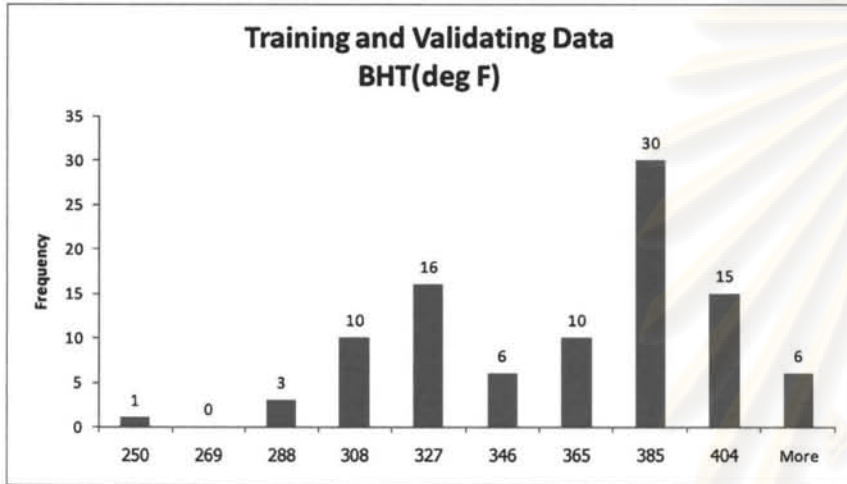


Figure 5.51 Data distribution histogram (continued)

Table 5.36 Training result

Network#	Learning rate	Momentum	#node 1 st hidden layer	#node 2 nd hidden layer	#node 3 rd hidden layer	Training error	Validation error	R2 testing	Total connect	Learning cycle
1	0.7	0.8	4	3	3	0.005265	0.00569	0.400	52	200,000
2	0.7	0.8	5	4	1	0.002802	0.00768	0.570	59	200,000
3	0.7	0.8	6	5	1	0.009298	0.00343	0.511	77	200,000
4	0.7	0.8	6	4	3	0.002844	0.00286	0.787	78	200,000
5	0.7	0.8	7	3	3	0.000213	0.00662	0.882	79	200,000
6	0.7	0.8	7	2	8	0.003025	0.00365	0.889	79	200,000
7	0.7	0.8	8	2	1	0.001072	0.02122	0.770	74	200,000
8	0.7	0.8	9	1	8	0.008145	0.00330	0.508	80	200,000
9	0.7	0.8	2	33	0	0.000100	0.03200	0.256	80	200,000
10	0.7	0.8	3	19	0	0.003032	0.00612	0.749	78	200,000
11	0.7	0.8	4	13	0	0.001752	0.00783	0.781	80	200,000
12	0.7	0.8	5	9	0	0.002831	0.00281	0.804	80	200,000
13	0.7	0.8	6	6	0	0.019712	0.00487	0.024	78	200,000
14	0.7	0.8	7	4	0	0.000093	0.01025	0.879	77	200,000
15	0.7	0.8	8	3	0	0.000466	0.00996	0.690	80	217,674
16	0.7	0.8	9	1	0	0.001030	0.01120	0.815	72	273,887
17	0.7	0.8	10	1	0	0.000557	0.01039	0.815	80	200,000
18	0.7	0.8	11	0	0	0.000018	0.00631	0.187	77	200,000
19	0.7	0.8	3	0	0	0.006177	0.00660	0.520	21	200,000
20	0.2	0.8	3	0	0	0.004592	0.00175	0.782	21	200,000
21	0.2	0.8	7	2	8	0.000396	0.00250	0.709	79	200,000
22	0.2	0.8	7	4	0	0.000302	0.02128	0.460	77	200,000
23	0.2	0.8	9	1	0	0.009150	0.00339	0.526	72	200,000
24	0.2	0.9	10	1	0	0.008612	0.00231	0.556	80	200,000
25	0.2	0.9	3	19	0	0.000080	0.03197	0.306	78	200,000

Table 5.37 Training result sorted by ascending training error

Network#	Learning rate	Momentum	#node 1 st hidden layer	#node 2 nd hidden layer	#node 3 rd hidden layer	Training error	Validation error	R2 testing	Total connect	Learning cycle
18	0.7	0.8	11	0	0	0.000018	0.00631	0.187	77	200,000
25	0.2	0.9	3	19	0	0.000080	0.03197	0.306	78	200,000
14	0.7	0.8	7	4	0	0.000093	0.01025	0.879	77	200,000
9	0.7	0.8	2	33	0	0.000100	0.03200	0.256	80	200,000
5	0.7	0.8	7	3	3	0.000213	0.00662	0.882	79	200,000
22	0.2	0.8	7	4	0	0.000302	0.02128	0.460	77	200,000
21	0.2	0.8	7	2	8	0.000396	0.00250	0.709	79	200,000
15	0.7	0.8	8	3	0	0.000466	0.00996	0.690	80	217,674
17	0.7	0.8	10	1	0	0.000557	0.01039	0.815	80	200,000
16	0.7	0.8	9	1	0	0.001030	0.01120	0.815	72	273,887
7	0.7	0.8	8	2	1	0.001072	0.02122	0.770	74	200,000
11	0.7	0.8	4	13	0	0.001752	0.00783	0.781	80	200,000
2	0.7	0.8	5	4	1	0.002802	0.00768	0.570	59	200,000
12	0.7	0.8	5	9	0	0.002831	0.00281	0.804	80	200,000
4	0.7	0.8	6	4	3	0.002844	0.00286	0.787	78	200,000
6	0.7	0.8	7	2	8	0.003025	0.00365	0.889	79	200,000
10	0.7	0.8	3	19	0	0.003032	0.00612	0.749	78	200,000
20	0.2	0.8	3	0	0	0.004592	0.00175	0.782	21	200,000
1	0.7	0.8	4	3	3	0.005265	0.00569	0.400	52	200,000
19	0.7	0.8	3	0	0	0.006177	0.00660	0.520	21	200,000
8	0.7	0.8	9	1	8	0.008145	0.00330	0.508	80	200,000
24	0.2	0.9	10	1	0	0.008612	0.00231	0.556	80	200,000
23	0.2	0.8	9	1	0	0.009150	0.00339	0.526	72	200,000
3	0.7	0.8	6	5	1	0.009298	0.00343	0.511	77	200,000
13	0.7	0.8	6	6	0	0.019712	0.00487	0.024	78	200,000

Table 5.38 Training result sorted by ascending validation error

Network#	Learning rate	Momentum	#node 1 st hidden layer	#node 2 nd hidden layer	#node 3 rd hidden layer	Training error	Validation error	R2 testing	Total connect	Learning cycle
20	0.2	0.8	3	0	0	0.004592	0.00175	0.782	21	200,000
24	0.2	0.9	10	1	0	0.008612	0.00231	0.556	80	200,000
21	0.2	0.8	7	2	8	0.000396	0.00250	0.709	79	200,000
12	0.7	0.8	5	9	0	0.002831	0.00281	0.804	80	200,000
4	0.7	0.8	6	4	3	0.002844	0.00286	0.787	78	200,000
8	0.7	0.8	9	1	8	0.008145	0.00330	0.508	80	200,000
23	0.2	0.8	9	1	0	0.009150	0.00339	0.526	72	200,000
3	0.7	0.8	6	5	1	0.009298	0.00343	0.511	77	200,000
6	0.7	0.8	7	2	8	0.003025	0.00365	0.889	79	200,000
13	0.7	0.8	6	6	0	0.019712	0.00487	0.024	78	200,000
1	0.7	0.8	4	3	3	0.005265	0.00569	0.400	52	200,000
10	0.7	0.8	3	19	0	0.003032	0.00612	0.749	78	200,000
18	0.7	0.8	11	0	0	0.000018	0.00631	0.187	77	200,000
19	0.7	0.8	3	0	0	0.006177	0.00660	0.520	21	200,000
5	0.7	0.8	7	3	3	0.000213	0.00662	0.882	79	200,000
2	0.7	0.8	5	4	1	0.002802	0.00768	0.570	59	200,000
11	0.7	0.8	4	13	0	0.001752	0.00783	0.781	80	200,000
15	0.7	0.8	8	3	0	0.000466	0.00996	0.690	80	217,674
14	0.7	0.8	7	4	0	0.000093	0.01025	0.879	77	200,000
17	0.7	0.8	10	1	0	0.000557	0.01039	0.815	80	200,000
16	0.7	0.8	9	1	0	0.001030	0.01120	0.815	72	273,887
7	0.7	0.8	8	2	1	0.001072	0.02122	0.770	74	200,000
22	0.2	0.8	7	4	0	0.000302	0.02128	0.460	77	200,000
25	0.2	0.9	3	19	0	0.000080	0.03197	0.306	78	200,000
9	0.7	0.8	2	33	0	0.000100	0.03200	0.256	80	200,000

Table 5.39 Training result sorted by ascending testing R2

Network#	Learning rate	Momentum	#node 1 st hidden layer	#node 2 nd hidden layer	#node 3 rd hidden layer	Training error	Validation error	R2 testing	Total connect	Learning cycle
13	0.7	0.8	6	6	0	0.019712	0.00487	0.024	78	200,000
18	0.7	0.8	11	0	0	0.000018	0.00631	0.187	77	200,000
9	0.7	0.8	2	33	0	0.000100	0.03200	0.256	80	200,000
25	0.2	0.9	3	19	0	0.000080	0.03197	0.306	78	200,000
1	0.7	0.8	4	3	3	0.005265	0.00569	0.400	52	200,000
22	0.2	0.8	7	4	0	0.000302	0.02128	0.460	77	200,000
8	0.7	0.8	9	1	8	0.008145	0.00330	0.508	80	200,000
3	0.7	0.8	6	5	1	0.009298	0.00343	0.511	77	200,000
19	0.7	0.8	3	0	0	0.006177	0.00660	0.520	21	200,000
23	0.2	0.8	9	1	0	0.009150	0.00339	0.526	72	200,000
24	0.2	0.9	10	1	0	0.008612	0.00231	0.556	80	200,000
2	0.7	0.8	5	4	1	0.002802	0.00768	0.570	59	200,000
15	0.7	0.8	8	3	0	0.000466	0.00996	0.690	80	217,674
21	0.2	0.8	7	2	8	0.000396	0.00250	0.709	79	200,000
10	0.7	0.8	3	19	0	0.003032	0.00612	0.749	78	200,000
7	0.7	0.8	8	2	1	0.001072	0.02122	0.770	74	200,000
11	0.7	0.8	4	13	0	0.001752	0.00783	0.781	80	200,000
20	0.2	0.8	3	0	0	0.004592	0.00175	0.782	21	200,000
4	0.7	0.8	6	4	3	0.002844	0.00286	0.787	78	200,000
12	0.7	0.8	5	9	0	0.002831	0.00281	0.804	80	200,000
17	0.7	0.8	10	1	0	0.000557	0.01039	0.815	80	200,000
16	0.7	0.8	9	1	0	0.001030	0.01120	0.815	72	273,887
14	0.7	0.8	7	4	0	0.000093	0.01025	0.879	77	200,000
5	0.7	0.8	7	3	3	0.000213	0.00662	0.882	79	200,000
6	0.7	0.8	7	2	8	0.003025	0.00365	0.889	79	200,000

Result

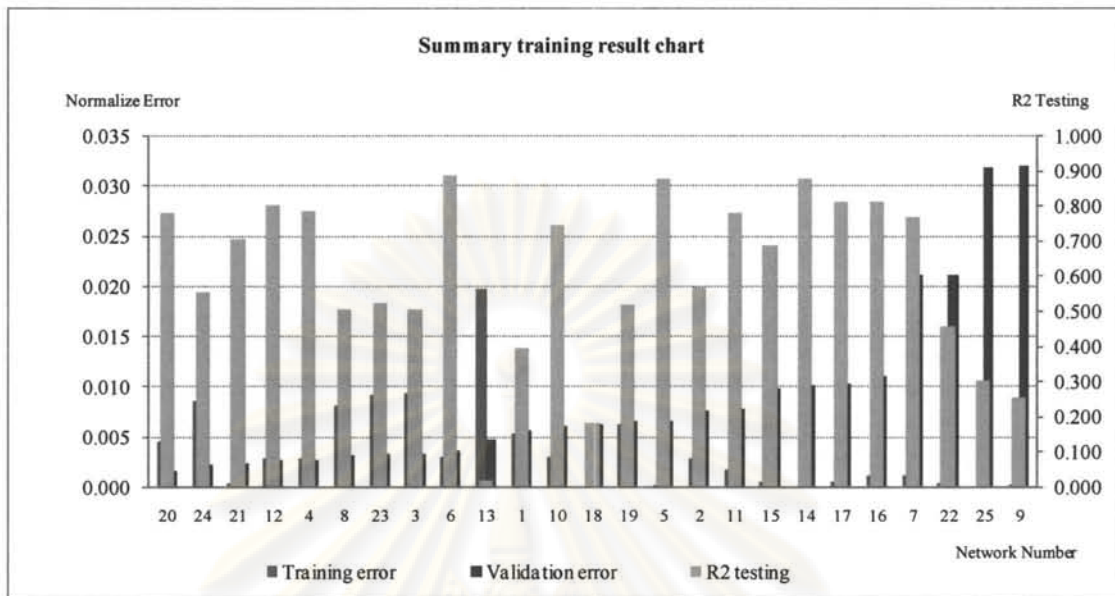


Figure 5.52 Summary of the result from all network

After the data were categorized, several distinctive structures of neural networks were trained, validated, and tested. The numbers of nodes in the hidden layers, the learning rate and the momentum used in the training, and the error associated with the training and validating data set as well as R^2 of the testing data set are tabulated in Table 5.36. Table 5.37 and 5.38 show the training result based on training and validating error sorted by ascending respectively. Table 5.39 shows sorted network based on ascending R^2 of testing data set.

Based on Tables 5.36 to 5.39 and Figure 5.52 which summarizes the result of the training, validating and testing process, Network #20 was selected for the prediction of terminal rate because it has the lowest validation error but the training error is roughly in the median which should not cause overtrained. Its R^2 was the 8th highest ranking. It also has the lowest number of connection which can ensure prevention of over-fitting and provides highest test accuracy as per Equation 3.40.

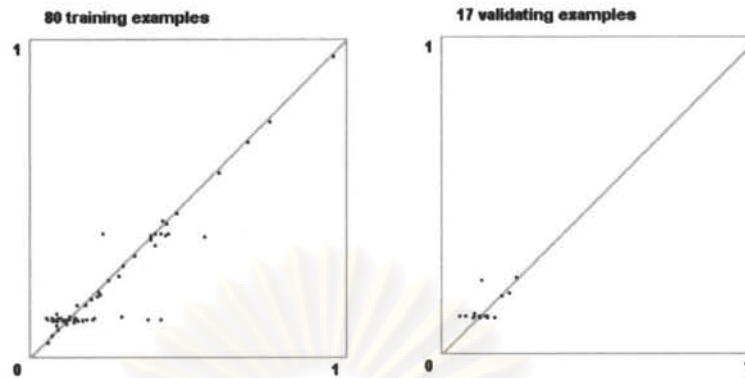


Figure 5.53 Training and validating result of Network #20

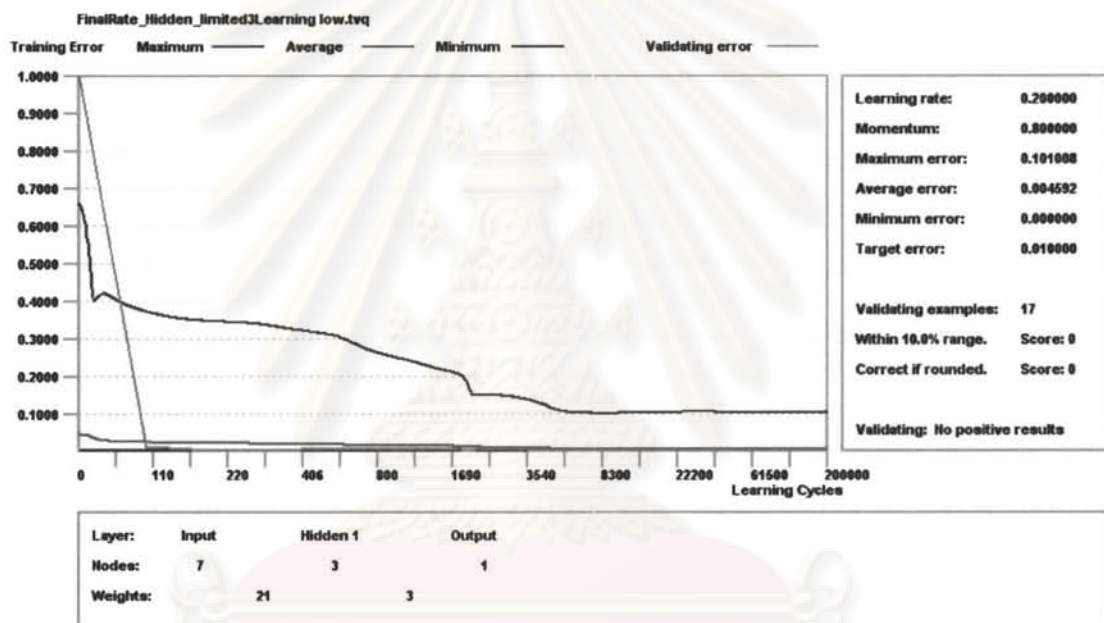


Figure 5.54 Training and validating progress chart of Network #20

Figure 5.53 shows result of training and validating error of each data records. Figure 5.54 shows the progress of validating error and each type of training error as the training cycle progresses.

Network #20 was selected as the best network with the following properties characteristics:

- 1 hidden layer with 3 neurons
- Training error 0.004592

- Validation error 0.00175
- $R^2 = 0.782$

The results of Neural Network (NN) #20 prediction compared to both actual rate and rate calculated by Turner's equation are shown in Figure 5.55. The rate predicted by the NN is much more in line with the actual rate and provide a fairly good fit to the actual data.

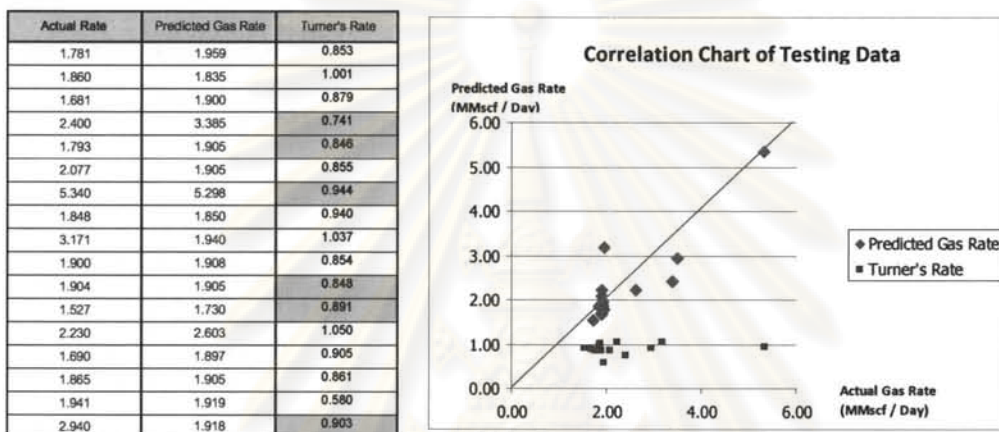


Figure 5.55 Testing result of network #20, comparison with Turner's

ศูนย์วิทยทรัพยากร
จุฬาลงกรณ์มหาวิทยาลัย

CHAPTER VI

CONCLUSIONS AND RECOMMENDATIONS

6.1 Zonal OGIP and aquifer determination

In this study, the necessity of having zone by zone OGIP information for better well intervention decision and improvement of water shut off success was pointed out. Limitation and capability of the commercial software (MBAL and GAP) used for constructing a multi-tank commingle model and a self-developed program for automatic history matching were investigated. Simulated data with different conditions and actual field data from three different wells were tested to illustrate validity of the model and capability of the automatic history matching spreadsheet. The results obtained from the proposed methods were compared with result from other methods to evaluate its performance.

6.1.1 Conclusions

- 1) Using a depletion drive multi-tank model to history match a system which has water drive reservoir when water does not break through the wellbore will likely to **overestimate** OGIP of the reservoir that has the water drive. The error depends on the strength (size) of the aquifer. However, the estimates of OGIP for other tanks in the system which have depletion drive should not have a significant amount of error. It is necessary that we need to assume all tank have depletion drive before water breaks through the wellbore because we don't know if there is any water on any sands unless there is accurate geological information which seems to be rare in such complex reservoirs in the Gulf of Thailand. Using Cole plot to identify water drive requires a good representative average reservoir pressure of the system and even though we had that good accurate reservoir pressure of the commingle system, we can only perform analysis at the well level. The effect of water drive may dilute out (if the aquifer is small compared to other tanks with high OGIP but without aquifers) or we still cannot point out which sand has the aquifer support. In addition, the geological setting of area in which the study focuses on is known to be highly faulted and compartmentalized. This limits the possibility of having a big aquifer which can give a strong water drive

support to the level that the depletion drive assumed for history matching would have high error. Most of the times, we would see watered out sands deplete to as low as non-watered out sands.

- 2) GAP despite its capability to model the pressure drop between sands in a commingled system is not effective in modeling cross flow during well shut in. MBAL which does not model the pressure drop between sands can model cross flow to some extent that at least the material balance due to cross flow during shut in should be better modeled than with GAP. For this reason MBAL was used for this work.
- 3) Using MBAL to construct a multi-tank model without pressure drop between sands to model an actual commingled well will result in fairly correct OGIP of the top sand but **under estimate** OGIP of the sand below. The significance of error depends on the pressure drop gradient, which translates to the distance from the top sand to that particular sand. The effect will be pronounced if bottom sand produces significant amount of liquid which creates significant hydrostatic pressure drop. This underestimated error could also be offset with overestimation of matching pressure support reservoir with a depletion type model.
- 4) Weighting factors also have an effect on convergence. From the experiments, it can be concluded that we should start with an equal weight on all residuals, and then try again with a weighing factor ten times more on all residuals. Then, we need to compare the answers that best fit WT and PLT data. After determining the best value of all equal weighing factor, increase the weighing factors of PLT data by ten times and compare the fitness of residual to that of the best equal weighting factors. Using too small weighting factor or normalized weighting factor has the same effect as using big λ . The solution vector will move slightly and perhaps converge to values very close to the initial guess values which are the wrong solutions. Using high weighting factors may overshoot the optimal solutions and could prematurely terminate the algorithm due to excessive solution from the algorithm. It is best to start with one which is the fair value on all weighing factors.

- 5) Water production modeled with MBAL tank could be difficult even though a correct aquifer model is used since the water production depends on many unknown factors such as correct relative permeability data and heterogeneity of the watered out layer. MBAL which is zero dimension reservoir model cannot model heterogeneity of the watered out layer. Otherwise, relative permeability (such as parameters in Corey function) will be another matching parameter used for history match for pseudo relative permeability of the watered out layer. Using water end point as the matching parameter built into automatic history matching spreadsheet cannot be done in this thesis due to the fact that the architecture of the software (using MBAL to communicate with calculation in Excel VBA Openserver) does not provide fast computation time which is essential as numbers of matching variables increase. The problem of local minimum of the optimization algorithm will be severe as the number of matching parameters increases especially when the initial guesses are far from the true solution.
- 6) To get a good history match of commingled multi-tank system, PLT is needed to constrain the solutions especially in the case that the algorithm used in the automatic history matching process cannot find the global minimum.
- 7) Apart from heterogeneity problem to model water production, water producing mechanism in the GOT might be more complex than any available models can mimic such as the problem of gas cap drive aquifer that communicate through leaking fault to the domain reservoir.
- 8) Algorithm with normalized error function worked better than standard error function.
- 9) The values of initial guesses have big effect on accuracy of the solutions since the algorithm used in the automatic history matching spreadsheet can yield the solutions that are trapped in local minimum, which leads to ambiguity of the solution answers when converges. In this case, the answers could be suboptimal value. Therefore, initial guesses should be as close as possible to the actual numbers and cannot be randomly chosen. Good initial guesses can be determined from the volumetric calculation method. Then, we can use a manual match spreadsheet to adjust those parameters to best possible fitted with actual data

graphically. We may use these adjusted variables for the automatic history matching routine.

- 10) The multi-tank commingled model built with MBAL coupled with the automatic history matching spreadsheet macro gives similar OGIP calculation from CWM (well A) and relatively different to CWM on well B and similar total OGIP to conventional P/Z technique on well C.

6.1.2 Recommendations for Future Work

- 1) A better optimization routine which is effective in finding the global minimum should be used to reduce the problem of local minimum trap.
- 2) The computational time used in the automatic history matching spreadsheet in combination with MBAL model used in this thesis is too long since the derivatives of the objective function need to be evaluated numerically. Automatic history match features should be built into MBAL or any software that can be used to build multi-layer system to eliminate numerical differentiation.

6.2 Critical Gas Rate Prediction by Neural Network

In this study, a neural network was built to predict a critical gas rate by training and validating sudden death well records. The result from neural network model was tested and compared with Turner's critical gas velocity and founded to be better matched with actual data.

6.2.1 Conclusions

A sudden death well database which stores critical gas well loading information was used to train, validate and test the constructed neural network. The result of the model can be summarized as follows:

- 1) All rates in sudden death well report were over critical gas well loading velocity calculated with Turner's model at the wellhead condition. The velocities in the record are not the terminal velocities but are the last record velocities. So, they are larger than Turner's velocities.
- 2) Due to above reason, the neural network model was constructed with last gas rate before the wells died instead of actual gas critical velocity. The result of model

testing was good but if high confidence is needed, more testing data should be used due to a limited number of records in the database used in the training and testing.

6.2.2 Recommendations for Future Work

- 1) More training set is needed to allow the network to recognize better relationship among the data.

6.3 The comprehensive sub surface water management

Individual gas in place determination from the multi-tank commingle model and terminal rate determination by the neural network can be used for improvement of the production optimization process on water management. The reserve or gas in place volume per individual sand can be determined by the method proposed in this thesis to increase the knowledge of value of each sand (reserve or volume in place at the time to decide if water shut off should be pursued) when it needs water shut off intervention. The future production profile of each sand can be obtained from the model that is well calibrated by history matching. The model can be used to predict the result of water shut off in terms of rate gain and reserve after intervention. This profile could also be used for planning for the timing for perforation of subsequent batches to prevent cross flow into depleted sands. The critical rate determined from the neural network can be used for planning on the timing of production logging to identify water producing sand before the well stop flowing. The success ratio of water shut off and recovery efficiency of commingled reservoirs in monobore wells should be increased by combining these tasks into water management process.

ศูนย์วิทยทรัพยากร
จุฬาลงกรณ์มหาวิทยาลัย

REFERENCES

- [1] Prasit K., Nick Last. *Comingled Wellbore Model*, Abstract, Unocal Thailand
- [2] Ahmed H., El-banbi, Robert A. Wattenbarger. *Analysis of Commingled Tight Gas Reservoir*, SPE 36736 at SPE Annual Technical Conference and Exhibition in Denver, CO, USA., 1996
- [3] J.P. Spivey., *Estimating Layer Properties for Wells in Multilayer Low-permeability Gas Reservoirs by Automatic History Matching Production and Production log Data*, SPE 100509 presented at SPE Gas Technology Symposium held in Calgary, Alberta, Canada, 2006
- [4] Calvin C. Mattax, Robert L. Dalton. *Reservoir Simulation*, SPE Monograph Series, 1990: 154-157
- [5] B.C. Craft and M.F. Hawkins. *Applies Petroleum Reservoir Engineering 2nd Edition*, Prentice Hall Englewood Cliffs, NJ 07632: 14-31, 76-90
- [6] L.P. Dake. *The Practice of reservoir Engineering, Development in Petroleum Science*, 36, ELSEVIER SCIENTIFIC PUBLISHING COMPANY, 1994: 471-477, 483-492
- [7] J.L. Pletcher. *Improvements to Reservoir Material Balance*, SPE, Marathon Oil Co.
- [8] L.P. Dake. *Fundamentals of Reservoir Engineering, Developments in Petroleum Science*, 8, ELSEVIER SCIENTIFIC PUBLISHING COMPANY, 1978: 303
- [9] H. Malyadi, R. Amin. *Core Laboratories, Practical Approach to Determine Residual Gas Saturation and Gas-Water Relative Permeability*, SPE 71523
- [10] Maio Alvarey Grima. *Neuro-Fuzzy Modeling in Engineering Geology, Application to Mechanical Rock Excavation, Rock Strength Estimation, and Geological Mapping*, A.A. Balkema / Rotterdam / Brookfield, 2000: 40-44
- [11] Daniel T. Larose. *Discovering Knowledge in Data: an Introduction to Data Mining*, Copyright @ 2005 by John Wiley & Sons, Inc.: 129-142

- [12] R.G. Turner, M.G. Hubbard, A.E. Dukler. *Analysis and Prediction o Minimum Flow Rate for the Continuous Removal of Liquids from Gas Wells*, SPE 2198
- [13] S.B. Coleman, H.B. Clay, D.G. McCurdy and H.L. Norris III, *A New Look at Predicting Gas-Well Load-up*, SPE 20280
- [14] Agarwal, *Unsteady-State Performance of Water-drive Gas Reservoirs*, PhD Thesis, Texas A&M, 1967



ศูนย์วิทยทรัพยากร
จุฬาลงกรณ์มหาวิทยาลัย



APPENDICES

ศูนย์วิทยทรัพยากร
จุฬาลงกรณ์มหาวิทยาลัย

APPENDIX A

EFFECT OF SHUTTING IN THE WELL ON GAP AND MBAL SOFTWARE

GAP

While simulating well shut in (in red cycle), both high and low pressure tanks take fluid which is not what actually happens in the multi-tank system.

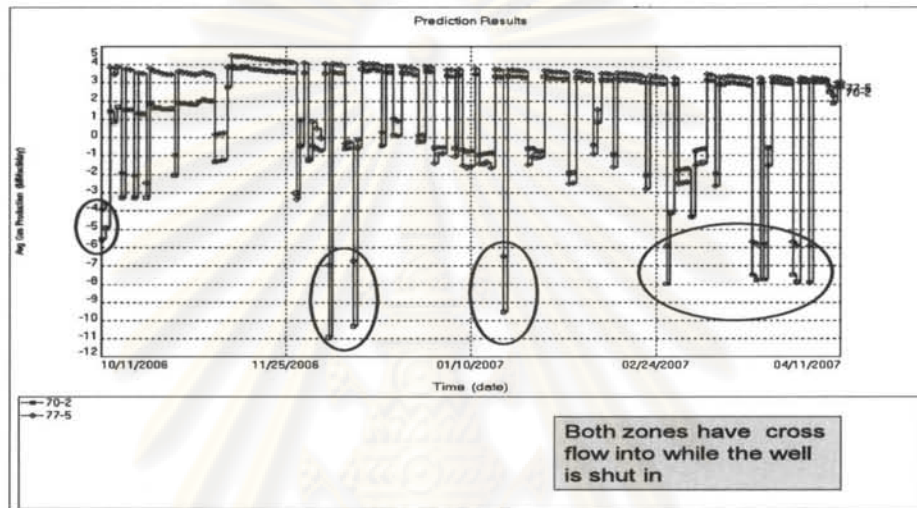


Figure 7.1 System production profile simulated by GAP during shut in

Table 7.1 Tank 77-5 production profile during shut in simulated with GAP

Date	Reservoir Pressure (psig)	Avg Oil Production (STB/day)	Avg Gas Production (MMscf/day)	Avg Water Production (STB/day)
10/11/2006	3600	-128.6	-3.91	0
10/12/2006	3617.03	0	-3.61	0
10/13/2006	3632.3	126.6	3.85	0
10/14/2006	3615.36	114.3	3.47	0

Table 7.2 Tank 70-2 production profile during shut in simulated with GAP

Date	Reservoir Pressure (psig)	Avg Oil Production (STB/day)	Avg Gas Production (MMscf/day)	Avg Water Production (STB/day)
10/11/2006	3100	0	-5.56	0
10/12/2006	3119.19	-161.1	-4.9	0
10/13/2006	3136.45	48.2	1.46	0
10/14/2006	3131.06	29.5	0.9	0

MBAL

While the well is shut in, cross flow will be from high pressure reservoir to low pressure reservoir with total flow rate equal to zero.

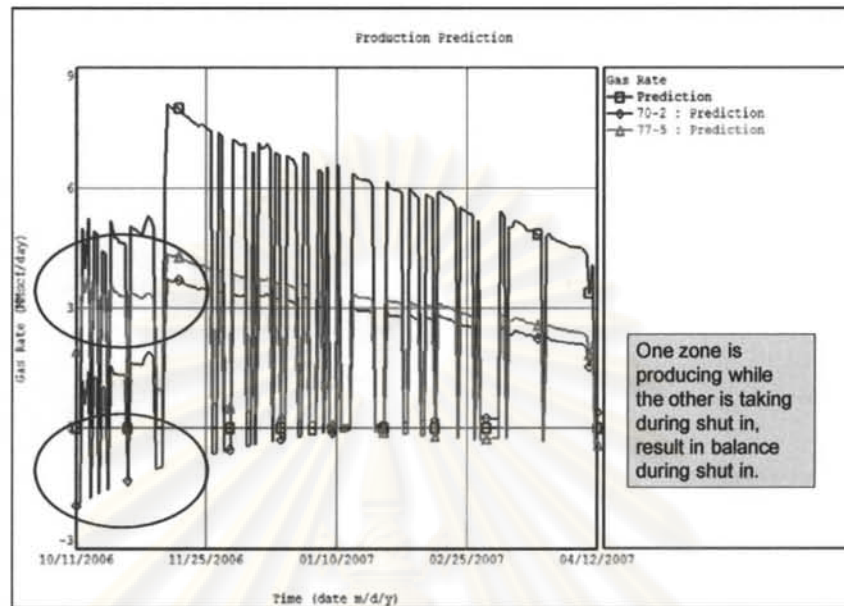


Figure 7.2 System production profile during shut in simulated with MBAL

Table 7.3 Tank 70-2 production profile simulated by MBAL

Date	Tank Pressure (psig)	Gas Recovery Factor (%)	Oil Rate (STB/day)	Gas Rate (MMscf/day)	Water Rate (STB/day)
10/11/2006	3100.00	0.00	-96.45	-1.93	0.00
10/12/2006	3106.71	-0.19	-94.37	-1.89	-0.02
10/13/2006	3113.29	-0.38	59.41	1.19	0.00
10/14/2006	3109.15	-0.26	30.13	0.60	0.00
10/15/2006	3107.05	-0.20	70.61	1.41	0.00

Table 7.4 Tank 77-5 production profile simulated by MBAL

Date	Tank Pressure (psig)	Gas Recovery Factor (%)	Oil Rate (STB/day)	Gas Rate (MMscf/day)	Water Rate (STB/day)
10/11/2006	3600.00	0.00	96.45	1.93	0.00
10/12/2006	3591.81	0.19	94.37	1.89	0.02
10/13/2006	3583.81	0.38	189.25	3.79	0.08
10/14/2006	3567.80	0.76	170.92	3.42	0.18

APPENDIX B

PROCEDURE TO SET UP COMMINGLE MODEL WITH MBAL AND PROCEDURE TO USE AUTOMATIC HISTORY MATCHING SPREADSHEET

1) Procedure to construct MBAL multi-tank model and how to use automatic history matching spreadsheet

Required information to build the multi-tank commingle model with MBAL (gas)

- 1) PVT properties for the well (if each individual tank property is known, it can be input separately)
 - a. Gas SG
 - b. CGR
 - c. Separator pressure when measured CGR
 - d. Condensate API
 - e. Impurities (N₂, H₂S, CO₂) mole percentage
 - f. Water salinity
- 2) Individual reservoir (tank or layer) properties
 - a. Initial pressure
 - b. Reservoir temperature
 - c. Connate water saturation
 - d. Porosity
 - e. Start date (date that sand is perforated)
 - f. Relative permeability data if that reservoir is to have aquifer model.
- 3) Well information to generate VLP in PROSPER such as completion, deviation survey data, BHT and WHT, FTP and BHP to select most fitted VLP correlation.

- 4) PLT data (multi rate or single rate) to build IPR of each reservoir. Multi rate PLT will provide information of P_{wf} and Q_g to build IPR. Fit these data with IPR correlation such as back pressure C&N or Forchheimer. PLT interpretation software (Emeradue, PLWin) has the feature to use S.I.P (selective inflow performance) technique to obtain the average reservoir pressure and well deliverability parameters. PLT data is also used for history match to obtain collect OGIP and aquifer size.
- 5) Wellhead pressure history since day 1 (initial perforation) and well test history preferable more than 6 months.

2) Procedure to set MBAL Multi-tank model

- 1) Choose material balance option in tool menu
- 2) System option: reservoir fluid = gas, tank model = multiple tank, production history by well.
- 3) Click add tank button on the left.
- 4) Choose PVT menu and fluid properties. Input information and choose viscosity correlation.
- 5) Double click on added tank. Input name and reservoir information. Choose aquifer model if needed in the second tab and relative permeability data. If no aquifer select, this information may not need to be accurate just ensure that residual water saturation is same as connate water saturation in first page. Gas residual saturation may be assumed to be 0.5 S_{gi}. Other parameter in Corey function may be assumed to be 1. If aquifer is selected, we may use need to use correlation to estimate relative permeability if the core flow test is not available. In this thesis, Boatman and Willie correlation were used.
- 6) Use plus sign to duplicate the tank that was just set up as many as required number of tanks in the system. Input the reservoir parameters as done previously on all tanks.

- 7) Go to production prediction menu. Choose Predict by production profile with well model. Prediction step size = automatic. Prediction start = start of production. Prediction end = User define (this will be filled up automatically by macro).
- 8) Add well. Connect all tanks to this new added well. Click on the small rectangular in the connecting line of the well to input IPR parameter. Click on well-Outflow performance. Click edit. Then import the VLP database generated from PROSPER.
- 9) Click on production prediction, choose well schedule. Input the start date on the earliest production date of any tanks. Select the well that we have and put zero downtime in the right column next to it.
- 10) All connection in the screen should not be grey out. We are now ready to use automatic history matching spreadsheet to set up well Prediction and Production Constraint to set up wellhead pressure.

3) Procedure how to use Automatic History Matching Spreadsheet (AHMS)

After finish setting up Multi-Tank model in MBAL, follow steps below:

Prepare the data in the spreadsheet

- 1) Copy Well Test (WT) data for the period to be used for history matching in Excel Format which is downloaded from PetroWeb of the particular well to be worked on onto "WT" worksheet of AHMS.
- 2) Copy Well Situation data from the start date of production until the end of simulation period onto "WellSituation" worksheet of AHMS. It is required to cut and insert tubing head pressure to Column B since. Date is to be left in the original column, A.
- 3) Turn to worksheet "Inputdata". Follow the steps below:
 - a. Input number of WT record for the period of history matching in cell B1.
 - b. Input number of tanks (reservoirs or layers) in cell B2.
 - c. Input number of tanks which has aquifer model (that particular tank needed to be preset in MBAL to have a small pot aquifer influx model).

- d. Input the starting Landa value for Levenberg-Marquardt optimization algorithm. Leave it at default value at 0.001 unless there is no other way to obtain convergence with reasonable answer.
- e. If this is the first time to work on this well, clear all the data in row 4-18.
- f. Input tank name into cell A4 and the other tank into other cells below. Maximum 15 tanks is allowed in the existing spreadsheet format. Name of the tanks must be the same as what were input into MBAL multi-tank model. Input initial guess OGIP and Pot Aquifer volume in column B and C corresponding to each particular tank in column A. Pay attention to units for OGIP and Aquifer volume. They must be the same as what have been used in MBAL.
- g. Input start simulation date in cell B20 and end date in cell B21. Data that is of date type must be input in format mm/dd/yyyy.
- h. Input “Y” in cell B22 if there is PLT data to use for history matching. If no PLT available, input “N”. Spreadsheet will only match total well gas rate. If “Y” is input, total gas rate, individual tank pressure and gas rate will be matched.
- i. Input number of PLT survey to be used for history matching in cell B23.
- j. Input date of 1st PLT survey in cell D19, 2nd one, if any, in cell E19 and so on for the next PLT survey.
- k. If there is water production and PLT survey and need to match water (both total well production and individual tank water production, input “True” in cell B24. Otherwise, input “False”. There is not possible to match water if there is no PLT survey data.
- l. Input maximum iteration loop required until program stops in case of none convergence can be reached in cell B25.
- m. If weighting factors of each residual to be put by message box, input “True” in cell B26. Message box will pop up when start running program for weighting factors for each individual. It is recommended to use for the first trial since after the program run it will write residual names and its corresponding weighting factor in cells A29/B29 and below. For the following run, this cell should be input as “False” so that we don’t need to repeat putting the weighting factors again. The program will read from cell B29 and below for all the residual. Change weighting factors as needed. The first time that run the

program, all data in cells A29/29 should be cleared so that when the program writes weighting factors and residual name obtained via message box won't be mixed with data that resides earlier in the spreadsheet.

- n. Same fashion with weighting factor PLT data could be entered via message box if it is the first matching. Input "True" in cell B26 for this purpose. The data obtained from message box will be written in cell D4 and other cells on the left (depends on how many PLT survey, how many tank in the system, and if water production of each individual tank needed to be matched).

Set manifold pressure schedule in MBAL

Macro "Set Schedule" will pull date and its corresponding tubing head pressure from "WellSituation" worksheet and input into MBAL's Prediction and Production constrain sheet after clearing the table automatically. This will reduce time consumption to input wellhead data which is on the daily basis for the whole simulation period.

Run Macro for manual History Matching and automatic History Matching

- 1) The initial value to be input for history matching should be OGIP from volumetric method calculated from inferred area. The initial guess for aquifer volume of water out sand may be from geological data if available otherwise it may starts with 5 MMrb.
- 2) Go to "Manual" worksheet. Select the macro "Manualmatch". This Macro will run the model simulation with input parameters which have been entered in the "Inputdata" worksheet and compared with observed value (WT data and PLT data) as per the option selected in the "Inputdata" worksheet. In case on any WT date, FTP in WT record is different from tubing head pressure reported in WellSituation table, this macro will also change manifold pressure (tubing head pressure) in "Wellsituation" worksheet to FTP reported in WT record. The manifold pressure in MBAL "Prediction Production and Constraints" on any WT date that is different from WT FTP will also be changed to WT FTP automatically.
 - a. Run the macro "Manualmatch". The table of result of history matching will be generated. All residuals selected as per input option in "Inputdata" worksheet

will be shown in this table. Observed data will be shown along with calculated data from the result of simulation. Create graph and chart for easy comparison for easier visualization to help easier adjusting matching parameters for manual matching.

- b. Adjust matching parameters in “Inputdata” worksheet and use manual match worksheet adjust matching parameters until it is best possible matched.
- 3) Use the matching parameters determined from manual match previously to input in “Inputdata” worksheet. Now it is ready for automatic history matching. Go to “Summary” worksheet. Select “Mainbody” macro and run it. This will perform automatic history matching. Detail of the progress of each loop will be shown in this page such as OGIP of each tank, $\Sigma R2$ (converge 2) and convergence parameters, OGIP of each tank from previous iteration (in case Sigma R2 increases), solution (ΔG) of each iteration, Aquifer volume of aquifer tank(s), previous iteration Aquifer volume of aquifer tank(s) in case $\Sigma R2$ increases.
 - 4) Macro will keep running until calculation meets convergence criteria or meet maximum iteration specified in “Inputdata” worksheet. There are other causes that can make the macro stops prematurely, i.e.,
 - a. Exaggerate value of matching parameter(s) makes the simulation result end before simulation period specified in “Inputdata” worksheet.
 - b. Exaggerated value of residual parameter(s) calculated from MBAL is over the limit of the type of variables declared for those residual parameters.
 - 5) When the macro run finishes, go to “Result1” worksheet to see the result of matching for each residual. It is in the same format as in “Manual” worksheet.

APPENDIX C
AUTOMATIC HISTORY MATCHING MACRO CODE

(Available upon request)



ศูนย์วิทยทรัพยากร
จุฬาลงกรณ์มหาวิทยาลัย

VITAE

Name: Polpipat Suthichoti

Date of Birth: 21 January 1974

Place of Birth: Bangkok, Thailand

Education: B.E., Chemical Engineering, 1995
Kasetsart University
Bangkok, Thailand

M.S., Engineering Management, 1996
University of Missouri at Rolla
Rolla, Missouri, USA.

Professional Experience: Schlumberger Oilfield Services
Engineer, 1998–2003
Unocal Thailand, Ltd
Well Services Engineer, 2003–2005
Chevron Thailand E&P, Ltd.
Completion Engineer to date

ศูนย์วิทยทรัพยากร
จุฬาลงกรณ์มหาวิทยาลัย